PRESTIGE WORLDWIDE
EST. 2023

PW-24 Harpy

Heavy Lift Mobility Platform Design Proposal

2023-24 AIAA Undergraduate Design Competition

COLLEGE OF ENGINEERING
KEVIN T. CROFTON DEPARTMENT OF AEROSPACE AND OCEAN ENGINEERING
VIRGINIA TECH.

Prestige Worldwide Team

Ryan Abbou
Team Lead, CAD, &
Deliverables
AIAA: 1603320
Signature:

Jack Schramm
Aerodynamics
AIAA: 1602741
Signature:

Grant Mellinger
Stability & Control
AIAA: 1180682
Signature:

Jimmy Martino
Maintenance & System
Integration
AIAA: 1602744
Signature:

Liam Schwarz
Maintenance
AIAA: 1603541
Signature:

Thomas Klein
Propulsion & Performance
AIAA: 1179226
Signature:

Nick Turletes
System Integration
AIAA: 1602740
Signature: Nicholas Turletes

Matthew Vorster
Project Management &
Weights
AIAA: 1603321
Signature: M Vorster

Sami Qasrawi
Structures & Weight
AIAA: 1314629
Signature:

Pradeep Raj, Ph.D.
Faculty Advisor

Table of Contents

List of Figures

List of Tables

Nomenclature

$(\frac{T}{W})_{TO}$	Takeoff Thrust Loading	V_{max}	Maximum Speed
$(\frac{W}{S})_{TO}$	Takeoff Wing Loading	$(\frac{W}{S})_L$	Landing Wing Loading
ω	Ratio of Ground-Run Retardation Force to Takeoff Thrust	δ	Induced Drag Factor
ρ_{SL}	Density at Sea Level	C_{lmax}	Maximum Coefficient of Lift (2D – airfoil)
g	Gravity	$(\frac{C_l}{C_d})_{max}$	Lift to Drag Ratio (2D – airfoil)
σ	Atmospheric Density Ratio	C_{dmin}	Minimum Coefficient of Drag (2D – airfoil)
$(C_{Lmax})_{TO}$	Maximum Coefficient of Lift During Takeoff (aircraft)	$(\frac{t}{c})_{max}$	Maximum Thickness to Chord Ratio
s_{TO}	Takeoff Distance	C_{m0}	Zero-Lift Moment Coefficient (2D – airfoil)
$(\frac{T}{W})_{OEI}$	One Engine Inoperable Thrust Loading	C_{MAC}	Aerodynamic Center Moment Coefficient
$n_{engines}$	Number of Engines (per aircraft)	c_t	Tip Chord
$\frac{L}{D}$	Lift to Drag Ratio (aircraft)	c_r	Root Chord
γ	Climb Angle (during takeoff)	c_A	Average Chord
$(\frac{T}{W})_{ROC_{max}}$	Maximum Rate of Climb Thrust Loading	α	Angle of Attack
ROC_{max}	Maximum Rate of Climb	$C_{HT\,(VT)}$	Horizontal (Vertical) Tail Volume Coefficient
C_{Lopt}	Optimized Coefficient of Lift (aircraft)	$l_{HT\,(VT)}$	Horizontal (Vertical) Tail Moment Arm
K	Drag Due to Lift Factor	$S_{HT\,(VT)}$	Horizontal (Vertical) Stabilizer Planform Area
C_{D0}	Zero-Lift Drag Coefficient	S_{ref}	Wing Planform Area
$(\frac{T}{W})_{V_{cr}}$	Cruise Speed Thrust Loading	W_e	Aircraft Empty Weight
V_{cr}	Cruise Speed	W_f	Fuel Weight
e	Wing Efficiency Factor	ρ	Fuel Density
$(\frac{T}{W})_{V_{max}}$	Maximum Speed Thrust Loading	$Cost_f$	Fuel Cost
$\frac{T}{W}$	Thrust Loading	CL	Coefficient of Lift (3D)
CD	Coefficient of Drag (3D)	M_{DD}	Drag Divergence Mach Number
$\frac{t}{c}$	Thickness to Chord Ratio	κ_A	Korn Equation
Λ	Leading Edge Wing Sweep	$CDtot$	Total Drag Coefficient (3D)
CDi	Induced Drag Coefficient	$CDleak$	Leakage Drag Coefficient
$CDtrim$	Trim Drag Coefficient	$CD0$	Parasite Drag Coefficient
V_{TO}	Takeoff Velocity	V_{50}	Approach Velocity (@50ft AGL)
V_{CL}	Climb Velocity	V_{TD}	Touchdown Velocity
S_G	Ground Run Distance	S_A	Approach Distance
S_{TR}	Transition Distance	S_B	Braking Distance
θ_{CL}	Climb Angle	θ_{app}	Approach Angle
$C_{m_{\delta e}}$	Elevator Deflection Induced Moment	$C_{M\alpha}$	Momentum Stability Derivative with Respect to Alpha
ζ_{dr}	Dutch Roll	$C_{n\beta}$	Yawing Moment Due to Sideslip Angle

T_{2s}	Spiral Period		$C_{l\beta}$	Rolling Moment Due to Sideslip Angle
ζ_{ph}	Phugoid		T_R	Roll Period
ζ_s	Short Period			

Acronyms

AAM	Air-to-Air Missile		**INS**	Inertial Navigation System
ACN	Aircraft Classification Number		**LRU**	Line Replaceable Unit
AI	Artificial Intelligence		**MBT**	Main Battle Tank
AIAA	American Institute of Aeronautics and Astronautics		**MDD**	Drag Divergence Mach Number
APU	Auxiliary Power Unit		**MIL-SPECS**	Military Specifications
AR	Aspect Ratio		**MLG**	Main Landing Gear
BC	Bus Controller		**MMH/FC**	Maintenance Man Hours per Flight Cycle
CDU	Control Display Unit		**MMH/FH**	Maintenance Man Hours per Flight Hour
CFRP	Carbon Fiber Reinforced Plastic		**MoM**	Measures of Merit
COTS	Commercial Off-The-Shelf		**ND**	Navigational Display
DAPCA	Development and Procurement Costs of Aircraft		**NLG**	Nose Landing Gear
DME	Distance Measuring Equipment		**O&S**	Operation and Support
DoD	Department of Defense		**OEI**	One-Engine-Inoperable
ECS	Environmental Control System		**PANDA**	Predictive Analytics and Decision Assistant
ECS	Environmental Control System		**PFD**	Primary Flight Display
EFB	Electronic Flight Book		**RAT**	Ram Air Turbine
EFIS	Electronic Flight Instrument Panel		**RDT&E**	Research, Development, Test, Evaluation
EHA	Electro-hydrostatic Actuators		**RFP**	Request for Proposal
EICAS	Engine Indicating and Crew Alert System		**RWR**	Radar Warning Receiver
EIS	Entry Into Service		**SAM**	Surface-to-Air Missile
EMA	Electro-mechanical Actuators		**SATCOM**	Satellite Communications
EMU	Engine Monitoring Unit		**SFC**	Specific Fuel Consumption
FAA	Federal Aviation Administration		**SSL**	Standard Sea Level
FADEC	Full Authority Digital Engine Control		**TACAN**	Tactical Air Navigation System
FAR	Federal Aviation Regulations		**TACAN**	Tactical Air Navigation System
FMS	Flight Management System		**TBW**	Truss Braced Wing
GPS	Global Positioning System		**TOGW**	Takeoff Ground Weight
HLA	Heavy-Lift Aircraft		**UHF**	Ultra-High Frequency
HLMP	Heavy Lift Mobility Platform		**US**	United States
HUD	Heads-Up Display		**USAF**	U.S. Air Force
ICAO	International Civil Aviation Organization		**VDT**	Video Display Terminal
IFF	Identification Friend or Foe		**VHF**	Very High Frequency

1. Executive Summary

Prestige Worldwide is pleased to offer the PW-24 Harpy, shown in figure 1, in response to the 2023-2024 AIAA RFP. The next gen Heavy Lift Mobility Platform is an innovative solution designed to bridge the capability gap in strategic lift mobility aircraft. The USAF's aging C-5 and C-17 fleets are moving toward retirement. Through its payload capacity, range, and rapid reconfiguration, the Harpy is best suited to fulfill these needs. Named after the Harpy eagle due to its superior ability to carry heavy weights, the PW-24 Harpy is a wide-bodied, 4-engine aircraft, whose dimensions exceed those of the C-5 and rivals the Antonov AN-225. A technologically advanced next-generation strategic military airlifter, the Harpy has global reach while transporting hundreds of tons of cargo.

The Harpy utilizes innovative high aspect ratio truss-braced wings that benefit from reduced weight and improved L/D ratios as compared to traditional cantilever wings. The folding wingtips allow the Harpy to operate out of ICAO Class F airfields without sacrificing the performance benefits of its extended wingspan. The Harpy is equipped with four Rolls Royce Trent 1000-J2 engines and implements a more electric subsystem architecture that requires no bleed air from these engines. The Harpy's tail design is a cruciform T-tail, to avoid interactions of the horizontal stabilizer with the wake of the high-wings and engines, and to allow for a clear path for paratrooper exits from the aircraft during flight. To ensure rapid redeployment capability, the Harpy has a nose cone that folds up for loading in addition to the aft loading ramp. These two loading ramps provide access to a spacious cargo hold, capable of housing three M1 Abrams tanks, forty-eight 463L pallets, or 430 passengers. In addition to the cargo hold, the PW-24 Harpy has a second floor housing the flight deck and 100 paratrooper seats. With a unit price of $421 million for a production run of 160 units for the USAF and 20 for niche commercial market, the PW-24 Harpy is a highly cost-effective aircraft that satisfies all mission requirements defined in the RFP; the payload and range capabilities are highlighted in Table 1 below. Due to its unprecedented technology and innovative lifting-body surfaces, the PW-24 Harpy will satisfy the need of the US Air Force to carry on its strategic military airlifting operations as well as support long-range transportation of tactical payloads.
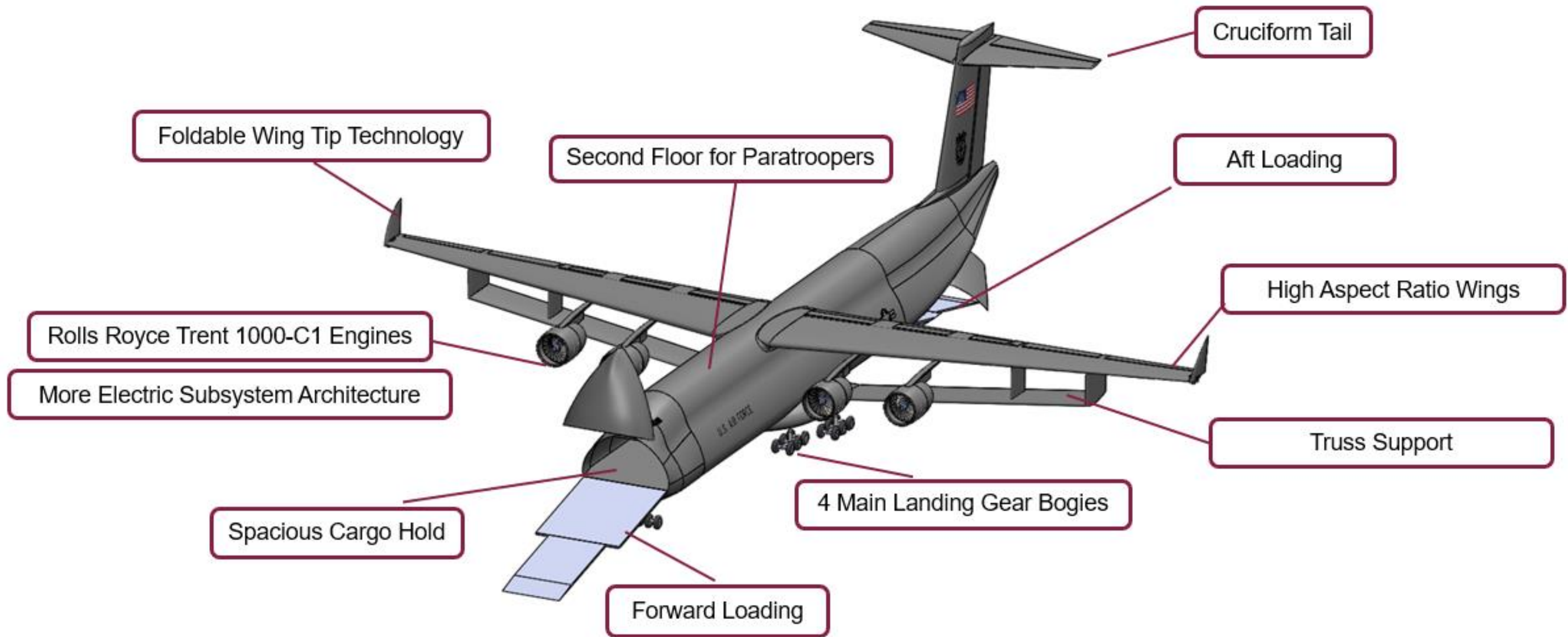
Figure 1. PW-24 Harpy walk-around chart.

Table 1. Key Parameters of the PW-24 Harpy

Trait	Value
Aircraft Empty Weight	435,000 lbs.
Max Payload Weight	430,000 lbs.
Maximum TOGW	1,080,000 lbs.
Cargo Hold Volume	55,000 cu. ft.
Ferry Range	8000 nmi.
Medium Load Range	5000 nmi.
Max Payload Range	2500 nmi.
Unit Price	$421 million
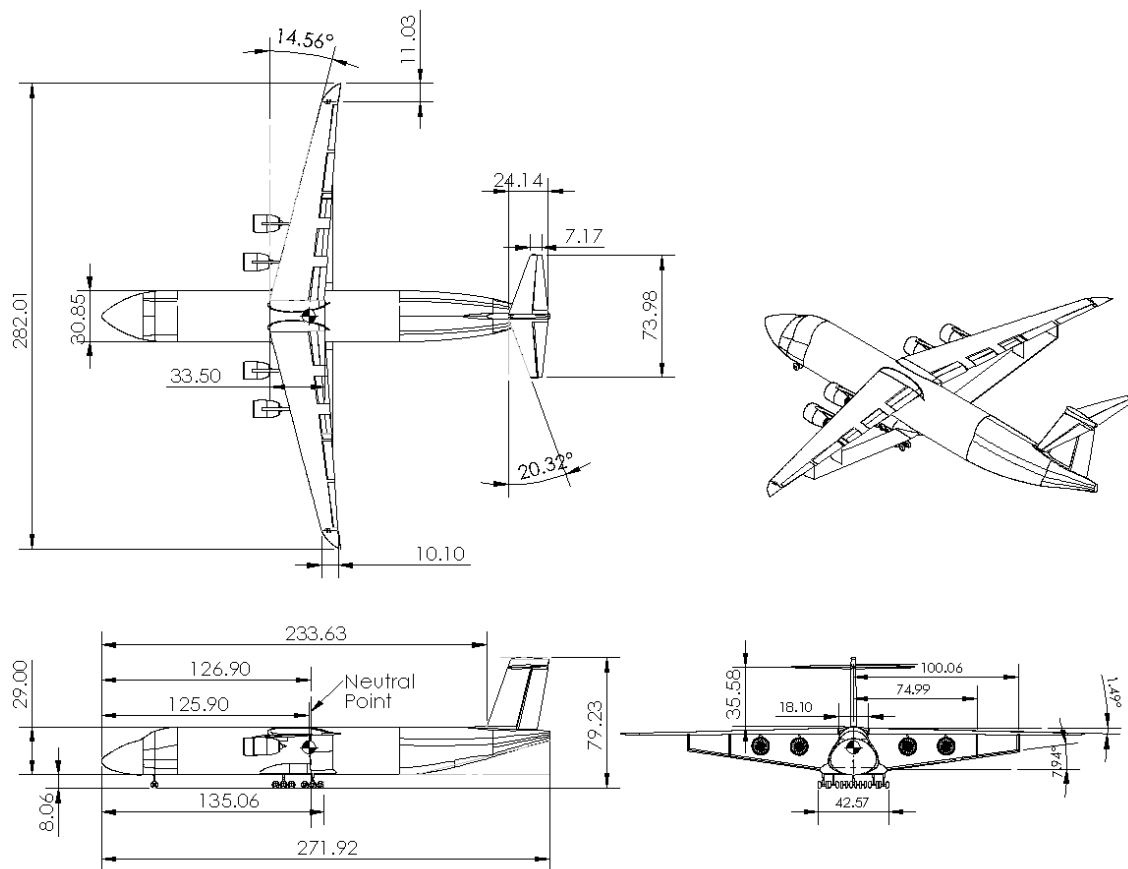
Figure 2. The PW-24 Harpy three-view drawing, all dimensions in feet.

2. Understanding of the Problem

In response to the Request for Proposal (RFP), put forth by the American Institute of Aeronautics and Astronautics (AIAA) for a Heavy Lift Mobility Platform (HLMP), Prestige Worldwide first developed a comprehensive understanding of the problem as described in this section.

2.1 Genesis of the Problem

The US Air Force (USAF) Air Mobility command faces a need for a next-generation Heavy-Lift Aircraft as the C-17 and C-5 reach the end of their service life. Their successor must be capable of bridging this gap in strategic lift capabilities. The proposed HLA must deliver 430,000 lbs. of payload over an unrefueled range of 2,500 nm at Mach 0.80, meeting the demand for rapid global mobility. The challenge lies in ensuring technical feasibility and affordability. The anticipated production of 160 units for the USAF and allies, along with 20 units for a commercial market, emphasizes the HLA's unique outsized cargo capability. The current USAF fleet contains the C-17 and C-5 cargo transporters, however they do not meet the mission's cargo and range needs. In order to rapidly adapt to the global needs of today's world, the USAF needs a heavy lift aircraft capable of transporting massive loads worldwide.

2.2 Requirements

2.2.1 Requirements and Constraints

The RFP contains requirements that are split into three main categories: general requirements, design requirements, and project management requirements. The design requirements contain information about the aircraft's range, cargo, personnel needs, entry into service, and information about its required mission profile. The design requirements are split into several subcategories including propulsion, operations, structure, maintainability, electric/hydraulic/fuel systems, avionics/displays/ECM, stability and control, and cargo handling. Lastly, the project management requirements include cost and production rate targets, certifications, development programs and financing, sourcing of components, and marketing goals.

To adequately ensure that the needs outlined in the RFP are met, we developed a compliance matrix, where we filter the requirements into their respective categories and labeled them with their respective status:

to-be-done, in-progress, current-design meets (requirement), or requirement satisfied. Note that these requirements are specifically derived from the RFP.

This section was intentionally left blank.

Table 2. Compliance Matrix

Requirement Section	Requirement Owner(s)	Mandatory/Tradable	Requirement	Requirement Met?
Structures	Structures	M	+3 and -1.5 gs load factor at any loading condition	X
Structures	Structures	T	Primary airframe made of any combination of aircraft grade alloy or composite materials	X
Structures	Structures	M	Safety factor of 1.5 used in analysis of ultimate design loads	X
Structures	Maintenance/Structures	M	Structure service life ≥40,000 hours	X
Maintenance	Maintenance	M	MMH/FH ≤24	X
Maintenance	Maintenance/Configuration	M	Easy access to all primary systems	X
Maintenance	Subsystems	M	Primary systems must be LRUs with self diagnostic capabilities and permit easy removal/replacement	x
Maintenance	Maintenance	M	Minimal need for unique support equipment	x
Electric, Hydraulic and Fuel Systems	Subsystems	M	Independent electrical and hydraulic power systems	X
Electric, Hydraulic and Fuel Systems	Subsystems	M	Fuel systems may consist of integral or self-sealing tanks with integrated fire suppression	X
Electric, Hydraulic and Fuel Systems	Subsystems	M	Must facilitate ground refueling from a single pressurepoint with gravity refueling as a backup	X
Electric, Hydraulic and Fuel Systems	Configuration	M	Internal fuel must not be stored in the same structure as the cargo/passenger bay	X
Avionics	Subsystems	M	Must include COTS avionics	x
Avionics	Subsystems	M	Primary pilot and copilot reference instruments must be a COTS HUD	X
Avionics	Subsystems	M	Must employ military qualified VHF/UHF radio, IFF transponder, and SATCOM	X
Avionics	Subsystems	M	Must employ terrain following radar with corresponding slaved digital flight controls	X
Avionics	Subsystems	M	Must incorporate a radar warning and electronic warfare/countermeasures suite	X
Stability and Control	Subsystems/Stability/Propulsion	M	Must employ a redundant FADEC system. The system must be closed loop with an automated flight control system.	x
Stability and Control	Stability	M	Static and dynamic stability characteristics must meet MIL-F-8785B requirements	X
Stability and Control	Stability/Configuration	T	The aircraft may have positive static and dynamic stability, but unstable designs in the longitudinal axis are acceptable given it augmented with a stability system.	X
Cargo Handling	Subsystem/Configuration	M	Must incorporate traditional heavy lift loading and egress systems	x
Cargo Handling	Subsystem/Configuration	M	Cargo must be contained within contiguous cargo hold	X
Cargo Handling	Subsystem/Configuration	M	The cargo hold must have internal dimmensions of ≥13.5ft high and 19ft wide	X
Cargo Handling	Subsystem/Configuration	M	Outsized cargo loading acceess must be provided	X
Cargo Handling	Subsystem/Configuration	M	≥1 cargo access locations	X
Cargo Handling	Subsystem/Configuration	M	Cargo ramp with down angle of ≤12°	X
Cargo Handling	Subsystem/Configuration	M	Cargo ramp toes with down angle of ≤16°	X
Cargo Handling	Configuration	M	≥2 paratroop doors	x

Requirement Section	Requirement Owner(s)	Mandatory/Tradable	Requirement	Requirement Met?
General Requirements	Project Management	M	EIS of 2033	X
General Requirements	Configuration	M	HLA must be fixed wing	X
General Requirements	Performance	M	HLA must be capaable of transpotring 430,000lbs in all of the following configurations: • Three (3) M1A2 Tanks; or • Forty-eight (48) 463L pallets; or • One humdred (100) passengers/troops in a separate compartment and three hundred-thirty (330) troops on the main cargo bay.	X
General Requirements	Propulsion	M	HLA must utilize airbreathing engines that are currently available or expected to enter service within 5 years	X
General Requirements	Configuration/Subsystems	M	Minimum crew size of four (4) with provisions for four (4) more	X
General Requirements	Subsystems	T	Zero-zero crew escape system	X
General Requirements	Subsystems	M	Cockpit must be designed for crew comfort and visibility	X
General Requirements	Subsystems	M	Controls and instruments must be arranged to reduce crew workload	X
General Requirements	Subsystems/Structures	M	Cabin must be pressurized throught flight envelope	X
General Requirements	Subsystems	M	Life support systems must have adequate emergency backups	X
Performance	Performance	M	Unrefueled range ≥2,500nm (plus reserves) at ≥Mach 0.8 and maximum payload	X
Performance	Performance	M	Maximum cruise speed of Mach 0.82	x
Performance	Performance	M	Unrefueled range ≥5,000nm (plus reserves) at Mach 0.8 and 295,000lb payload	X
Performance	Performance	M	Unrefueled ferry range ≥8,000nm	X
Performance	Performance	M	Initial cruise altitude ≥31,000ft with maximum payload	X
Performance	Performance	M	Service ceiling ≥43,000ft	X
Performance	Subsystems/Propulsion	M	Provisions for in-flight refueling	X
Operations	Configuration/Structures	M	Operate from ICAO code F or E airports	X
Operations	Performance	M	Operate from a 9,000 x 1,500ft airfield at SL on an ISA +15°C day	X
Operations	Structures	M	Landing gear must be suitable for civilian and appropriate military airfields	X
Operations	Structures	M	The ACN at MTW must be ≤55 for flexible pavement with subgrade B	X
Operations	Structures	M	Retractable landing gear must survive 15ft/s vertical descent rate	X
Operations	Stability	M	Takeoff and land with crosswinds of 30kt at 90°	X
Operations	Subsystems	M	Be designed witth self-start capability	X
Operations	Performance	M	Of all weather type	X
Operations	Subsystems	M	Incorporate deicing, terrain following, and terminal avoidance systems	X

2.2.2 FAA Requirements and MIL Standards

Tables 3 and 4 include FAA requirements and MIL standards in relation to a military transport category aircraft. The specific requirements listed in these tables were selected from their respective sources as they were not already covered by the requirements in the RFP.

Table 3. Applicable FAA Requirements [1]

CFR	Brief	Requirement Description
25.105	Takeoff Critical Icing	Stall speed at MTOW in icing conditions cannot exceed the greater value between 3 knots CAS and 3% VSR
25.107	Takeoff V2MIN	V2MIN cannot be less than 1.08*VSR
25.111	Takeoff Path	After reaching altitude of 400ft above takeoff surface climb gradient must be ≥1.7%
25.121	Takeoff OEI	• Gradient of climb must be ≥ 0.5% with landing gear extended • Gradient of climb must be ≥ 3% with landing gear retracted • Gradient of climb must be ≥ 1.7% in en route configuration
25.147	Directional Control	Must be possible to change heading up to 15 degrees in direction of critical inoperative engine(s) (up to two engines)
25.147	Lateral Control	Must be possible to make 20 degree banked turns with and against inoperative engine
25.149	Minimum Control Speed	VMC may not exceed 1.13*VSR
25.161	Longitudinal Trim	Must maintain longitudinal trim during climb at speed not more than 1.3*VSR1
25.233	Stability and Control	Must be no uncontrollable ground-looping tendency in 90 degree cross winds, up to a wind velocity of 20 knots or 0.2*VSR0, whichever is greater

Table 4. Applicable MIL Requirements (MIL-A-8861B, MIL-HDBK-516-1) [2], [3]

CFR	Brief	Requirement Description
3.1.3.1.3	Emergency Stores Release	Emergency release of the most critical combinations of stores shall not result in unacceptable aircraft motions or exceedance of limit strength of the airplane
3.1.7	Pressurization	The limit pressure differential between pressurized portions of the structure and the ambient atmosphere shall be: • 1.33 times the maximum attainable pressure with 1-G flight loads • Zero and the maximum attainable pressure combined with flight loads • 1.33 times the maximum attainable pressure combined with the loads due to ground test support equipment for pressurization tests
3.2.3	Takeoff/Landing	The design weight for takeoff and landing shall be the maximum design weight for each scenario
3.3.3.9	Evasive Maneuvers	Consideration shall be given to evaluate aircraft strength for evasive maneuvers such as jinking, missile break, etc.

4	Quality Assurance Provisions	Unless otherwise stated, the contractor is responsible for performance of all inspections and compliance of all items
16.1.1	Maintenance Instructions	Verify that servicing instructions are provided for all systems that require servicing; for example, fuel, engine oil, hydraulic systems, landing gear struts, tires, oxygen, escape system, etc.
16.1.2	Cautions and Warnings	Verify that cautions and warnings have been included in maintenance manuals, aircrew checklists, and ground crew checklists
16.1.3	Maintenance Checklists	Verify that maintenance checklists are available for critical maintenance tasks, such as fuel and oxygen serving procedures; towing procedures and restrictions; jacking procedures; engine operation during maintenance; lifting procedures; integrated combat turn procedures, etc.
16.1.4	Support Equipment	Verify that support equipment will not adversely impact the safety of the air vehicle

2.3 Concept of Operations

The following scenario demonstrates the initial operational capabilities of the HLMP in a typical end user case:

The USAF requires 3 M1A2 Abrams tanks to be delivered from Dover Air Force Base for use in Afghanistan. Two loadmasters assigned to the HLMP secure the 3 tanks after they are driven on by their respective crews using the aft loading ramp. Due to the flight distance being ~6,800nm, plans for aerial refueling with 2 KC-135 Stratotankers are arranged prior to takeoff. After takeoff from Dover AFB, with two loadmasters and two backup relief flight crews, the HLMP reaches its cruising altitude and flies to Bagram Airfield nonstop in ~10 hours. After landing in Bagram, drive-off unloading through the front ramp is organized by the two loadmasters and refueling is completed simultaneously by ground crew. Now empty and refueled, the HLMP completes takeoff for a return trip to Dover AFB and completes the trip unrefueled within its ferry range of 8,000nm.

The above scenario along with Figure 3 allows us to understand the overall mission of the HLMP and focus on the requirements throughout the design process. The versatility of the designed HLMP is of utmost importance, allowing for transport of rolling and non-rolling cargo along with personnel over long distances with minimal downtime between maintenance and refueling. To meet this focus, the cargo bay needs to be optimized for quick changes between rolling and non-rolling cargo. Cargo fastening and access to primary systems will be made readily accessible to reduce the workload while loading and performing routine maintenance.
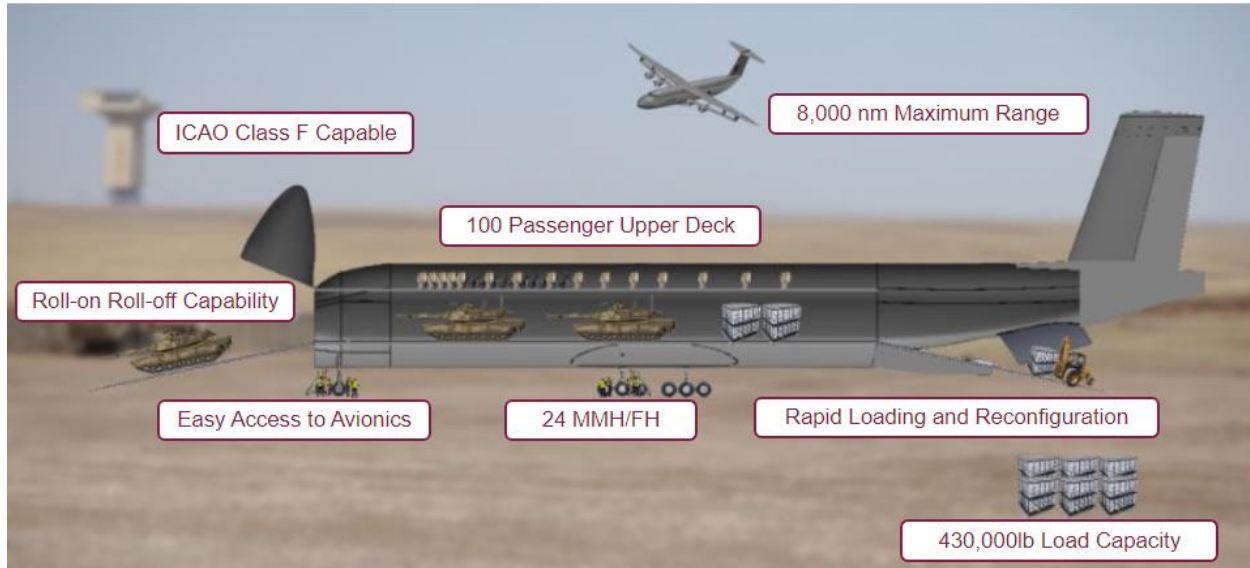
Figure 3. Concept of Operations

2.4 Comparator Aircraft

The team identified three different comparator aircraft in the strategic transports class of air vehicle – the C-5 Galaxy, the C-17 Globemaster, and the Antonov An-225. The specs of these three aircraft along with the RFP requirements are tabulated below in Table 5.

Table 5. Comparator Aircraft Parameters

	Lockheed C-5 Galaxy [4]	Boeing C-17 Globemaster [5]	Antonov AN-225 [6-7]	Specified in RFP
Payload Weight	36 Pallets (260,000 lbs)	18 Pallets (170,900 lb)	420,000 lb capacity	48 Pallets (430,000 lb)
Tanks	Two M1-A1 Abrams Tanks	One M1 Abrams Tank	Not Specified	Three M1-A2 Abrams Tanks
Passengers	270 Passengers	102 Paratroopers/ 134 Troops	Not Specified	330 Troops + 100 paratroopers
Ferry Range	7,000 nmi	6,230 nmi	8,300 nmi	8,000 nmi
Max Payload Range	2,300 nmi	2,420 nmi	2,170 nmi	2,500 nmi
Cruise Speed	Mach 0.77	Mach 0.74 - Mach 0.79	Mach 0.78	Mach 0.8 – Mach 0.82
Service Ceiling	34,000 ft	45,000 ft	36,000 ft	43,000 ft

Currently, the USAF utilizes the C-5 and the C-17 for its strategic military aircraft operations. These two aircraft present a capability gap as they offer payload capacities of 261,000 lbs. and 170,900 lbs. respectively, falling short of the RFP payload requirement of 430,000 lbs. Moreover, both aircraft are incapable of transporting three M1A2 Abrams tanks as requested by the USAF. The two aircraft also fall short of the 8000 nm. ferry range and the 2500 nm. max payload range requirement. The C-5 has a ferry range of 7000 nm. and a max payload range of 2300 nm [4]. The C-17 has a ferry range of 6230 nm. and a max payload range of 2420 nm [5]. Clearly, these two aircraft are incapable of meeting the RFP's requirements. The Antonov An-225 on the other hand nearly meets the key requirements, with a max payload of 420,000 lbs., a ferry range of 8,300 nm., and a max payload range of 2,170 nm [6]. However, the An-225 is not a viable option for the USAF since just a single An-225 was ever produced and is currently rendered inoperable as it is destroyed. Projections to rebuild the An-225 eclipse $500 million [7], thus the An-225 is simply not a realistic option for the USAF. The capability gap and lack of viable aircraft for the USAF's RFP highlight the justification for the development of a new HLA.

2.5 Measures of Merit

Measures of Merit (MoMs) are criteria the Prestige Worldwide team has decided on to show the improvement of the final design and market differentiators that give us an edge over competitor aircraft. The chosen of MoMs are shown in Table 6.

Table 6. The PW-24 Harpy's Measures of Merit (MoMs)

Category	Aspect
Financial	- Minimal cost for development and production of aircraft - $400 million unit cost (C-5 historical and AN-225 projection)
Mission & Maintainability	- Lowest possible time for reconfiguration of cargo bay between cargo and passenger configurations - Manned maintenance hours per flight hour below 20
Environmental Factors	- Less than 100 dB of sound produced at takeoff/landing, similar to comparator aircraft (C-5 Galaxy) - Minimize emissions during production/manufacturing
Structures & Weights	- Minimum weight while meeting performance criteria

Further dissecting the categories, we placed certain goals for each measure of merit to verify once it is 'achieved'. First, we set minimal cost for development/production and a unit cost of $400 million as the

goals of the financial category. For mission & maintainability, we desire the lowest possible reconfiguration time and manned maintenance hours per flight hour below 20. Finally, we aim to achieve fewer than 100 dB of sound produced during takeoff and landing for aerodynamics & propulsion and a minimum takeoff gross weight while still being able to meet the performance criteria. While these measures show viable achievements to the customer, they also proved to be useful in the final down selection we used to identify our preferred system concept.

2.6 Promising Technologies

The AIAA's RFP for an HLMP presents several engineering challenges such as maintenance of a large-scale aircraft, pilot comfort, and energy efficiency that may require new and emerging technologies to solve. The Prestige Worldwide team has identified and investigated several developing technologies that will allow us to tackle these engineering challenges and to design a concept fit for the US Air Force's feet. The technologies listed below are currently in varying stages of development but have a sufficiently high TRL such that they will be commercially available before the HLA is ready for production.

2.6.1 Continuous Health Monitoring Using Artificial Intelligence

The first promising technology we propose to integrate into our solution is an Artificial Intelligence (AI) system that monitors the aircraft's maintenance needs. AI has the capability to more accurately predict when maintenance or replacement is needed for aircraft parts or subsystems. The AIAA RFP specifies that the "HLA must meet a Maintenance Man Hours per Flight Hour (MMH/FH) no greater than the C-17 (20 MMH/FH) plus 20%." The factors that go into the MMH/FH are complex, but one way to reduce the MMH/FH is to reduce the amount of maintenance needed for the aircraft over its lifespan. AI aims to accomplish this using complex models and historical data to predict when maintenance is needed and proactively prevent future need for maintenance hours.

As of May 2023, the Air Force has designated the Predictive Analytics and Decision Assistant (PANDA) as a system of record. This system is an "artificial intelligence and machine learning tool for predictive maintenance" [8]. PANDA and similar systems integrate AI and machine learning to increase reliability of aircraft systems. This technology has been under development since 2019 and is currently in use by the US Airforce. However, it is not done being updated and optimized, giving it a TRL of ~6-7.

Furthermore, with the rapid development of AI in recent years, this technology will be ready by the entry into service date.

2.6.2 Dire BAE LiteWave Heads-Up Display (HUD)

The BAE LiteWave Heads-Up Display is the latest HUD developed by BAE Systems. This system is designed for installation on a wide range of both military and commercial aircraft [9]. The AIAA RFP states that the aircraft must be capable of delivering a "430,000 lbs payload over an unfueled range of no less than 2,500 nm." An aircraft able to carry such a heavy payload must minimize weight while meeting performance criteria which the BAE HUD will aid in. This HUD "represents a 70% reduction in size and weight of this kind of product compared to conventional HUDs."

This technology not only is a significant reduction in weight and size, but also an improved eye motion box, which ensures the pilot can view the HUD information while having a greater range of vision when compared to standard HUDs. Additionally, the LiteHUD systems have been in development since 2010, and have been integrated into aircraft since 2017. The latest version, LiteWave, has been demonstrated in various aircraft as well. This correlates to a TRL of ~8-9, meaning that it will be ready before the technology freeze.

2.6.3 Truss-Braced Wing

The final emerging technology of interest is the revolutionary truss-braced wing, initially proposed by Northrop Grumman for long-range bombers. In recent years, Boeing and NASA have been conducting research on how to implement this technology on transport aircraft. The RFP's requirements on cargo and weight surpass the capability of existing aircraft. This generates the need for new lifting technology, such as the truss-braced wing. The truss structure under the wing provides structural support, enabling far larger aspect ratios than traditional wings. Higher aspect ratio wings correlate to a lower lift induced drag, leading to reduced wing weight compared to cantilever wing of same aspect ratio, and ultimately increased payload capability from an increase in aerodynamic efficiency [10]. The truss under the wing also helps to reduce aeroelastic effects and flutter, two important factors that constrain an aircraft's design space, enabling more possibilities for our aircraft and its performance capabilities.

2.7 Development Timeline

The development timeline, including milestones of the HLA project is shown in Figure 4. Starting in the summer of 2023, the conceptual design phase marks the beginning of the project and lays the groundwork for the subsequent phases. The period from 2024 to 2028 is devoted to the detailed design, a comprehensive phase that ensures the accuracy and viability of the HLA's specifications. In 2027, a milestone is reached with the technology freeze. Additionally, it is the beginning of the production line development, a critical point that signifies the consolidation of design decisions. The following years, 2028 to 2030 will implement the production of the aircraft, transforming the detailed design into a viable aircraft. In 2030 to 2032 the focus shifts to ground and flight testing and certification. The culmination of these milestones occurs in 2033, marked by the Entry into Service of the HLA, signifying its operational deployment and the fulfillment of the strategic goals of this development initiative.

Summer 2023:
Begin Conceptual Design

2024 - 2028:
Detailed Design

2028 - 2030:
Manufacturing

Early 2033:
Receive Aircraft Certification

2024:
Begin Preliminary Design

2027:
Technology Freeze and Production Line Development

2030-2032:
Ground/Flight Testing and Certification

End of 2033:
EIS
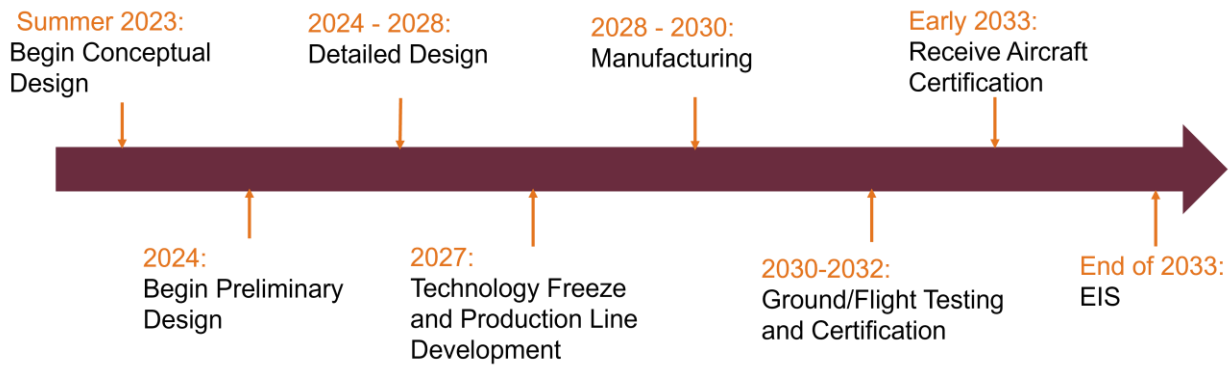
Figure 4. Project Timeline of HLA Design

2.8 Key Design Drivers

The key features that drive the design are the following:

- Cargo Volume: The ability to provide space, and transport large-scale military equipment and paratroopers is essential for the aircraft to successfully carry out its missions.
- Reconfiguration: Reconfiguring the internal structure of the aircraft allows for the accommodation of transporting both tanks and troops and then rearranging to a cabin capable of transporting solely troops.
- Low Production Cost: Lowering the production costs and expenses when producing the HLMP can reduce the selling price. This makes it more affordable for the customer while maintaining profit.
- Low Maintenance Time: Minimizing maintenance time while assuring that the plane is providing full protection for the troops and equipment onboard.

2.9 Design Objectives and Strategy

The team created design strategies which would most effectively achieve the key design objectives of this project. The key objectives are: include being rapidly deployable and reconfigurable, a large, fixed wing aircraft, made of modern materials, and safe/maintainable. The corresponding strategies are:

- Optimize reconfiguration and deployment time,
- Maximize wing size while satisfying ICAO Code E/F requirements,
- Utilize modern materials and manufacturing techniques, and
- Prioritize safety and maintenance of the aircraft and its production process.

The aircraft is to be designed with large cargo access points in both the forward and aft portions of the plane. These are then to be enhanced with the inclusion of technology to lower the loading crew's workload. To maximize wing capabilities within the constraints of the RFP, non-traditional lifting bodies (such as a truss-braced wing) are to be implemented with folding-wing technology to increase span in flight and meet the aforementioned requirements in taxi and stationary situations. Cost and performance are balanced through efficiency, which is to be considered through the implementation of modern manufacturing systems and the use of contemporary composite materials. Above all else, however, the aircraft's production and lifespan must be monitored and controlled. This will be done through risk management assessments, automated health monitoring to decrease workload, and by utilizing modern, efficient propulsion systems to minimize the costs of flight.

2.10 Mission Profile

The mission profile for the HLMP is shown in Figure 5. The five primary sections of flight are included for the aircraft, along with specific values for cruise speed and altitude specific to its capabilities.

4   **33,000 ft. altitude**   **6**

5

3   **7**

1   **2**   **8**   **9**

1: Taxi
2: Takeoff
3: Climb
4: Transition to Cruise
5: Cruise
6: Transition to Descent
7: Descent
8: Landing
9: Taxi
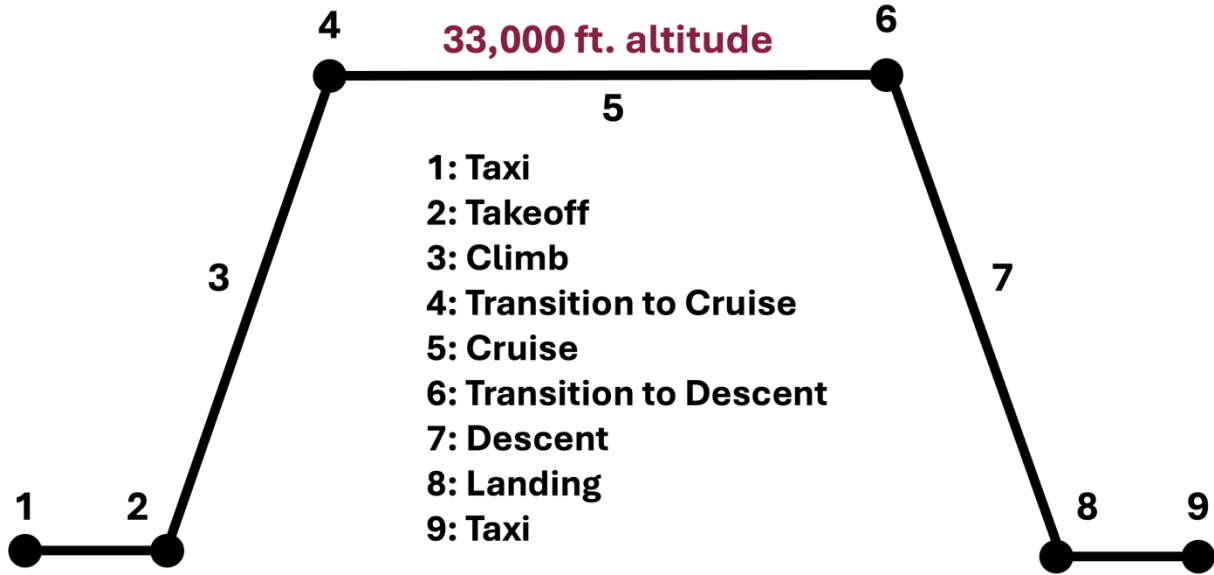
Figure 5. Mission Profile

The HLMP's mission profile, as outlined in Figure 5, accounts for the varying range and load conditions dictated by the RFP. Generally, the mission profile remains unchanged with the varying load cases, i.e., the HLMP will follow the same five-phase flight profile with every load case. The only variable in this scenario is the total range of the aircraft which varies from 2,500 nm (heavy load case) to 8,000 nm (ferry range).

3. Design Evolution

In this section we highlight the evolution of the preferred system concept (PSC) as a best solution to the problem outlined in section 2. We first highlight the final PSC in section 3.1 and then discuss how it was developed from scratch in the subsequent sections.

3.1 The PW-24 Harpy

Prestige Worldwide's preferred system concept, the PW-24 Harpy is shown in Figure 6. The PW-24 Harpy is a truss-braced wing aircraft featuring a high aspect ratio wing capable of producing high lift and reducing the overall thrust required for flight when compared with other concepts of similar empty weight. The high span wings offer foldable wingtips allowing the Harpy to operate at smaller airfields without sacrificing its high efficiency wing design. Due to its large size, the Harpy is compatible with a wider variety of engines when compared to similar aircraft, thus opening the possibility of the use of highly efficient, bleed-less engines. Unlike the C-5 and the C-17, the PW-24 Harpy can carry payloads of up to 430,000 lbs and has enough volume for the three requested configurations: three M1 Abrams tanks, forty-eight 463L pallets, or 330 passengers. Each of these three configurations also accounts for the separate 100 paratrooper cabin. The Harpy is pictured in Figure 6.
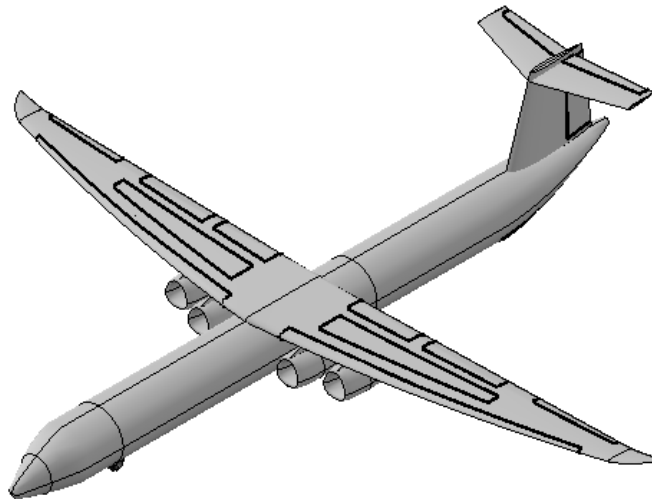
Figure 6. PW-24 Harpy Model from NASA's OpenVSP Modeling Software

3.2 Initial Viable Concepts

Each member of the Prestige Worldwide team sketched a concept of their HLA design. This allowed for a wide range of different concepts, from which we could combine desirable aspects and down select to a preferred system concept. As shown in the highest level of Figure 7, the initial concepts included: truss-braced wing, tri-jet, blended-wing body, wedge-nose, standard four-engine configuration, V-tail, T-tail, and compound delta wing aircraft.
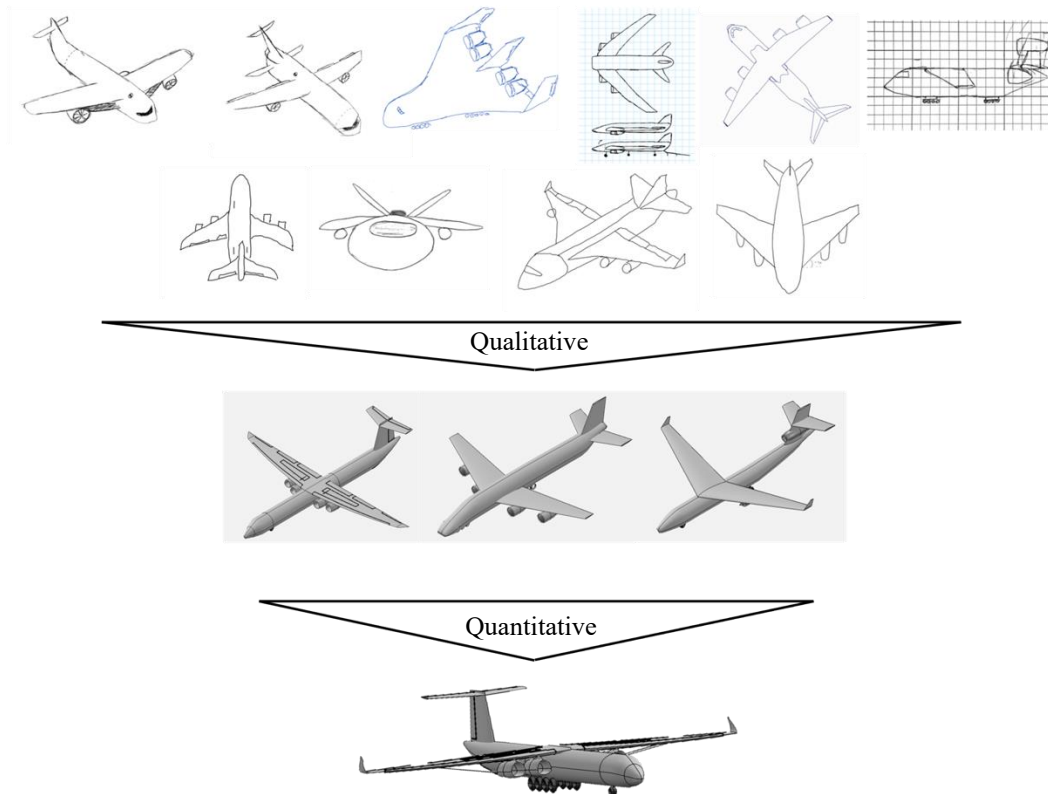
Figure 7. Design Down Selection Pyramid Beginning with Initial Design Phase

3.3 Three Most Promising Concepts

To down select to three most promising concepts, we defined a decision matrix with selection criteria shown in Figure 8 and in descending order are cost, range, cargo capability, innovation, aircraft weight, maintainability, stability, sizing, fuel efficiency, reconfigurability, and ease of production and manufacturing. We created a matrix allowing each member to submit their criteria scores for each of the concepts. The TBW, tri-jet, and wedge-nosed aircraft scored the highest primarily due to their better affordability, weight, and

innovation when compared with the other concepts. The TBW's additional wing support led to a higher aspect ratio wing and ultimately greater lift capabilities when compared with the other concepts. The wedge nose's fuselage shape acted as an additional lifting body, providing greater lift capability than other designs. Finally, the tri-jet's three engine design led to high scores in cost and weight when compared to the other designs.
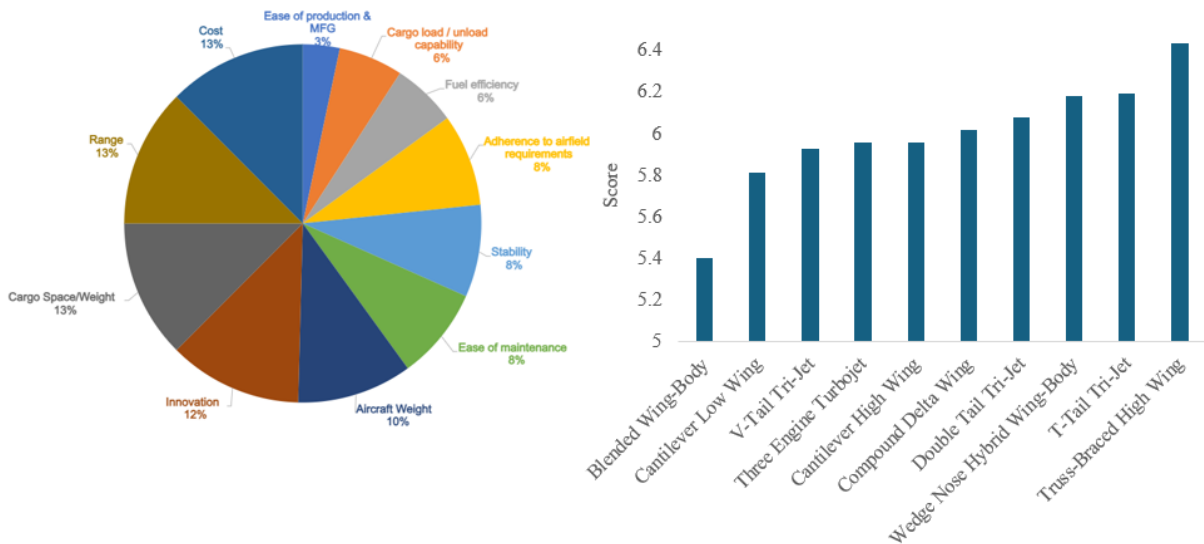
Figure 8. Design Down Selection Criteria with Heavily Weighted Towards Cost, Range, Payload, and Innovation.

3.4 Initial Sizing

3.4.1 Weight Sizing

To assess feasibility of the three down selected concepts, we estimated their takeoff gross weights (TOGW). We found these values using an iterative process of solving for the weight fractions of each stage of flight with an estimation of different weight parameters such as crew and cargo as well as estimations of the $(L/D)_{max}$ for each design as specified in Nicolai and Carichner [11]. The beginning of the process involved estimating fuel fractions pertaining to different stages of the mission profile including warm up & takeoff, climb, cruise, and landing. These phase fuel fractions were multiplied together to obtain the total mission fuel ratio, accounting for reserve fuel for 45 minutes of flight at cruise speed and altitude, per FAA requirements. Once we calculated the overall fuel ratio, we iterated through an array of test takeoff weights estimating the weight of the fuel, empty available, empty required, and their difference. We defined a convergence criteria of 1% difference on aircraft weight empty required., and we calculated the takeoff gross weight for the respective

load condition. Table 7 shows each design's TOGW in the heavy payload (430,000 lbs) scenario, fuel ratio, and fuel weight utilizing estimated parameters such as aspect ratio and $C_{L,max}$ from historical data.

Table 7. Weight Sizing for Selected Designs

	Truss-Braced Wing	Wedge Nose	Tri-Jet
Takeoff Gross Weight	1,080,000 lbs	1,170,000 lbs	1,180,000 lbs
Fuel Ratio	0.166	0.200	0.203
Fuel Weight	179,000 lbs	233,000 lbs	240,000 lbs

3.4.2 Feasible Design Space

To size each design, we developed constraint plots to determine a feasible design space. Constraint plots utilize specific aircraft performance equations that model the different phases of flight to plot thrust loading (T/W) for a range of wing loading (W/S). The constraint equations we used to determine our design region included: takeoff, takeoff OEI, rate of climb, cruise, max speed, and landing. The constraint equations, obtained from Nicolai and Carichner [11], contained aerodynamic assumptions specific to each design. These assumptions varied from C_{Lmax} to SFC to accurately estimate a feasible design region for our aircraft. Once we identified the feasible region, we utilized a 5% buffer from the closest constraint lines, allowing us to operate within the design region but optimizing the design point we select. Each design yielded a different design point location due to their unique features. For example, the TBW design's constraint plot yields the largest wing loading of the three concepts due to its relatively high AR. On the other hand, the Tri-Jet has the highest thrust loading in large part because it is a 3-engine design and requires more thrust per engine in the OEI scenario compared to the 4-engine designs. To demonstrate these differences to the customer, we overlaid historical data of similar class aircraft including the C-17, C-5 Galaxy, and the AN-225. Ultimately, the constraint plots aided in our search for an optimum design point as well as preferred system concept. We used them to determine the sizing of each design's engines, wing planform area, chord, span, and other aerodynamic sizing parameters. The equations used to generate our constraint plots are listed below:

$$\textbf{Takeoff: } \left(\frac{T}{W}\right)_{TO} \geq \frac{1.44\,(\frac{W}{S})_{TO}}{(1-\omega)(\rho_{SL}\,g\,\sigma)(C_{Lmax})_{TO}*\left\{s_{TO}-3.394\sqrt{\frac{(\frac{W}{S})_{TO}}{\sigma\,\rho_{SL}\,(C_{Lmax})_{TO}}}\right\}} \qquad (1)$$

Takeoff OEI:
$$\left(\frac{T}{W}\right)_{OEI} \geq \left(\frac{n_{engines}}{n_{engines}-1}\right)\left[\frac{1}{\left(\frac{L}{D}\right)} + \sin(\gamma)\right] \tag{2}$$

Rate of Climb:
$$\left(\frac{T}{W}\right)_{ROC_{max}} \geq \left[\frac{ROC_{max}}{\sqrt{\frac{2\left(\frac{W}{S}\right)}{\rho\, C_{Lopt}}}} + 2\sqrt{K\, C_{D0}}\right] \tag{3}$$

Cruise Speed:
$$\left(\frac{T}{W}\right)_{V_{cr}} \geq \left\{\frac{\rho\, V_{cr}^2}{2\left(\frac{W}{S}\right)}C_{D0} + \frac{2\left(\frac{W}{S}\right)}{\rho\, V_{cr}^2\,(\pi\, AR\, e)}\right\} \tag{4}$$

Max Speed:
$$\left(\frac{T}{W}\right)_{V_{max}} \geq \left\{\frac{\rho\, V_{max}^2}{2\left(\frac{W}{S}\right)}C_{D0} + \frac{2\left(\frac{W}{S}\right)}{\rho\, V_{max}^2\,(\pi\, AR\, e)}\right\} \tag{5}$$

Landing:
$$\left(\frac{W}{S}\right)_L \leq \frac{(\mu\, \rho_{SL}\, g)\sigma\,(C_{Lmax})_L}{1.3225}\left[S_L - \frac{h_{obstacle}}{\tan(\theta_{approach})}\right] \tag{6}$$

We generated three constraint plots (one for each initial concept) using the above equations. The resulting design parameters obtained from the constraint plots are shown in Table 8. Also, an example constraint plot for the TBW design is shown in Figure 9 below.

Table 8. Constraint Plot Results Information Summary

	Truss-Braced Wing	Wedge Nose	Tri-Jet
Wing Loading	186 lb/ft^2	148 lb/ft^2	154 lb/ft^2
Thrust Loading	0.275	0.28	0.32
Thrust per Engine	73,800 lbf	84,800 lbf	132,000 lbf
Aspect Ratio	13.7	6.5	7.9
Planform Area	5,790 ft^2	8,190 ft^2	7,930 ft^2

3.5 Preferred Concepts Down Selection
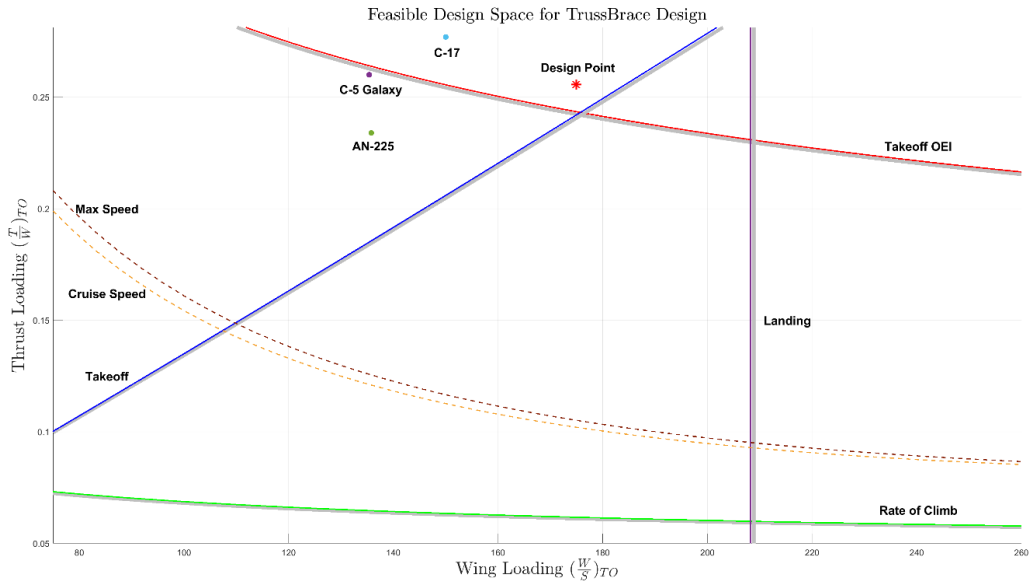
Figure 9. Constraint Plot for TBW Design

3.5.1 Constraint Assumptions

To accurately create the feasible design space within the constraint plots, assumptions for each design were required. First, we assumed the preferred concept (TBW design) to have an AR of 14 and an $(L/D)_{max}$ of 25. These assumptions came from NASA documents [10] discussing advancements in truss braced technology as well as the typical order of aspect ratio of wings that utilize it and how they effectively trim drag during flight. Next, the aircraft's C_{Lmax} was required. This estimation came from Nicolai and Carichner's [11] Figure 9.7, however we were not able to directly use this, as an AR of 14 is larger than the bounds of the chart. To estimate a proper C_{Lmax} we used linear interpolation of all the other historical aircraft data to identify a trend, and eventually come to the estimation of a C_{Lmax} of 3.36.

Finally, the last assumption that varied per design was the induced drag factor (δ) of 0.0248. This number came from the Lifting Line Theory and plotting it against an array of different taper ratios per AR. Since Nicolai and Carichner [11] identified an estimated taper ratio to be 0.3 for jet class transport aircraft, the

value of δ could be found. The other assumptions were held constant since they were made in terms of the class of our aircraft. These included a cruise C_{D0}, sfc of 0.000139 lb/s/lb, and a cruise altitude of 37,000 ft.

3.5.2 Measures of Merit

The identification of the preferred system concept involved the use of our previously listed measures of merit, which aided in the final selection of the design we deemed best fit for the customer and their needs. Table 9 shows the Truss Braced Wing (TBW) to be a clear frontrunner based on MoMs.

The TBW outperformed both the Wedge Nose and the Tri-Jet in every category. Coming in with a maximum TOGW of 1,080,000 lbs, a unit cost of $289 million, and 16.6 MMH/FH. It was clear to us that the TBW was the design best suited for the customer. We completed a cursory trade off study on engine cost to provide quantifiable information for narrowing down our designs. We selected the Trent 1000-C1, GE90-85B, and GE90-115B engines as representative engines that best satisfied the required thrust per engine for the TBW, wedge nose, and tri-jet designs, respectively. In narrowing down, we evaluated that while it is the biggest engine on the market, the GE90-115B still does not provide suitable thrust for the tri-jet aircraft's takeoff requirements; furthermore, our analysis showed an approximate cost of the Trent 1000-C1 to be $16.25 million (in 2023 dollars) [12] and the GE90-85B to be $40.8 million (in 2023 dollars) [13]. Therefore, to reduce costs and maintenance time, the TBW was chosen as the optimal design for proposal set by the USAF.

Table 9. Final PSC Selection Based on MoMs

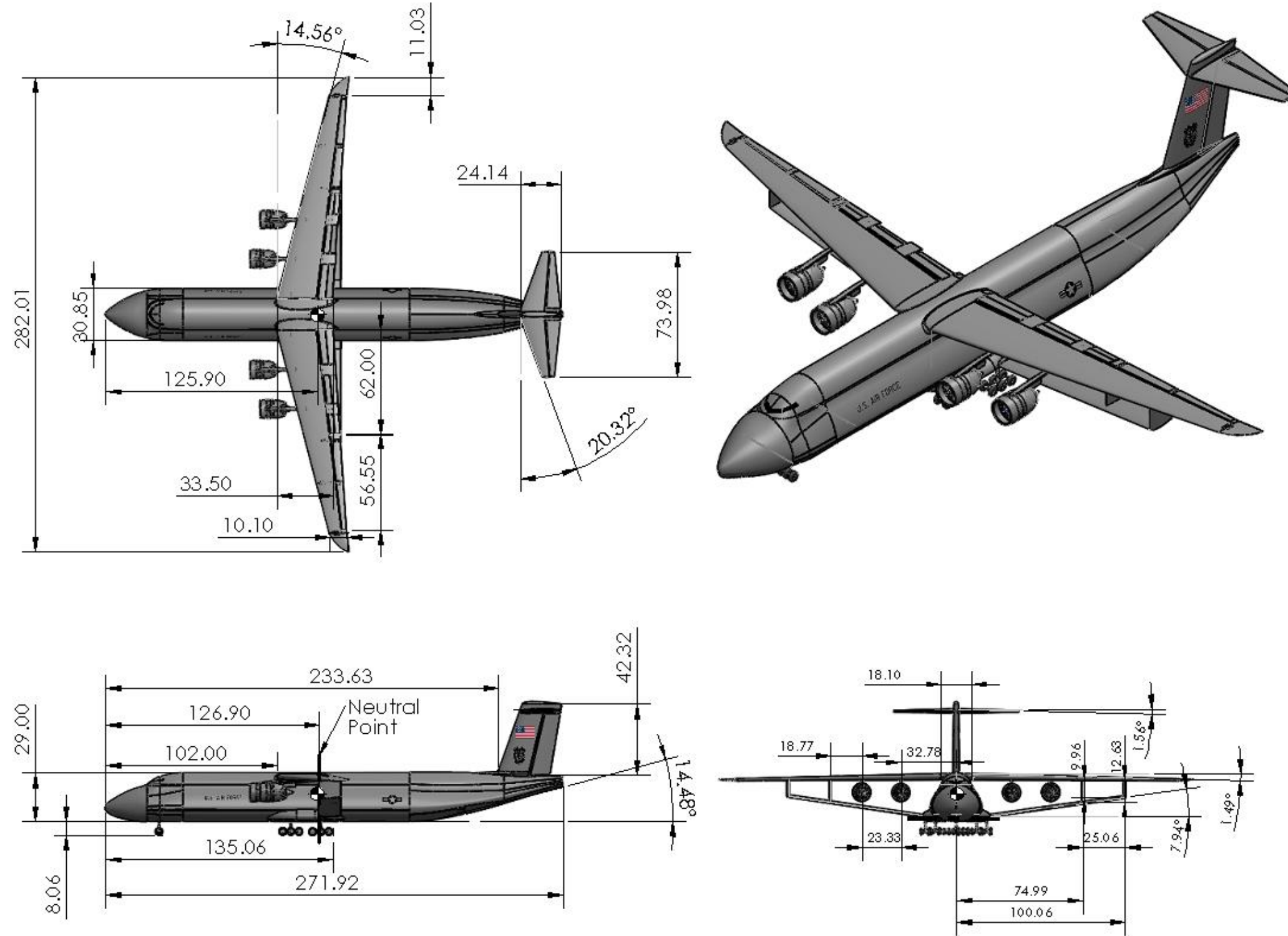|	Truss-Braced Wing	Wedge Nose	Tri-Jet
Maximum TOGW	1,080,000 lbs	1,210,000 lbs	1,240,000 lbs
Unit Cost (at down selection)	$289 million	$317 million	$319 million
MMH/FH	16.6	18.3	18.4

4. The PW-24 Harpy Configuration Design

Figure 10. Three-View Diagram of the PW-24 Harpy

4.1 Configuration Layout

The PW-24 Harpy is a 4-engine, wide-bodied aircraft whose identifying characteristic is its truss-braced wings. As shown in Figure 10, the Harpy's fuselage length is 272 ft, with a max fuselage width of 31 ft and fuselage height of 29 ft. Figure 11 shows the cross section of the fuselage.
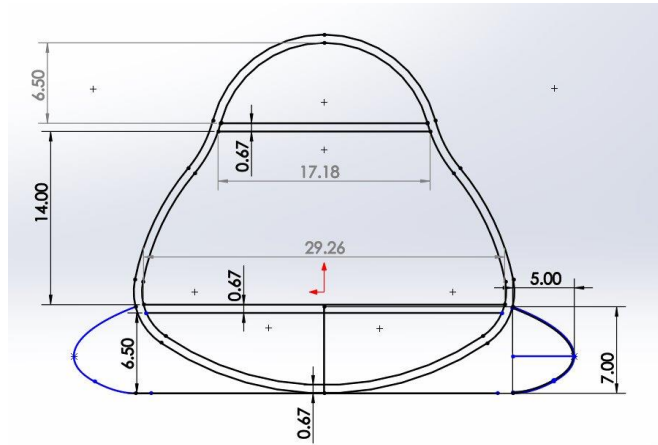
Figure 11. Cross section of the fuselage

As shown in Figure 11, the Harpy fuselage comprises three main sections. The lower section is 7 ft tall and has room for the landing gear when retracted, as well as the avionics bays and other subsystems. The middle section is 14 ft tall and houses the main cargo bay. The cargo bay stores pallets and oversized cargo, such as M1 Abrams tanks. The upper section is a second floor akin to that of the Lockheed C5 galaxy, the Airbus A380, or the Boeing 747. This second floor provides a separate paratrooper passenger bay. This section is 7 ft tall and also contains the flight deck, crew quarters, galley and bathroom, as well as environmental controls and the aircraft's auxiliary power units.

Figure 12 illustrates the internal layout of the aircraft's different configurations, while Figure 13 provides a cross section view. For center of gravity purposes outlined in Section 8, the main cargo bay is loaded as far back as possible, ending where the fuselage begins tapering. The pallets drove the required length of the fuselage. The pallets require about 120 ft of fuselage length, while every other configuration does not require as much space. The upper section is located directly behind the cockpit and offers paratrooper seating. The paratroops can walk down to the main cargo bay and head towards the aft ramp area where doors are located for quick paratrooper exit without any obstructions due to the nature of the cruciform T-tail design.
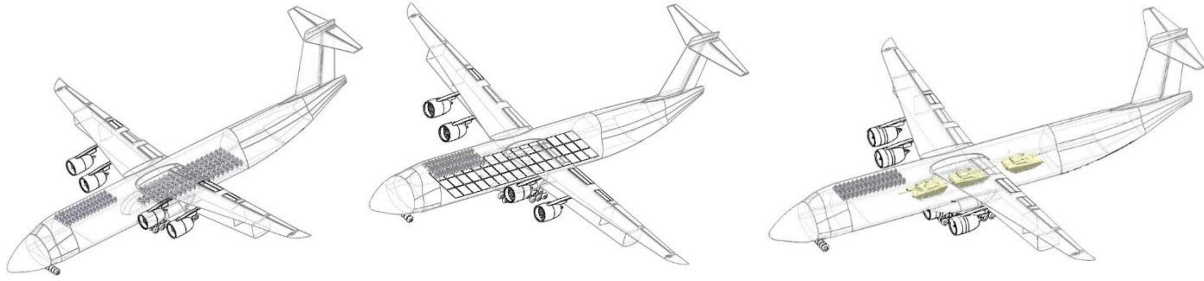
Figure 12. 330 Passenger Configuration (left), 48 463L Pallet Configuration (middle), Three M1 Abrams Tanks Configurations (right)
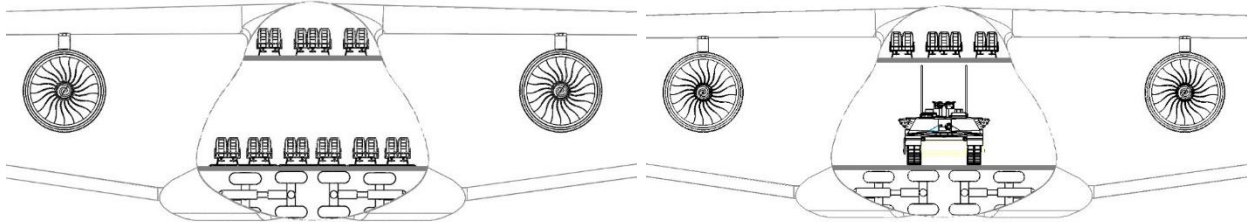
Figure 13. Cross section view of seating and pallet configuration (left) and of the tank configuration (right)

The left image of Figure 13 shows the cross-section view for the seating or palletized configuration. Because the 330 troop seats in the main cargo bay are attached to pallets, the loading layout for the seats and the pallets is identical. The right image in Figure 13 shows the tank configuration, and it is evident that the driver for the fuselage width was the pallet configuration. However, the driver for the main cargo bay height was the tank and oversized cargo configuration. The tanks are lined up in one row, while the pallets are lined up in three rows. The palletized seating thus seats twelve troopers across, with plenty of walking space between pallets. The upper deck sits seven across, in a 2-3-2 configuration with two aisles, similar to that of the Boeing 767 economy class layout. The width of aisles is 22 inches, while the seats have a 33-inch pitch, comparable to that of commercial airliner economy classes. These cross sections also show that the landing gear fits snugly in the lower compartment of the fuselage.

The Harpy's wings have a total wingspan of 282 ft, each wing equipped with an 11 ft long foldable wing tip, capable of folding down to a span of 260 ft, allowing the Harpy to operate out of ICAO Class F airfields without compromising on the performance benefits gained from a higher aspect ratio wing. Figure 14 provides a visual for the folding wingtip mechanism.
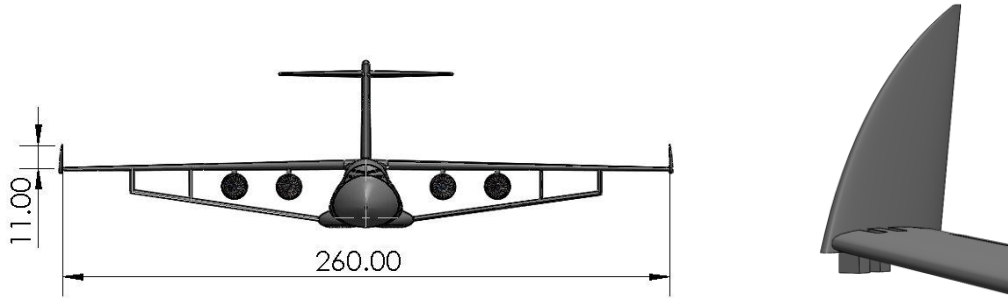
Figure 14. Wingtip effect on dimensions of wing (left) and a zoomed in view of wingtip mechanism (right)

The bottom of the Harpy sits at 8 ft above the ground, with provisions to kneel to a height of 18 in above the ground. The Harpy offers two loading locations, one at the aft and one at the front, with an opening ramp door and opening nose respectively. The nosecone is 25 ft long and opens above the flight deck to allow for front loading, while the aft ramp begins at the point at which the fuselage begins tapering, about 171 ft behind the nose. Figure 15 illustrates the loading capabilities of the Harpy.
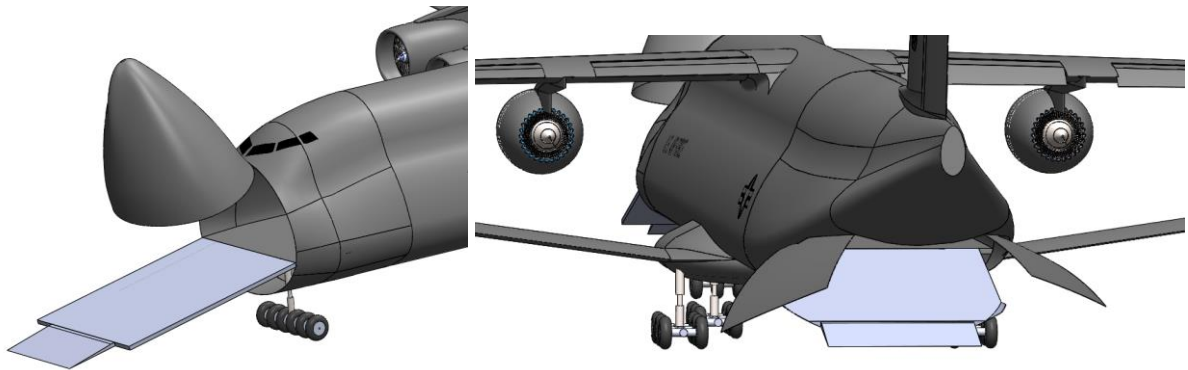
Figure 15. Forward loading depiction (left) and aft loading depiction (right)

5. Aerodynamics

5.1 Airfoil Section

The airfoil selection process for the PW-24 Harpy entailed effectively understanding its mission profile and necessities during flight. As per the RFP, the Harpy will have to cruise at speeds of up to Mach 0.82. This cruise condition is incredibly important, as it lies in the transonic regime. The transonic region

involves the creation of shock waves, thus increasing the amount of drag incurred over the airfoil. To combat this effect, supercritical airfoils were a necessary design feature. Because of their unique geometry, the supercritical airfoil allows flow to separate closer to the trailing edge, thus effectively decreasing the amount of drag induced over the top [14].

Due to the nature of the given mission, we chose four supercritical airfoils to analyze and determine which was best suited for the Harpy. These airfoils were the KC-135 Winglet, Lockheed-Georgia Supercritical Airfoil, NACA/Langley Symmetrical, and the Whitcomb Integral Supercritical Airfoil. Each of these has distinct differences, the most prevalent being the thickness to chord ratio. The t/c ratio was an important consideration when identifying the proper aerodynamic characteristics of the wing, its structural support, and its fuel capacity to be stored. Using the software XFLR5, characteristics such as CL and CD were identified for each airfoil and compared based on the angle of attack of the aircraft at a Reynolds number of 48.8 million simulating cruise conditions.

Figure 16. Coefficient of lift against aircraft angle of attack for each airfoil considered for the PW-24 Harpy
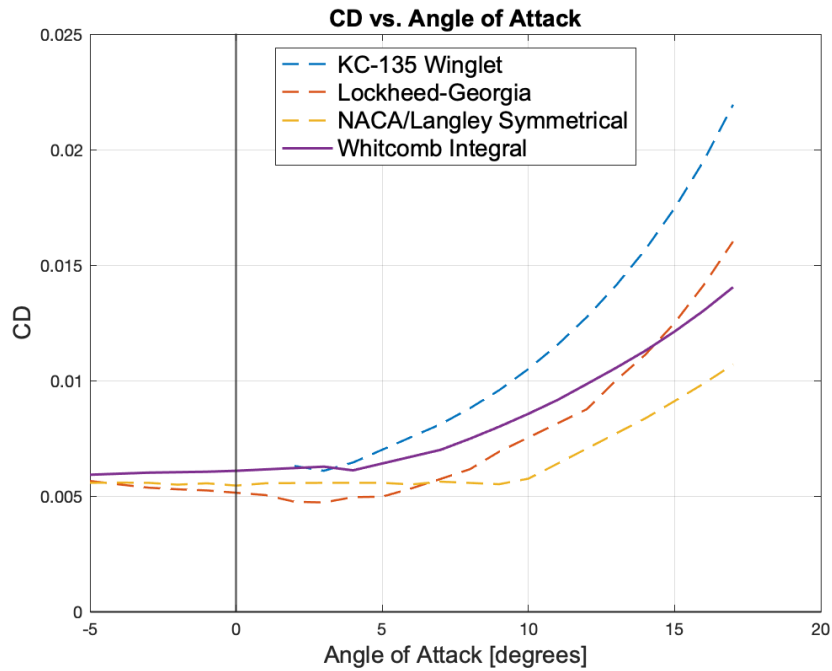
Figure 17. Coefficient of drag against aircraft angle of attack for each airfoil considered for the PW-24 Harpy
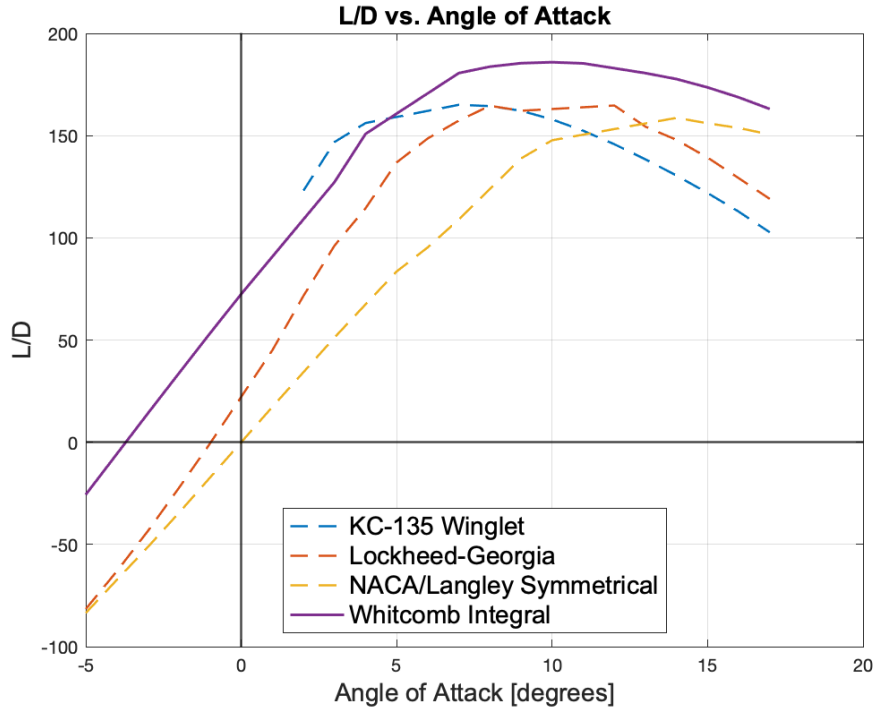
Figure 18. Lift over drag against aircraft angle of attack for each airfoil considered for the PW-24 Harpy
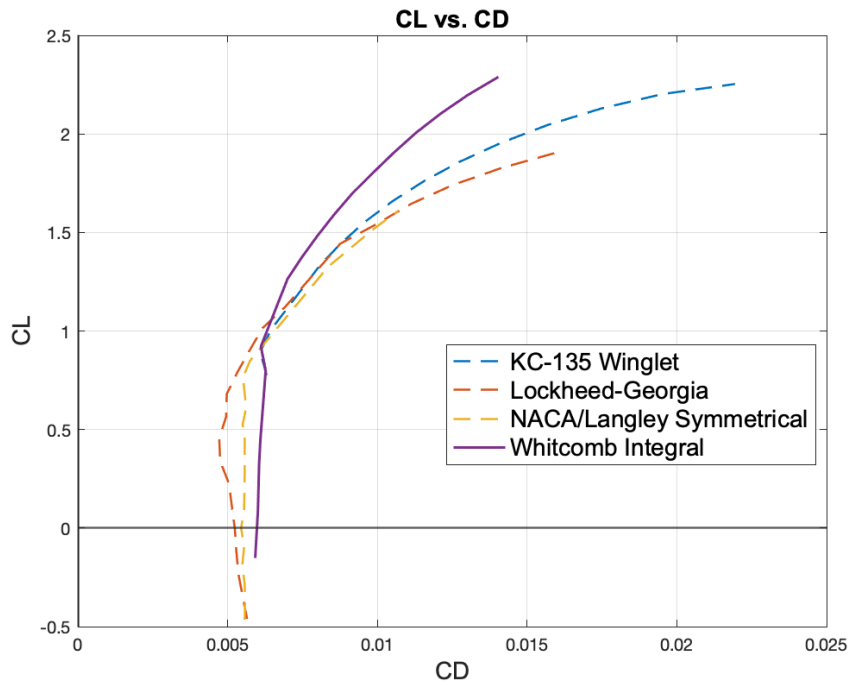
Figure 19. Coefficient of lift against coefficient of drag for each airfoil considered for the PW-24 Harpy

After analyzing the previous figures, we chose the Whitcomb Integral Supercritical Airfoil based on its ability to produce significantly higher CL v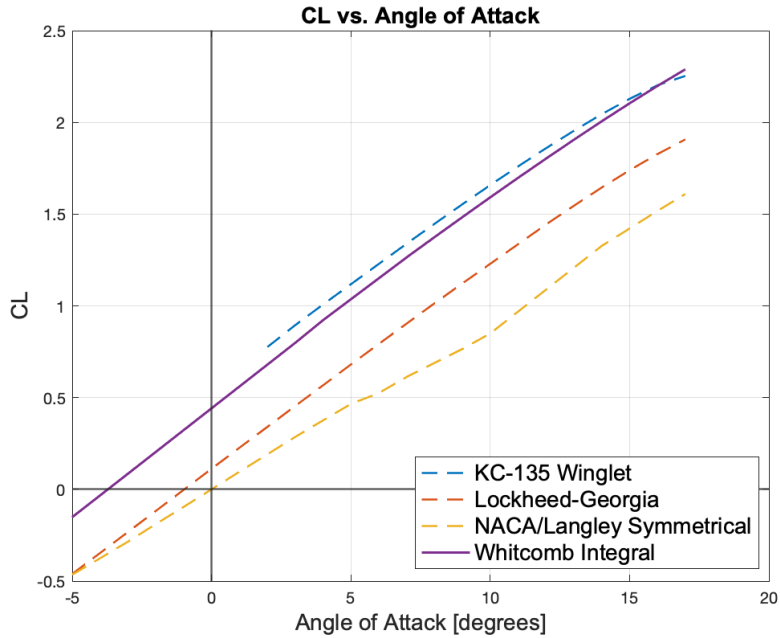alues compared to the other airfoils. Due to the heavy lift requirements of the PW-24 Harpy, the airfoil selected was needed to produce sufficiently large amounts of lift while also remaining relatively low on drag production. The Whitcomb fulfills both parameters at lower angles of attack with the given mission conditions. Finally, to complete the selection process, we computed the drag divergence Mach number (MDD). MDD is important to consider during aircraft design, as flying below the aircrafts MDD results in significantly lower drag counts [11]. These counts of wave drag increase exponentially once the MDD is reached, thus it is crucial to identify this number for the given airfoil. With the supercritical airfoil assumption, a t/c of 0.11, a sweep of 14.6 degrees, and a CL of 0.4 the following equation can be used to find an MDD of 0.8201, resulting in a significant drag reduction in cruise before Mach 0.8201. Equation 7 also allowed for the tradeoff study of identifying proper aircraft sweep and CL identification to satisfy the drag divergence Mach number conditions.

$$M_{DD} = \frac{\kappa_A}{\cos(\Lambda)} - \frac{t/c}{\cos^2(\Lambda)} - \frac{C_L}{10\cos^3(\Lambda)} \qquad (7)$$
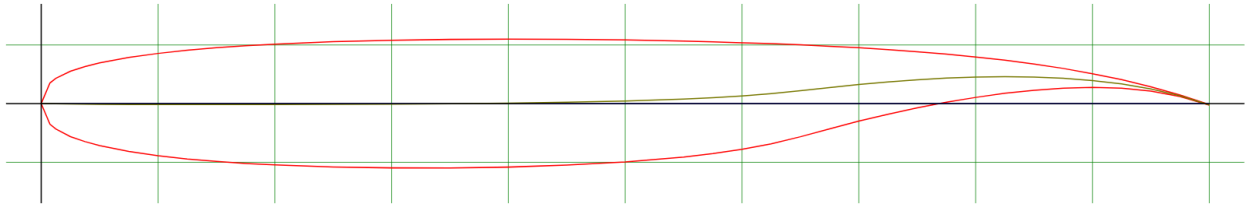
Figure 20. Profile of the selected Whitcomb Integral Supercritical Airfoil [15]

5.2 Wing Design

The PW-24 Harpy's wing design was an important step in the design process. Due to the plane's large cargo carrying capability, wing parameters were identified through the iterative process of takeoff gross weight estimation found in Nicolai [11]. Once historical estimations were inputted, design constraint plots could be formed highlighting the open design space for the aircraft. Because of the Harpy's truss-braced design, the wing's high aspect ratio of 13.7 allows for a reduction in induced drag resulting in an increase in efficiency.

Due to the nature of the Harpy's mission, increased efficiency was an important factor to consider when designing the dimensions of the wing. Another important design consideration was the storage of the massive aircraft. To comply with the ICAO Class F airport requirements, the PW-24 Harpy features foldable wing tips at a span of 260 feet, allowing for easy storage and maneuvering at a plethora of airports across the world. Boasting an unfolded wingspan of 282 feet and a sweep of 14.6 degrees, featured in the 3-View drawing, the Harpy is able to take off and carry massive loads huge distances all while remaining efficient in drag reduction and lift production during flight.

Table 10. PW-24 Harpy wing dimensions

Dimension	Size
Planform Area	5790 ft^2
Span (unfolded)	282 ft
Span (folded)	260 ft
Sweep	14.6°
Aspect Ratio	13.7
Taper ratio (ct/cr)	0.3
Tip Chord	10.1 ft
Root Chord	33.5 ft

5.3 Aerodynamic Characteristics

The aerodynamic characteristics of the PW-24 Harpy, such as CL, CD, and L/D were obtained using OpenVSP's VSPAero simulation utilizing a Vortex Lattice Method at steady level flight conditions. Figures 21 to 24 show the Harpy's estimated graphical polars with the outputted VSP data.
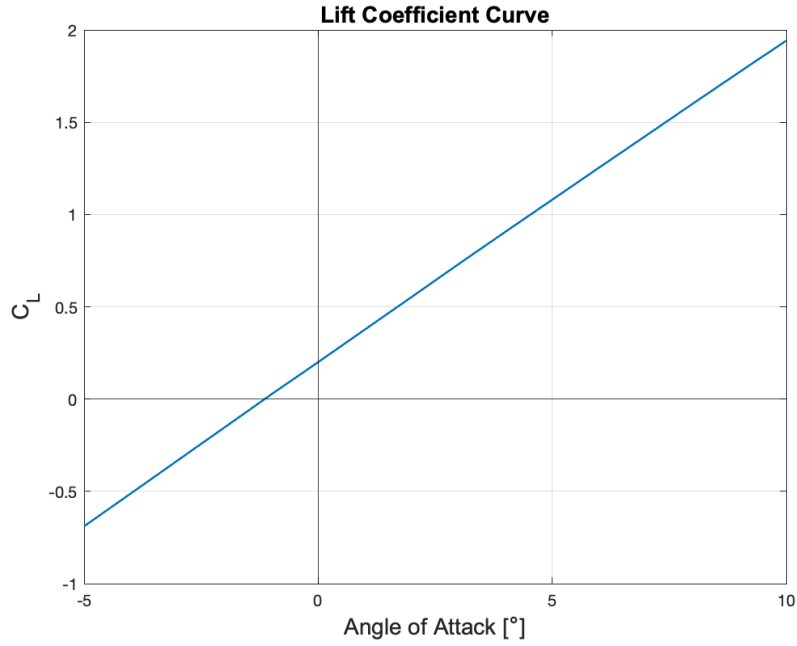
Figure 21. Lift coefficient curve outputted using the aircraft's geometry in OpenVSP
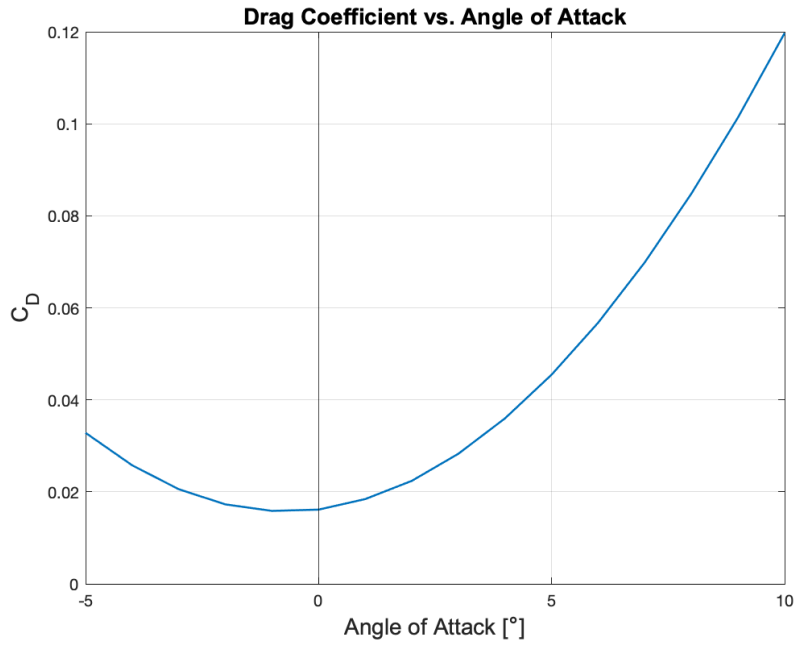
Figure 22. Coefficient of drag curve
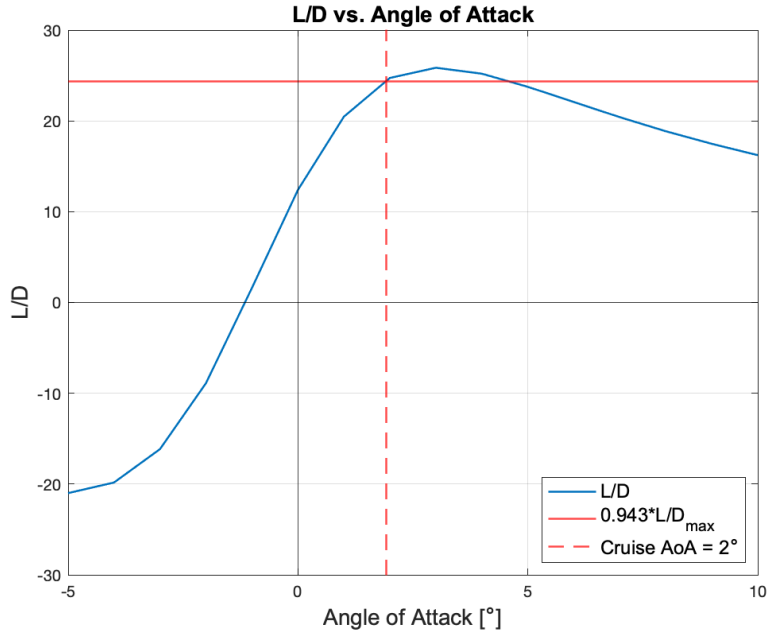
Figure 23. L/D vs. angle of attack, indicator at cruise angle of attack, at cruise M = 0.8
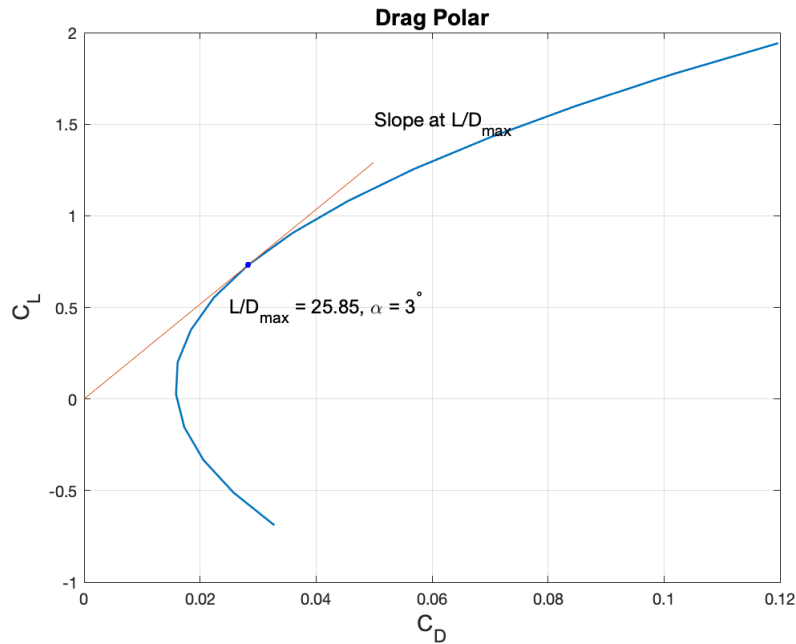
Figure 24. Drag polar outputted with OpenVSP, featuring L/D max and its slope

To ensure the most efficient cruise, the Harpy operates at constant throttle for maximum jet range, proven to be 94.3% of the maximum L/D [11]. This allows the cruise angle of attack to be identified at 2 degrees with a CL of 0.55, CD of 0.022, and an L/D of 24.4.

33

5.4 High Lift Devices

The high lift devices, with a CL of greater than 2.3 were necessary for takeoff and landing. To achieve C_{Lmax} of 2.3, double slotted trailing edge fowler flaps were selected. Fowler flaps feature the ability to extend the surface of the wing and continually curve down. The Harpy wings also include 20% Full span leading edge slats, these leading-edge slats curve down allowing for an increase in lift during takeoff and landing.

The next step in maturing the Harpy's high lift devices was identifying a flap deflection angle. These angles can vary from anywhere between 10 and 50 degrees based on certain flight conditions. In order to achieve the desired CL for takeoff and landing, the Harpy uses a takeoff flap deflection angle of 15 degrees and a landing flap deflection angle of 40 degrees. These angles provide enough lift for the massive payload carried by the Harpy while remaining below the typical region that drastically increases drag. Accounting for both leading edge slats and trailing edge flaps, the CLmaxes for takeoff and landing are 2.4 and 2.8 respectively, based on the process outlined in Chapter 9 of Nicolai [11].

In order to visualize these flap deflection angles with the selected Whitcomb airfoil, XFLR5 was used to import the flaps and slats and identify how the airfoil adjusts during takeoff and landing. Due to limitations in the XFLR5 software, only basic hinge flaps are capable of being displayed, however the sizing of the flaps remains the same as seen in Figures 25 and 26. The dimensions presented include a flap chord to wing chord ratio of 30%, resulting in the position of the trailing edge flaps hinge at 70% of the chord and the leading-edge slats hinge at 20% of the chord.
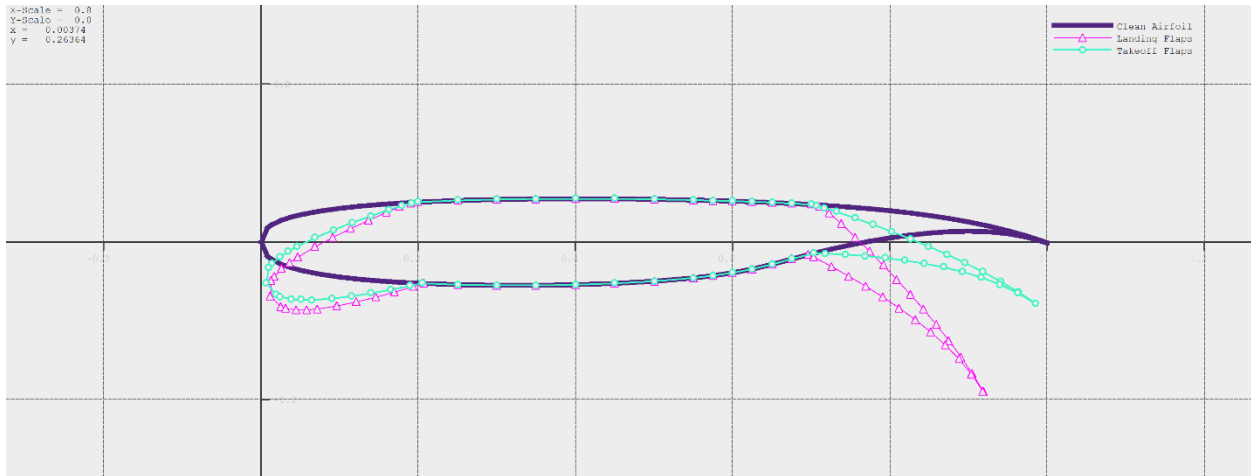
Figure 25. Cross section view of XLFR5, showing off different leading edge and trailing edge flap angles
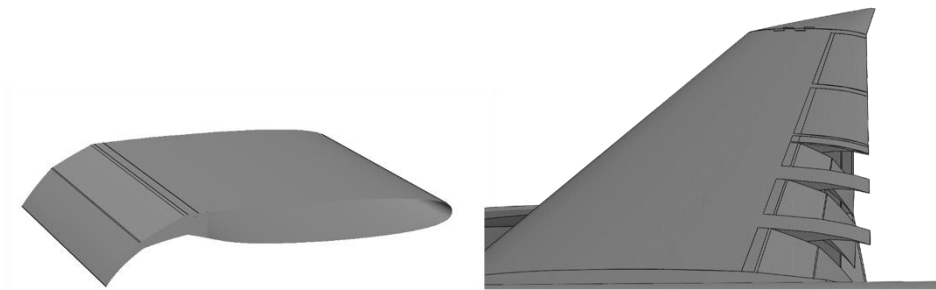
Figure 26. Double slotted Fowler flaps present on the Harpy
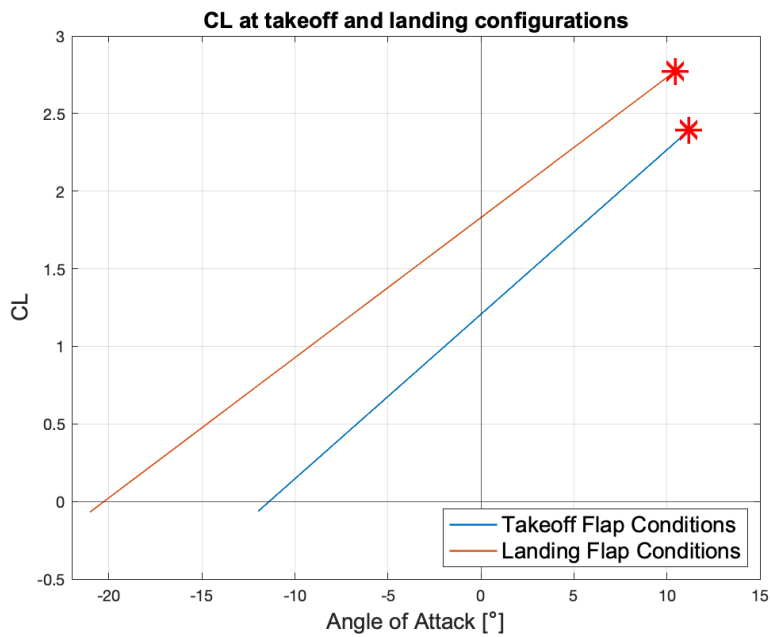
Figure 27. CL vs. Angle of Attack for flapped takeoff and landing conditions

Table 11. PW-24 Harpy takeoff and landing conditions

Takeoff and Landing Conditions	Value
Flap Deflection Angle (Takeoff)	15 degrees
Flap Deflection Angle (Landing)	40 degrees
CLmax (Takeoff)	2.4
AoA stall (Takeoff)	11.2 degrees
CLmax (Landing)	2.8
AoA stall (Landing)	10.7 degrees
cf/c (flap to chord length)	0.3

5.5 Drag Analysis

To calculate the parasitic drag buildup of the PW-24 Harpy, OpenVSP's parasite drag analysis was utilized. To reduce computation time the main components of the aircraft were utilized as the reference geometry including the fuselage, wings, truss, stabilizers, jury strut, and engines. The truss plays an important role in the reduction of drag due to the fact that the wing can be lighter with the increased support from the truss and jury strut. The parasite drag software utilizes the Blasius and Schlichting compressible equations to solve based on the given conditions. The model was run at cruise conditions of 774 ft/s and 37,000 ft. Finally, in order to account for 'real-life' effects, excrescence drags were estimated and added to the final CD0 calculation. Examples of these low types of drag include a fueling probe, angle of attack indicator, and a pitot tube, all of which were adapted from Roman [16] and can be seen in Table 12.

Table 12. Parasite drag build up summary

Component	Swet (ft^2)	CD	% Total
Fuselage	21,200	0.00669	31.57%
Wings	8,940	0.00456	21.49%
Truss	5,580	0.00317	14.94%
Horizontal Stabilizer	2,240	0.00118	5.58%
Vertical Stabilizer	2,150	0.00110	5.17%
Duct (out)	1,970	0.00095	4.47%
Duct (in)	1,960	0.00095	4.46%
Jury Strut	488	0.00028	1.34%
Nacelle (in)	206	0.00011	0.53%
Nacelle (out)	186	0.00010	0.48%
Excrescence	~	0.00211	10%
Total CD0	~	0.02120	100%

To continue approximating relevant drag produced by the Harpy, more counts of drag were identified including induced drag, leakage drag, trim drag, and finally flap drag. Induced drag can be identified as a

function of CL, AR, and efficiency factor, as seen in NASA documents [17]. Additionally, trim drag can be approximated as 10% of induced drag per Nicolai [11] and leakage drag can be estimated as 5% of the total parasitic drag. Finally, flap drag can be calculated utilizing the techniques seen in Nicolai chapter 9 [11], using functions of deflection and flap reference area.

Table 13. Total coefficient of drag calculation

Drag Parameter	Value
CD0 (parasite)	0.0212
CDi (induced)	0.0106
CDleak (leakage)	0.00106
CDtrim (trim)	0.00106
CDtot (unflapped)	0.0339

Table 14. Total drag coefficient during takeoff and landing flap conditions

Drag Parameter	Takeoff	Landing
Delta CD flapped	0.0254	0.0637
CDtot unflapped	0.0339	0.0339
CDtot flapped	0.0593	0.0976

5.6 Truss-Braced Wing

With the large-scale cargo load specified in the RFP, the PW-Harpy required innovative design techniques and implementation in order to achieve its current carrying power. Truss braces provide an increase in structural integrity within the wing, allowing for the implementation of a high aspect ratio. Because of this support, the wing of the aircraft can be longer and thinner, reducing the weight of the wing and effectively increasing its efficiency. This reduction in total wing area results in a decreased induced drag during flight, enhancing the performance of the aircraft making it ideal for long-range, heavy-cargo missions. Featuring a NASA SC(2)-0012 airfoil section, the sizing of the truss, as seen in Figure 28, was determined using concepts seen in the University of Michigan's published research regarding truss optimization for aircraft [18]. Further analysis of the structures behind the truss can be seen in a later section of this report.
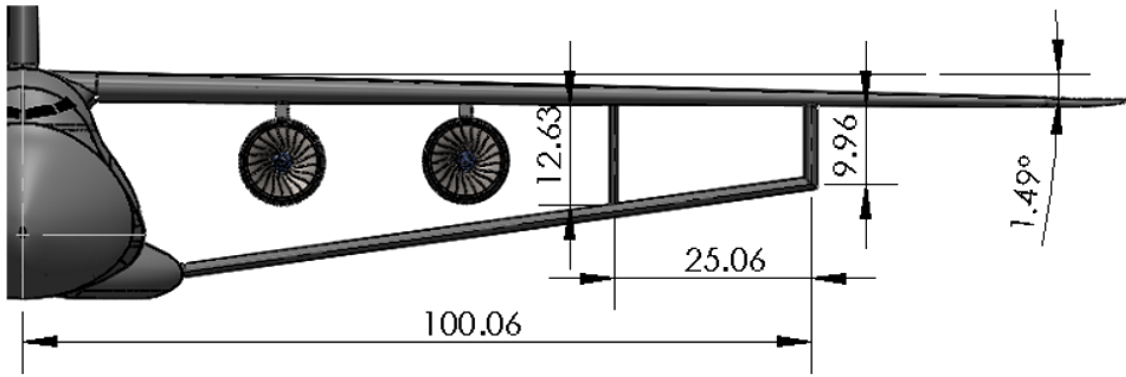
Figure 28. Dimensions of the truss brace used on the PW-24 Harpy

6. Propulsion and Performance

6.1 Engine Selection

6.1.1 Design Approach

The PW-24 Harpy is powered by four ultra-high bypass ratio turbofan Rolls-Royce Trent 1000-J2 engines. Each engine is capable of producing a total maximum takeoff thrust of 78,100 lbf and a maximum sustained thrust of 73,800 lbf [19]. This results in a total max takeoff thrust of 313,000 lbf and sustained thrust of 295,000 lbf for the Harpy. This maximum sustained thrust, in conjunction with our maximum takeoff weight of nearly 1.08 million pounds, results in a thrust loading of 0.275 for the Harpy. Shown in Figure 29 is the CAD model of the Rolls-Royce Trent 1000-J2 with the engine casing.
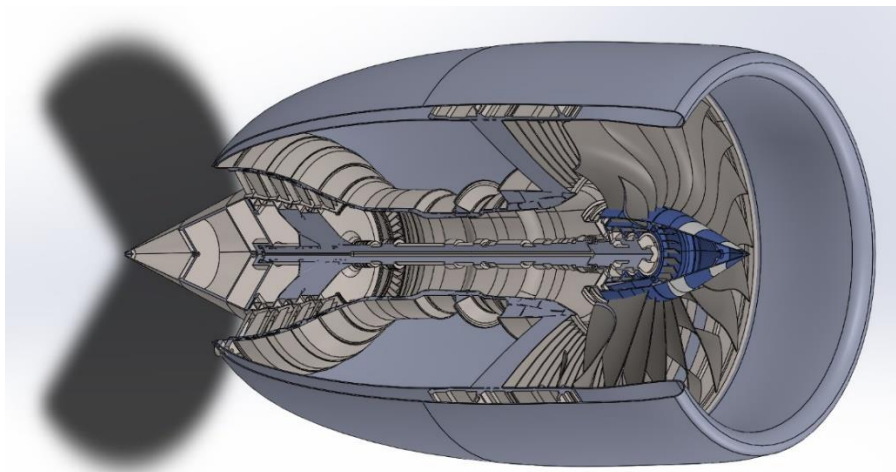
Figure 29. Rolls Royce Trent 1000-J2 CAD Model

6.1.2 Trade-off Studies

Our main considerations while selecting our aircraft's engines were meeting performance requirements and our measures of merit: reducing weight, cost, and environmental impacts. Initial aircraft sizing yielded a requirement of a thrust loading of slightly more than 0.25 and an initial takeoff thrust per engine requirement of 68,700 lbf, however refinements in our weights, aerodynamics, and thrust installation losses yielded a final takeoff thrust requirement per engine of 77,000 lbf. In selection of our engine, multiple options were taken into consideration, such as the GEnX-1B75 engine made by General Electric. A numerical comparison of useful engine parameters between the GEnX-1B75 and the RR Trent 1000-J2 engine are shown in Table 15 below. As can be seen, the Trent 1000-J2 beats out the GEnX-1B75 in maximum takeoff thrust, weight, efficiency, and estimated cost. Additionally, the Rolls-Royce Trent 1000 series incorporates bleedless engines, thus decreasing installation losses [20].

Table 15. Engine Parameters Comparison [19], [21], [22], [23], [20]

Engine	RR Trent 1000-J2	GEnX-1B70
Static Thrust	73,800 lbf	66,500 lbf
Fan Diameter	112 in	111.1 in
Weight	13,110 lbs	13,550 lbs
TSFC	0.506 lb/lbf/hr	0.5279 lb/lbf/hr
Bypass Ratio	11.0	9.0
Overall Pressure Ratio	52:1	58.1:1
Estimated Cost	$16.25 million	$17.9 million

6.2 Safety Considerations

The PW-24 Harpy's propulsion system is sized to ensure that it meets the takeoff and landing performance requirements set in the RFP, which include a balanced field length no longer than 9,000 feet. Should the PW-24 Harpy lose an engine during takeoff, it is recommended that the pilot abort the landing and immediately apply brakes if they are below the decision speed, V1, or continue to takeoff should they have exceeded the decision speed, which is outlined in the takeoff and landing analysis section of this report.

6.3 Engine Placement

Each engine on the PW-24 Harpy is placed two fan diameters ahead of and one fan diameter beneath the leading edge of the wing, as suggested by Raymer [24]. This is standard for large cargo aircraft such as the

C5-Galaxy and the Boeing 747, both of which have nearly this exact configuration. This placement is designed to reduce the installation losses due to interactions between the wing and the engine. Furthermore, this placement also ensures that the engines are sufficiently far from the truss so as not to cause any aerodynamic or structural complications.

Similarly, each wing carries two engines which are spaced 2.5 fan diameters (280 in.) and are slightly more than three fan diameters (395 in.) from the fuselage. This placement is selected such that interference drag between the engines is minimized [11]. The placement of the engines with respect to the rest of the wing-truss configuration is shown in Figures 30 and 31.
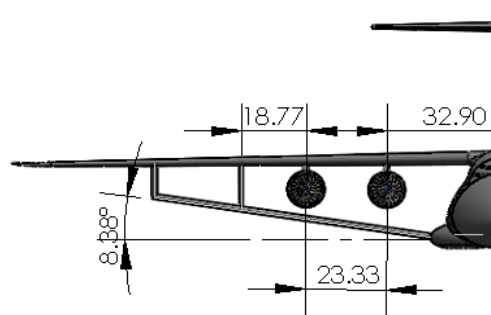
Figure 30. Front view engine placement diagram
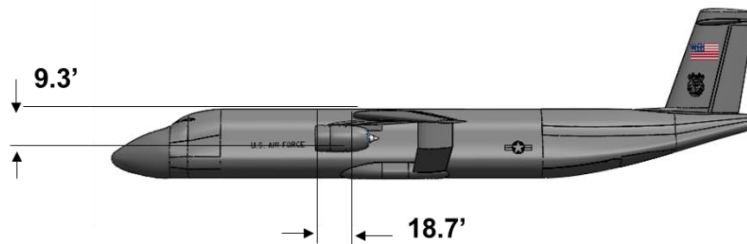
Figure 31. Front view engine placement diagram

6.4 Inlet and Nozzle Design

The inlet casing of the RR Trent 1000-J2 was designed to maximize the capture area during the optimal cruise speed of Mach 0.8. The casing has an outer inlet lip radius equal to 4% of the fan diameter, and the inner inlet lip has a radius of 8% of the fan diameter. Furthermore, the upper surface of the inlet casing has a 10 degree decline and the inlet face is angled 2 degrees downward to account for the angle of attack during

cruise, ensuring the flow aligns with the inlet face. A diagram of the inlet casing is shown in Figure 32. This inlet results in a mass flow rate of 2,760 lb/s [25]. A fixed convergent nozzle was chosen for the nozzle exit shape to minimize weight and manufacturing complexity. The nozzle exit area to capture area ratio was calculated to be 0.7 to maximize cruise efficiency, in accordance with suggestions from Raymer [24].
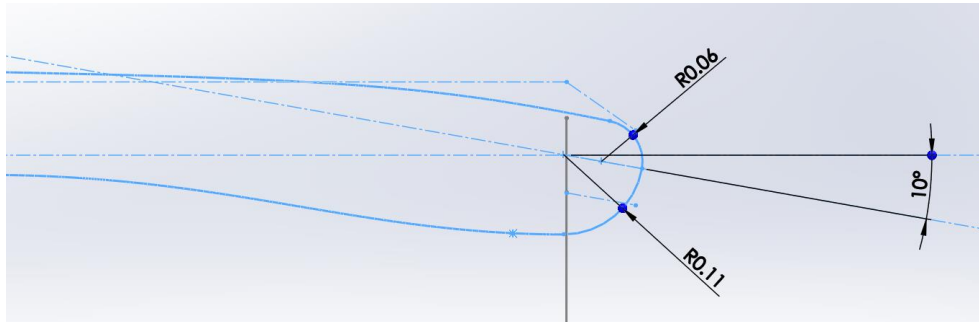
Figure 32. Inlet Casing Profile Diagram

6.5 Engine Properties

The performance characteristics of the Trent 1000 series engines are not publicly available, and therefore must be estimated using the equations in Raymer [24]. The thrust per engine as a function of the altitude is shown in Figure 33. The continuous thrust per engine at the cruising altitude becomes 21,300 lbf, which is more than sufficient to overcome the total cruise drag of 17,000 lbf. The installation losses were estimated to be approximately 8% using Nicolai [11] and are accounted for in the takeoff/landing and payload range performances, as shown in the subsequent Section 6.7.
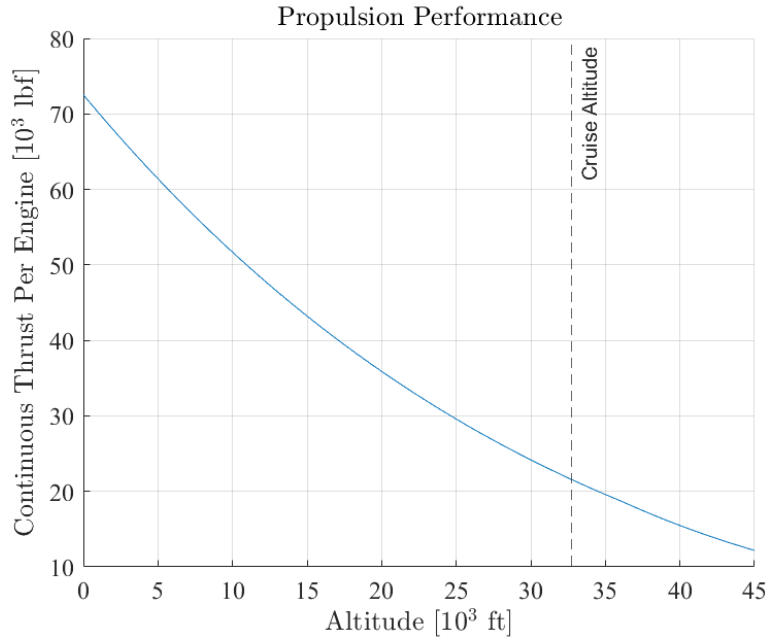
Figure 33. Propulsion performance with altitude

6.6 Takeoff and Landing

The PW-24 Harpy is designed to operate in ICAO Class F and Class E airports, utilizing current logistical structures. Additionally, it is designed to operate from airports with a minimum runway size of 9,000 ft. x 150 ft. on an ISA +15 degree Celsius day at sea level conditions. Furthermore, to satisfy MIL specifications, the Harpy must clear a 50 ft. obstacle on takeoff conditions [24]. The parameters used in calculating the takeoff and landing field lengths are shown in Table 16. A typical takeoff and landing profile is shown in Figure 34.

Table 16. Relevant takeoff and landing parameters

Parameter	Value
TOGW	1,078,000 lbs
Thrust Per Engine	78,100 lbf
S	5,790ft^2
Maximum CL with TO/LD flaps (15/40 deg)	2.4 / 2.8
Takeoff Lift/Drag Coefficient	1.26 / 0.0912
Landing Lift/Drag Coefficient	1.93 / 0.196
Stall Speed for TO/LD	151 / 131 kts
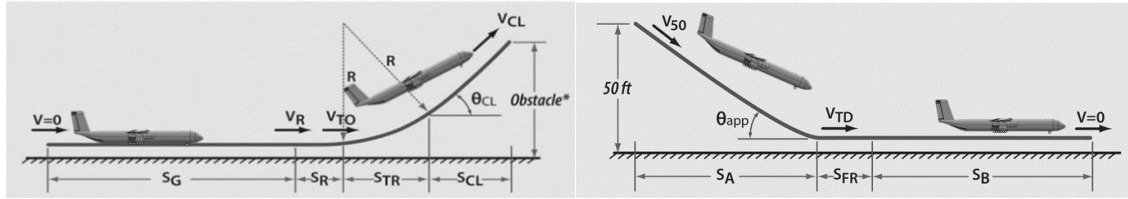
Figure 34. Takeoff and landing profiles

The PW-Harpy is able to achieve a maximum takeoff distance of 8,370 ft. and a maximum landing distance of 6,820 ft. in wet runway conditions. Furthermore, the balanced field length for the wet runway condition is 8,960 ft. for the maximum takeoff weight condition. The calculated takeoff and landing field lengths for the maximum load condition on a wet runway are shown in Table 17.

Table 17. Takeoff and landing field lengths

Takeoff Parameter	Value	Landing Parameter	Value
V_{TO}	167 kts	V_{50}	170 kts
V_{CL}	182 kts	V_{TD}	150 kts
S_G	6,270 ft	S_A	954 ft
S_{TR}	1,340 ft	S_B	5,110 ft
θ_{CL}	14.1 deg	θ_{app}	3 deg
Takeoff Field Length	8,370 ft	Landing Field Length	6,820 ft

The balanced field length was found by iteratively solving for the intersection between the acceleration stop and acceleration go curves given different decision speeds, V1. If the speed of the aircraft during an engine failure exceeds the V1 decision speed the pilot should continue their takeoff, whereas if the speed of the aircraft is less than the decision speed, the pilot should abort the takeoff and immediately apply the brakes. The balanced field length is the runway length needed to reach the V1 decision speed and either continue the one-engine-out takeoff or abort the takeoff. For dry runway conditions, the balanced field length was calculated to be 8,630 ft. with a decision speed of 145 kts. (244 ft/s); for wet runway conditions, the balanced field length was calculated to be 8,960 ft. with a decision speed of 145 kts. (245 ft/s). The acceleration stop and acceleration go curves are plotted as a function of the decision speed for both the dry and wet runway conditions in Figure 35.
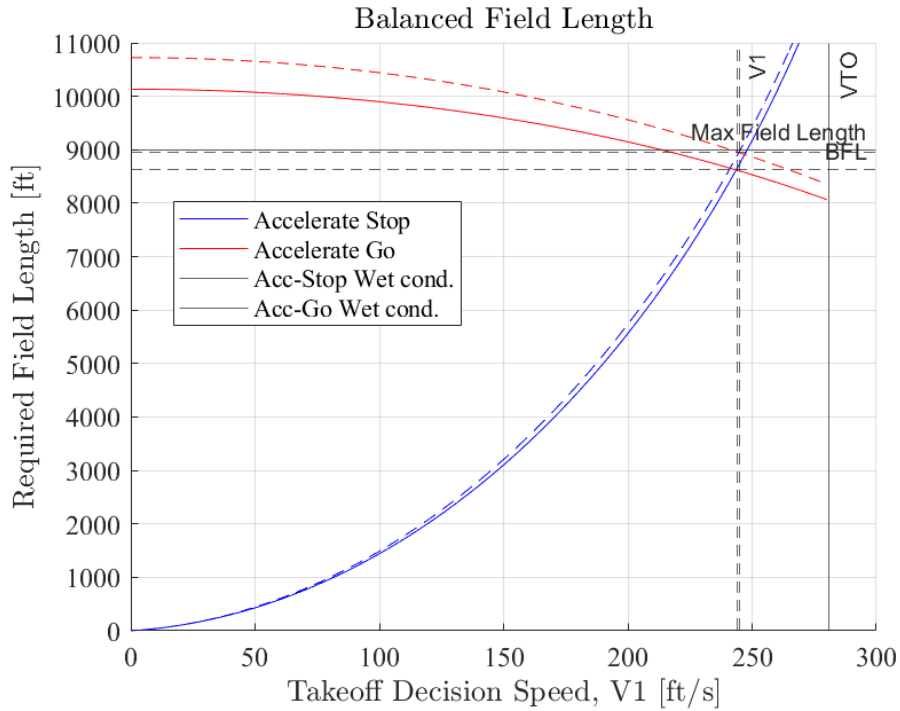
Figure 35. Balanced Field Length for dry (solid) and wet (dotted) runway conditions

6.7 Range

The PW-24 Harpy is required to be able to perform three different unrefueled missions with differing payload and range requirements. The RFP defines an 8,000 nmi ferry mission (no payload), a 5,000 nmi mission capable of carrying 295,000 lbs of payload, and a 2,500 nmi mission capable of carrying 430,000 lbs of payload. The range for each load configuration can be calculated using the fuel fractions for each mission segment, the results are shown in the payload-range diagram shown in Figure 36. Each load configuration mission is plotted along with the maximum range for a given payload. The maximum range curve is limited by the maximum payload limit, the maximum takeoff weight limit of 1.11 million lbs, and the maximum fuel capacity limit of the Harpy.
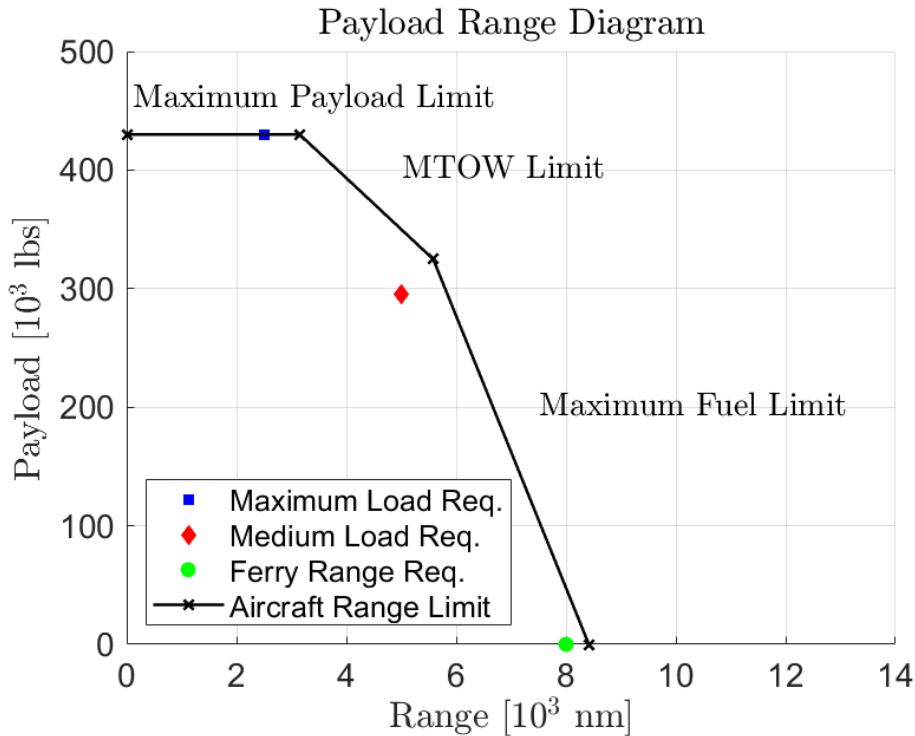
Figure 36. Payload range diagram

6.8 Cruise

The RFP dictates that the PW-24 Harpy has a cruise altitude between 31,000 and 43,000 ft and between a speed of Mach 0.8 and 0.82. The PW-24 Harpy has an optimum cruise at a speed of Mach 0.8 and an altitude of 33,000 ft. The drag divergence Mach number of the Harpy is 0.8205, allowing for the required maximum cruise speed of 0.82 to be met. Additionally, the four Trent 1000-J2 engines powering the Harpy are more than sufficient to allow the Harpy to reach the maximum service ceiling of 43,000 ft. as shown in the propulsion performance section of this report. A table of the applicable cruise performance parameters are shown in Table 18 below.

Table 18. Cruise Parameters

Parameter	Value
Optimum Cruise Speed	Mach 0.8
Maximum Cruise Speed	Mach 0.82
Altitude	33,000 ft
Angle of Attack	2°
L/D	24.4
CD_{tot}	0.0339

6.9 Emissions

Emissions are an important factor to consider in the manufacturing and operation of any large transportation project. The following analysis seeks to inform customers and consumers of the environmental impacts of the Harpy and outlines factors that contribute to greenhouse gas emissions. This analysis breaks down the emissions of this aircraft into CO_2 released during manufacturing and CO_2 released during operations. Calculations were done using production runs of 90, 180, and 270 aircraft, with total CO_2 production being shown in Figure 37.

Metal manufacturing produces a significant amount of carbon dioxide. To find the figure for amount of CO_2 produced per aircraft manufactured, the percentage of each material used to construct a Harpy was estimated which corresponds to the amount of each material that needs to be manufactured. Based on the weight analysis of the Harpy, 95% of its empty weight is made from high-grade aluminum, while 5% of its empty weight is made from steel. Other materials used in construction are absorbed into the weight of the aluminum. Currently, 9.2 pounds of CO_2 are produced per pound of high-grade aluminum manufactured, and 4.0 pounds of CO_2 are produced per pound of steel manufactured [26]. These figures were used to calculate the amount of CO2 produced per aircraft, which was 1940 tons.

Despite manufacturing producing a significant amount of CO_2, the operation of a Harpy produced significantly more due to the sheer amount of fuel needed for each flight. This aircraft burns 5250 gallons of fuel per flight hour and flies 1200 flight hours per year for a total service life of 40000 flight hours. Jet fuel produces 27 pounds of CO_2 per gallon of fuel burned [26]. Using these values each aircraft produces 71 tons of CO_2 per flight hour or 85000 tons of CO_2 per year. These are necessary figures to allow an aircraft of this scale to operate consistently and complete its mission. It is important to note that the Trent 1000-J2 engines have been approved for use by the FAA and meet all FAR 25 certification requirements [27]. A summary of the lifecycle CO_2 emissions is shown in Figure 37.
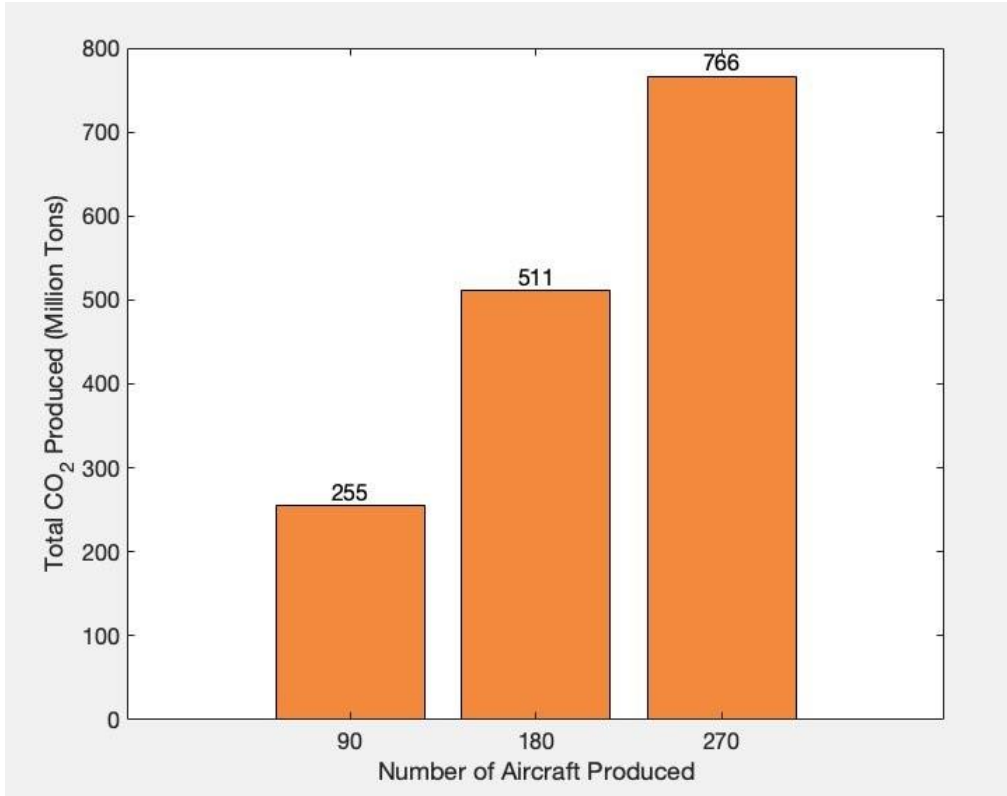
Figure 37. Lifecycle CO2 emissions for various production runs of the PW-24 Harpy

6.10 Acoustics

Noise emissions for the PW-24 Harpy were calculated to ensure the aircraft meets FAA and ICAO standards. An acoustic analysis of the aircraft was conducted for three different conditions: Take-off, cruise, and landing approach. The primary noise emissions of the aircraft were identified to be from the airframe and the engines. The methods used to calculate the overall sound pressure level emitted from these sources are described in Filippone, Chapter 17 [28]. To simplify the calculations made in this section, all aircraft parameters were converted to their metric system equivalents. All sound pressure levels were found at the aircraft's maximum take-off gross weight. For humans, the threshold of hearing occurs at 20 micro-Pascals which correlates to a reference sound intensity of 1×10^{-12} Watts per meter squared. This value was used as the reference intensity for all sound pressure level calculations.

Airframe noise, specifically wing noise, is a significant contributor to acoustic emissions. Filippone shows that this noise is dependent on freestream velocity, weight, altitude, the coefficient of lift, and atmospheric conditions in equation 17.10 [28]. During landing, the Harpy approaches at 87.4 meters per

second with a lift coefficient of 2.8. At the required altitude of 121.5 meters and standard sea level conditions, the airframe sound pressure level is found to be 71.0 dB. The airframe noise at cruise and take-off is found using the same method with necessary adjustments to altitude-dependent conditions. At cruise, the Harpy flies at an altitude of 10060 meters at 239 meters per second with a lift coefficient of 0.827, giving a sound pressure level of 53.9 dB. During takeoff, the air speed is 85.6 meters per second with a lift coefficient of 2.4. Sound is measured at an altitude of 300 meters. The sound pressure level at take-off from the airframe was found to be 52.0 dB

The four Trent 1000-J2 engines providing the thrust for the Harpy also produce a significant level of noise. Engine noise is dependent on the jet velocity, average speed of sound in the jet, jet mass flow rate, altitude of measurement, and atmospheric conditions, as shown in equation 17.19 in Filippone. For all conditions, the mass flow rate of the jet is 1210 kilograms per second. The jet velocities for approach, cruise, and take-off are 374, 310, and 357 meters per second, respectively. The average speed of sound in the jet was found for each condition by dividing the jet velocity by the local Mach number. The altitudes were taken to be the same as the previous section. This yielded sound pressure levels of 35.0, 40.6, and 30.2 dB for approach, cruise, and take-off conditions, respectively.

The overall sound pressure level for the aircraft at the listed conditions were determined by logarithmically adding the sound pressure levels from the air frame and engines. These are summarized in Table 19. These sound pressure levels fall within FAA and ICAO standards.

Table 19. Overall sound pressure level for the PW-24 Harpy at several flight conditions

Flight Condition	Measured Altitude (ft)	Overall Sound Pressure Level (dB)
Take-Off	400	52.1
Cruise	33,000	54.6
Landing Approach	1,000	72.0

7. Stability and Control

7.1 Empennage

The empennage is modeled after a standard T-tail configuration for the PW-24 Harpy. The decision was made after considering multiple designs including other cruciform and conventional horizontal stabilizer

options. The T-tail was selected for the best longitudinal stability performance of the options as well as the ability to locate the horizontal tail as far away from the wing's wake as possible. This is especially important when considering the added wake and drag that the truss would create behind the wing, reducing the horizontal stabilizer's effectiveness. The leading edge of the root chord of the vertical stabilizer is located 233 ft behind the tip of the nose and is placed by performing a static stability analysis of the CG location, static coefficients, and static margin. Iterating through different placements of the tail using analysis done in VSPAero led to the chosen location. The location of the empennage is also depicted in Figure 10.

7.1.1 Vertical Tail

The initial sizing of the vertical stabilizer was performed using the tail volume coefficient method. Initially the vertical tail volume coefficient was selected based on historical data of aircraft with similar characteristics and intended uses. A more refined approach was then used using the necessary requirements for the dynamic stability and rudder sizing needs, specifically the OEI and sideslip conditions. The minimum required surface area under these conditions for the vertical stabilizer is the OEI rudder only condition, which resulted in the vertical stabilizer area of 1,110 ft^2. The maximum rudder deflection angle used for the analysis was ± 30°. Initially based on historical data, this was confirmed by rudder analysis in Part 7.2.2 for extreme circumstances such as two engine out. Table 20 gives the characteristics of the vertical stabilizer and Figure 38 gives the side view with dimensions. All values were compared and follow typical values of aircraft in a similar class. The airfoil for the vertical stabilizer is the NASA SC(2)-0012. This is chosen as the supercritical airfoil is designed to handle the transonic speeds that the plane will experience at cruise conditions. It is also symmetric so there is no side force or moment generated during flight from the airfoil's shape.
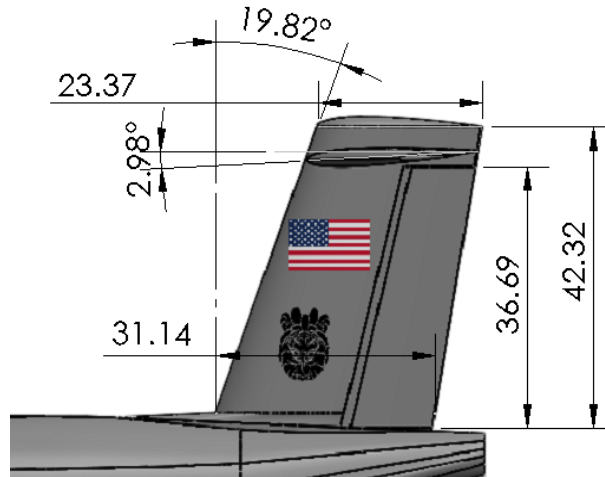
Figure 38. Vertical Stabilizer

Table 20. Vertical Stabilizer Parameters

Vertical Stabilizer	
Planform Area	1,109 ft^2
Chord	27.2 ft
Height	40 ft
Aspect Ratio	1.5
Tip Chord	23.1
Root Chord	30.8

7.1.2 Horizontal Tail

Like the vertical tail, the horizontal tail was initially sized using data of planes with similar profiles in [24] using the horizontal tail volume coefficient. A more accurate analysis was done then using scissor plots shown in Figure 39. The limits are computed using the neutral point from VSPAero and forward CG location from [29]. The scissor plots are computed using calculations presented by [30]. Comparing the tail volume coefficient with required maximum and minimum center of gravity locations, Figure 39 displays the tail volume coefficient used for the tail. Figure 40 gives the top view of the stabilizer along with its elevators. The horizontal tail parameters are provided in Table 21. The final values are consistent with airplanes in a similar class [24]. Like the vertical, the airfoil for the horizontal stabilizer is the NASA SC(2)-0012. Similar reasons apply to why this airfoil is chosen. It should also be noted that the NASA SC(2)-0012 is chosen over the NASA SC(2)-0010 for the lighter weight structure. There is also an added 2.98º incidence angle to the horizontal tail to keep the nose pitched up without using pitch control. The method to get this value is also given in [31]. The

5% static margin is calculated using the operational neutral point, Table 22 gives the values of the static longitudinal stability, calculated using VSPAero.
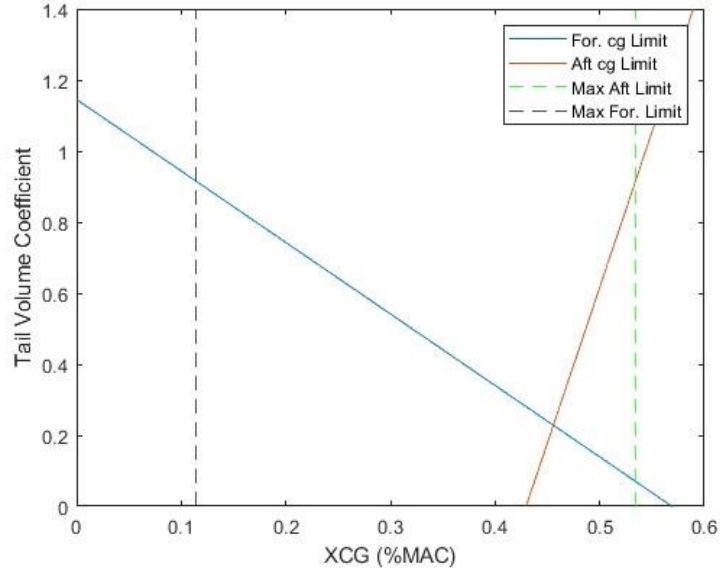
Figure 39. Horizontal Stabilizer Scissor Plot
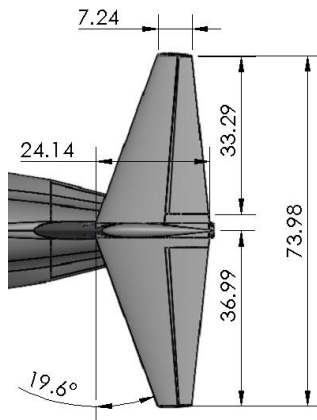
Figure 40. Horizontal Stabilizer

Table 21. Horizontal Stabilizer Parameters

Horizontal Stabilizer	
Planform Area	1,263 ft^2
Chord	17 ft
Height	73.9 ft
Aspect Ratio	4.3
Tip Chord	10.9
Root Chord	21.9

7.2 Control Surfaces

7.2.1 Aileron

The ailerons on the PW-24 Harpy are designed to be able to roll the plane at 30 degrees in 1.5 seconds, therefore meeting the requirements presented by MIL-F-8785C for the PW-24 Harpy's class of aircraft [32]. The chord is 30% of the wing's chord with dimensions pictured in Figure 41. This is in line with the flaps and the spars do not have any interference. The analysis and dimensions were computed using ideas given in [31]. The ailerons also have a maximum deflection of 20º.
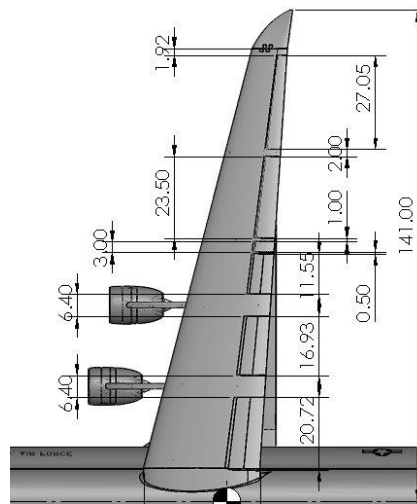
Figure 41. Flaps and Ailerons

7.2.2 Rudder

The maximum deflection for the rudder is ± 30º. Initial sizing for the rudder was computed using historical data. The chord ratio and area were then refined using techniques presented in [31] for the crosswind and OEI scenarios (for the PW-24 Harpy, this is the two engines out scenario). To ensure that the rudder could handle maximum sideslip conditions no aileron deflection was considered when performing the analysis. In addition, the methods presented in [31] helped to properly size the rudder to handle winds with a crosswind component of 30 kt at 90º during takeoff and landing. The rudder is 40% of the vertical tail's chord and 90% of the height. The rudder is shown in Figure 38.

7.2.3 Elevator

The maximum deflection for the elevators is ± 20º and were iterated through to make sure they met trim conditions. The initial sizing for the elevators were computed using historical data. The chord ratio and spanwise dimensions were then refined using techniques presented in [31]. These were found to the 39% of the horizontal stabilizer chord and 90% of the span. The exact elevator design and dimensions are given in Figure 40 and are sized to meet the trim conditions. Figure 42 shows the effect of elevator deflections and confirms that $C_{m_{\delta e}}$ exhibits longitudinal stability. It also demonstrates the two extreme cases where the elevators are deflected 20º and -20º. The results were computed using VSPAero.
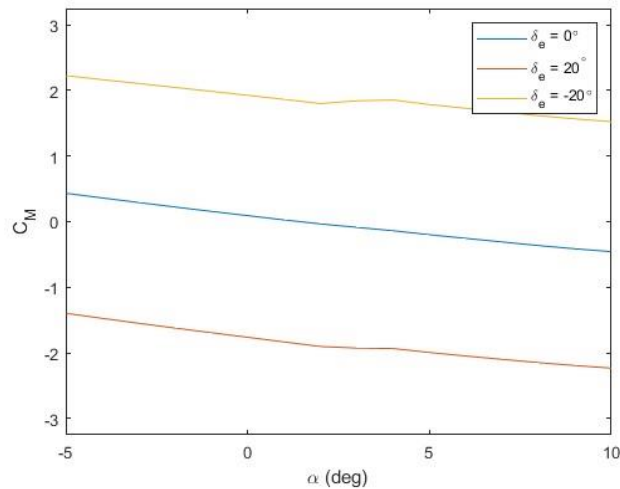
Figure 42. Elevator Deflections

7.3 Static Stability Analysis

The static margin for the aircraft is 5% for the ferry range condition. The furthest forward the cg moves under static conditions for the different configurations is the 3 tanks arrangement and this results in a static margin of 11%. The other configurations fall between the 5%-11% range which is largely in range of the recommended 5%-10% range given by [24]. All arrangements result in a statically stable aircraft. Other stability derivatives are presented in Table 22, and all meet the required values for stabilization. An anhedral angle of 1.49º is also added to the wings to achieve the desired values. It can also be noted that the aircraft is laterally symmetric and the CG is always located between the most forward and aft CG positions as shown in

Figure 43 with the neutral point being the aft condition. Figure 43 shows the unloaded configuration CG with rough dimensions.

Table 22. Static Stability Coefficients

Static Stability		
Static Margin	5 %	✓
$C_{M\alpha}$	-0.056/deg	✓
$C_{n\beta}$	0.0272/deg	✓
$C_{l\beta}$	-0.05/rad	✓
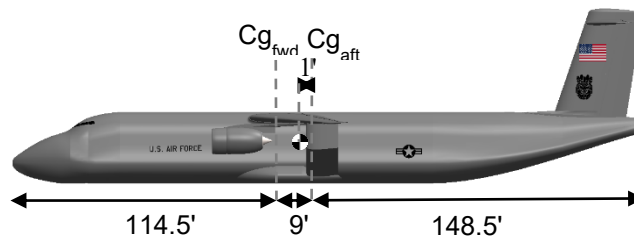
Figure 43. Forward and Aft C.G. Limits

7.4 Dynamic Stability Analysis

The dynamic stability of the aircraft is assessed using the AVL program by MIT for dynamic and trim conditions. The AVL program outputs the eigenvalues for the specific run case and the results are translated to the correct units given as comparisons by the mil standards. The results are tabulated in Table 23 below.

Table 23. Dynamic Stability Parameters

Dynamic Stability		
Dutch Roll	$\zeta_{dr} = 0.17$	✓
Spiral	$T_{2s} = 23\ s$	✓
Phugoid	$\zeta_{ph} = 0.044$	✓
Short Period	$\zeta_s = 0.56$	✓
Roll	$T_R = 0.69\ s$	✓

8. Structures and Weights

8.1 Material Selection

When considering the materials the aircraft would be composed of, the most common options were aluminum alloys or composite materials. The options that we down selected to are outlined below [33].

Table 24. Material Specifications

Material	Density (lb/in3)	Yield Strength (psi)	Ultimate Tensile Strength (psi)	Ultimate Shear Strength (psi)	Young's Modulus (ksi)	Poisson's Ratio
Aluminum 2024-T3	0.100	50.0e3	70.0e3	41.0e3	10.6e3	0.333
Aluminum 7075-T6	0.102	73.0e3	83.0e3	48.0e3	10.4e3	0.333
Carbon Fiber	0.0578-0.0795	N/A	247e3- 102e4	N/A	33.1e3-105e3	0.26-0.28
Steel 300M	0.284	230e3	280e3	N/A	29.7	0.280

While composites have superior material qualities, such as being lighter-weight, less likely to experience fatigue failure, and overall higher strengths, they also are much more expensive [34]. That is, the sourcing and maintenance of composites correlate to increased lifetime costs as compared to traditional materials. Additionally, composites are much more easily damaged than wrought materials. This, coupled with the fact that it is much harder to visually determine when a composite sustains damage, makes maintaining these materials much harder. Due to these reasons, the PW-24 Harpy will not utilize carbon fiber and will use aluminum instead.

The fuselage structure, fuselage skin, and lower wing skin will be constructed with aluminum 2024-T3. This material is standard for pressurized fuselages and offers slow crack growth, as well as high fracture toughness [35]. Additionally, it is useful for areas that see the regular application of tensile stresses. Furthermore, the upper wing skin and wing structure will be made from aluminum 7075-T6. Military aircraft structures routinely use this material, and it offers higher strength than its 2024-T3 counterpart. The upper wing skin primarily receives compressive loads as the wing flexes upwards in flight, for which 7075-T6 excels [35]. The landing gear will be made of a high strength steel alloy, 300M. This material has been hardened to high strengths, which is vital for landing gear carrying loads as large as the PW-24 Harpy.

8.2 Aircraft Load Analysis

8.2.1 V-n Diagram

To determine the aircraft loading at various airspeeds, we developed a V-n diagram. The flight envelope can be seen in Figure 44.
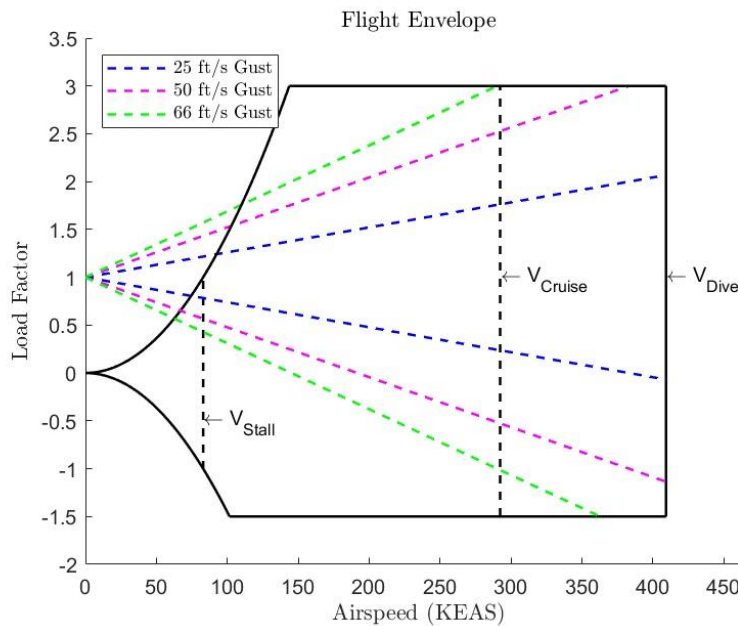
Figure 44. PW-34 Harpy V-n Diagram

This flight envelope consists of curves from Roskam V [36] and Nicolai's [11] textbooks. Additionally, the maximum load factor was set to +3 g's and the minimum load factor was set to -1.5 g's, taken from the RFP requirements. Stall speed and dive speed were calculated through additional equations outlined in Roskam V [36], and cruise speed was another parameter derived from the RFP. Specific speeds can be seen in Table 25.

Table 25. Aircraft Speeds

Stall Speed	Cruise Speed	Dive Speed
83.0 KEAS	292 KEAS	409 KEAS

This loading diagram will help to inform the structural layout of the Harpy. That is, the loading at each airspeed will help to determine how much support members of the aircraft structure will need to provide.

8.2.2 Wing Loading

To further analyze the loading on the aircraft, the lift distribution across the semi-span of the wing was calculated. This distribution was taken by averaging the trapezoidal and elliptical wing lift approximations, as outlined in Nicolai [11].
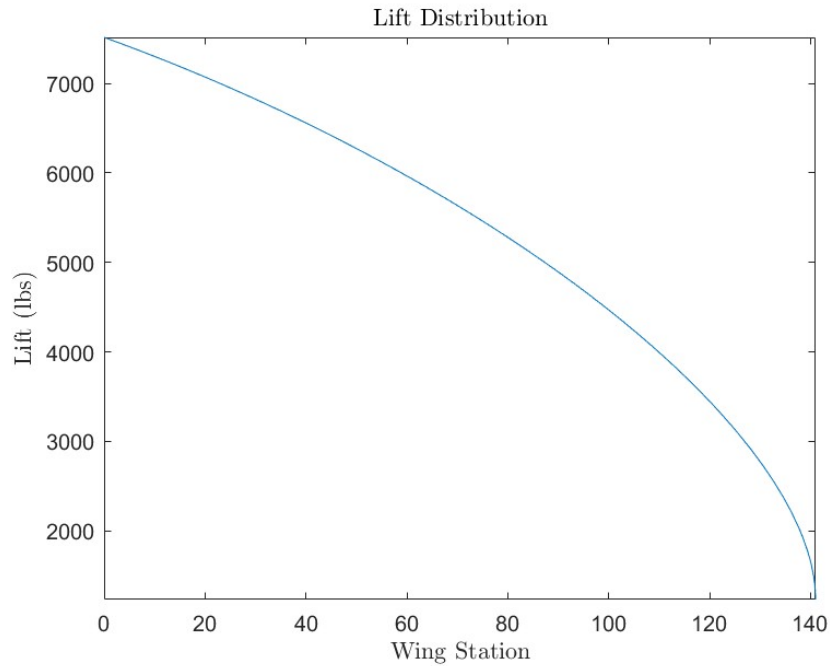
Figure 45. Wing Lift Distribution

The lift is the highest at the root of the wing and decreases steadily toward the tip. This indicates there will need to be more structural support near the wing root and less further along the wingspan.

8.3 Structural Layout

8.3.1 Wings

The structural layout was initially determined from a static structural analysis of the wing with the truss. This includes the jury truss and the main truss. The analysis calculated the forces of the wing under a 3g load, calculated with a factor of safety of 1.5, as outlined in the RFP. The result of this analysis can be seen in Figure 46.
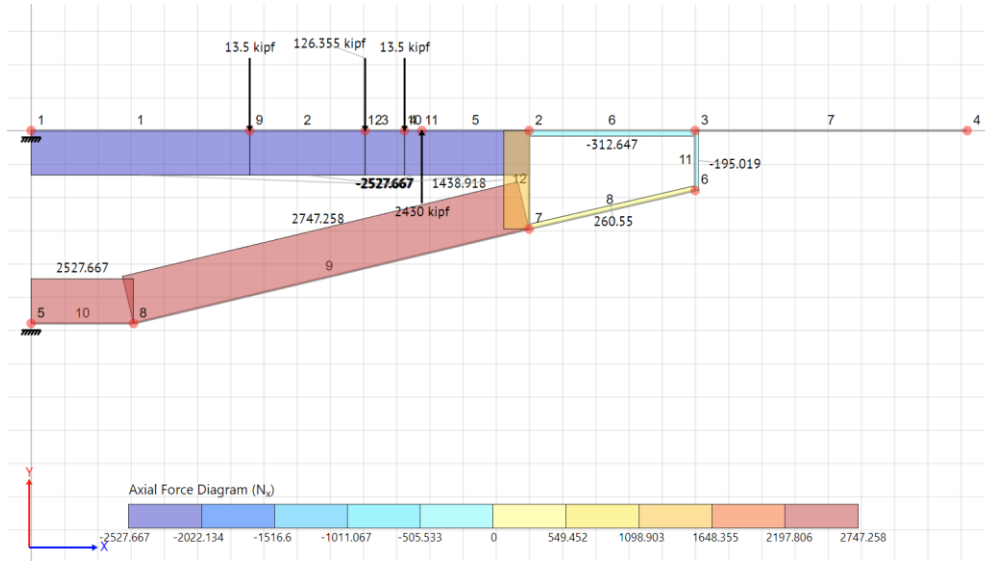
Figure 46. Wing Structure Axial Forces

The forces which contributed to the resultant axial stresses include the lift generated by the wing, the weight of the engines, and the weight of the wing itself. With the axial loads, the cross sections of the spars at the wing root can be sized based on the maximum stress seen along the wing, at 2530 kips. Knowing the ultimate stress, the required area to sustain the load can be easily calculated, based on the strength of the aluminum alloy.

Table 26. Main Structural Component Dimensions at Wing Root

Component	Height (in)	Maximum Width (in)	Cross-Sectional Area (in2)
Front Spar	2.75	38.3	36.1
Rear Spar	3.29	30.7	36.1
Main Truss Spar	N/A	N/A	39.1
Jury Truss Spar	N/A	N/A	20.6
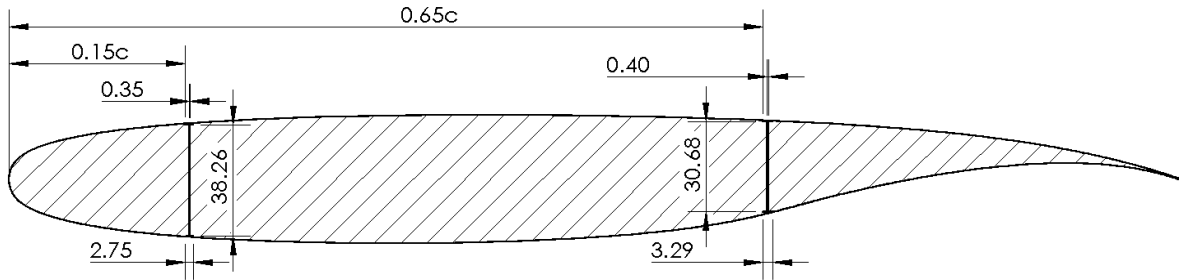
Figure 47. Wing Structure Cross-Section

The front and rear spars will be sized based on these dimensions at the wing root and decrease in size along the span of the wing. However, the jury and main truss will have a constant area shaped like a NASA SC(2)-0012 airfoil. Furthermore, the front and rear spars will be placed at 15% and 65% of the chord of the wing, as advised by Niu [35]. They will be in the shape of an I-beam, as is common for wing spars. There will be 62 ribs on each wing, 0.42 inches thick and spaced 26 inches apart. This is based on the total amount of shear the wing experiences, as well as advice from Dr. Kapania from Virginia Polytechnic Institute and State University.
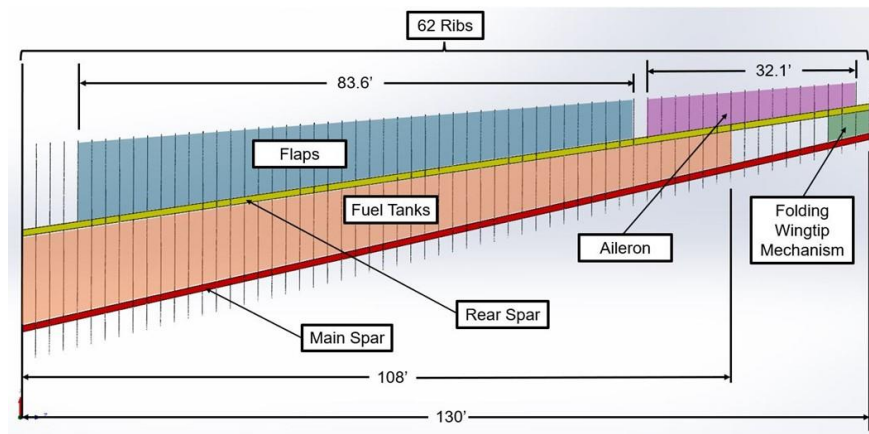
Figure 48. Wing Structural Layout

Truss braced wings offer significant weight savings due to the reduced wing skin thickness they need. Traditional cantilever wings have skin that is much thicker, over four times thicker than strut braced wings [37]. Due to our truss, our wing skin thickness can be much lower at the root of the wing, 0.02 inches.

8.3.2 Fuselage

The fuselage layout was determined from historical data and recommendations from Niu's [35] textbook. For transport aircraft, the fuselage frames are typically 20 inches apart and 8 inches thick. This is the layout that the PW-24 Harpy has as well. There will be more structural support where heavy loads are present. That is, the frames will be spaced closer together where heavy avionics bays and cargo are normally placed. Additionally, like the C-5. The stringers will be spaced 7.5 inches apart, with an L-shape.

Lastly, the cabin will be pressurized to 6000 ft sea level, and cruising up to 43000 ft. This correlates to a pressure differential of 9.42 psi. With that, the fuselage will need to be 0.05 inches thick at a minimum.
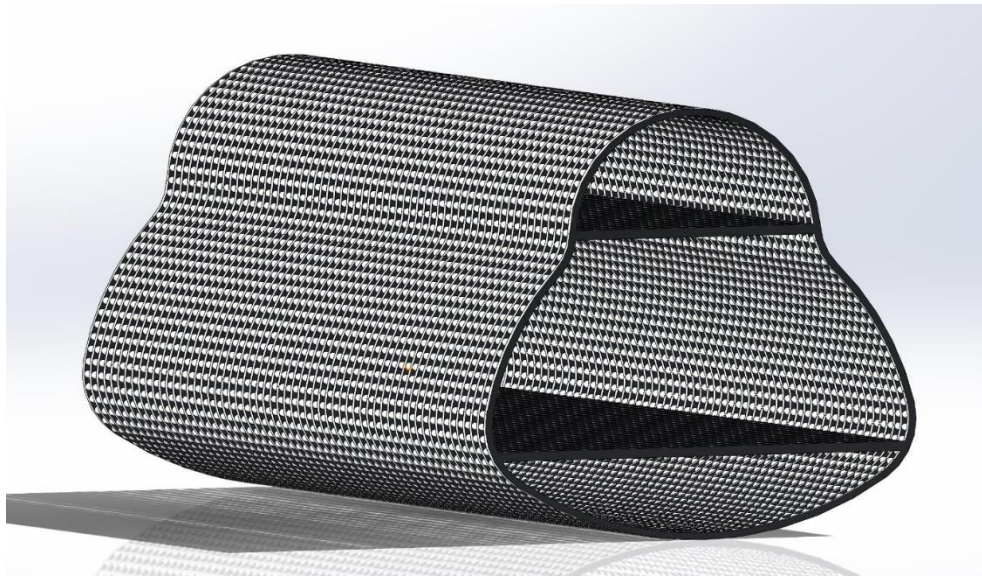
Figure 49. Fuselage Structure

8.4 Structural Analysis

To understand the behavior of the wing structure, an Ansys static structural analysis was used. This will help to get the deformation and max stresses across the wing, at the 3g loading condition. First, based on the V-n diagram, the wing was placed in Ansys fluent to get the pressure distribution at 3g loading with a factor of safety of 1.5.
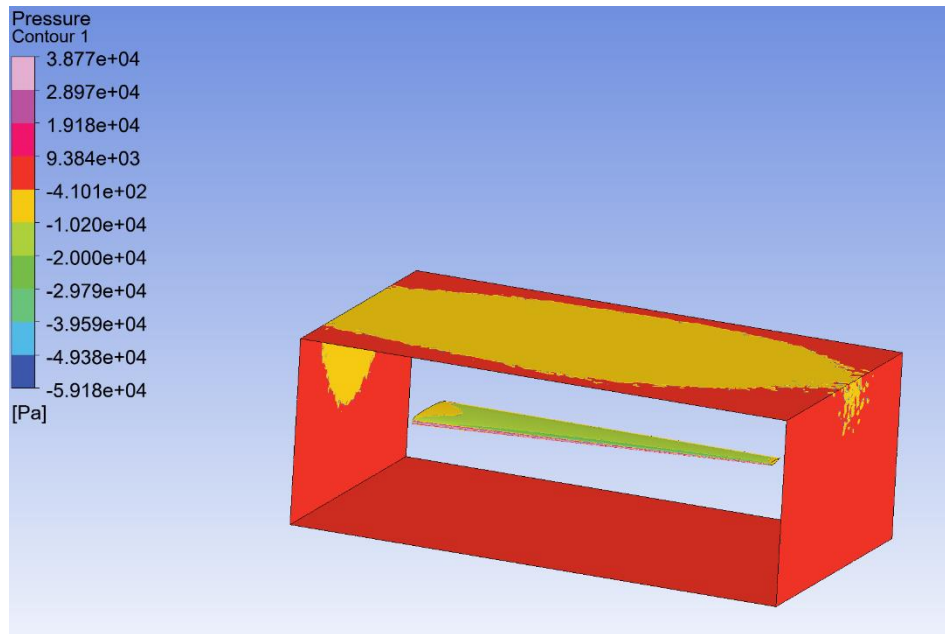
Figure 50. Wing Pressure Distribution

The leading and trailing edge have the highest pressure, which in turn will be subject to the most stress. After the Fluent study, this pressure distribution was exported to Ansys mechanical to get overall wing stress and deformation. The detailed pressure distribution, the engine's weights and support of the truss were included in the mechanical study.
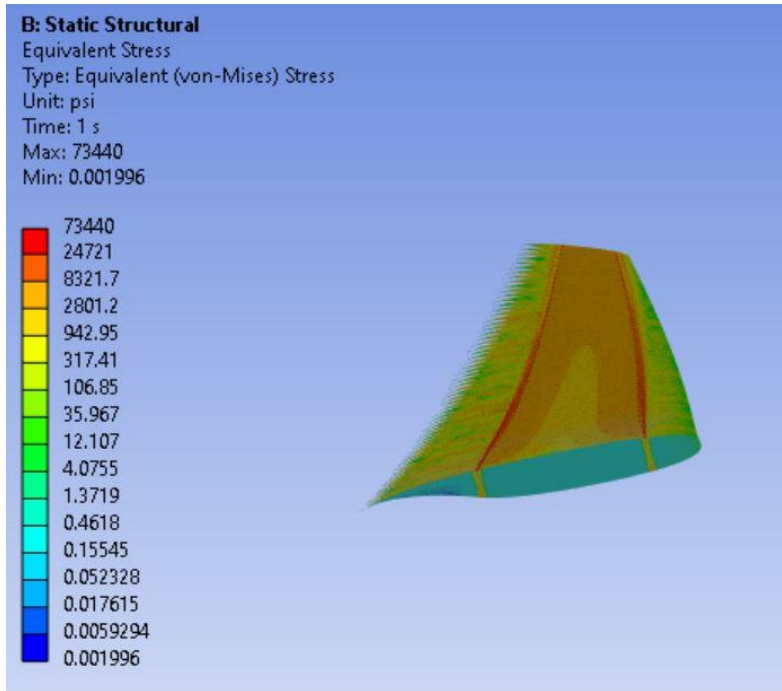
Figure 51. Wing Stress Distribution

From the analysis, the wing is seen to carry between 2.00e-6 ksi and 73.4 ksi. The lowest amount of

stress is near the wing root, while the maximum stress is held at the spars. In this max loading condition, the

wing can sustain the load as the ultimate tensile strength is never reached.
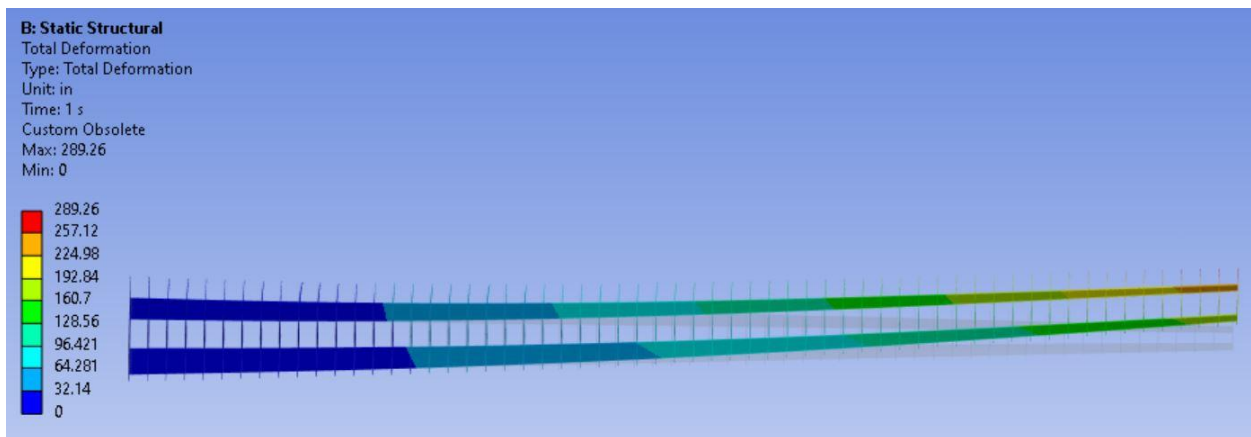
Figure 52. Wing Deformation

The wing deforms 289 inches at the tip in the max loading scenario. This is a significant deformation,

but the aluminum structure can withstand such deflection. Additionally, the wing skin was not included in this

analysis. This indicates that with the added support of the wing skin, the loading scenarios would be even more manageable than already shown.

8.5 Weights

8.5.1 Weight Assessment

One major task in the design of aircraft is weight distribution and center of gravity location. As mentioned in the subsystems and stability sections of this report, the c.g. location is most crucial for positioning landing gear and lifting surfaces, such as the wing and empennage. The evaluation of center of gravity location found its beginnings in determining the weights and longitudinal locations of key components of the aircraft, such as cockpit controls and passenger bays.

8.5.2 Hardware Weight Analysis

For the weight evaluation, Chapter 20 of Nicolai [11] was utilized, as well as Raymer [24] for the landing gear weight estimation. This provided acceptable weight estimations for structural, propulsion, and subsystem components which most greatly affect the center of gravity of an aircraft. Each calculation provided by Nicolai [11] had various equations, each for a different category of aircraft or type of system which was to be evaluated. However, some subsystems did not have weight equations within Nicolai [11] in which case an equation was located in Raymer [24]. For the engine system, the actual weights were used. The weight of the wing tip folding mechanism was calculated through Boeing's method.

These components and their weights define the empty weight of the aircraft. That is, the empty weight of the aircraft is all components default to the aircraft and not including fuel. To develop a comprehensive gross takeoff weight, the weight of the fuel must be taken into account. The equation for the weight estimation of this system considers the half span of the plane's wing, the length of wing desired to fold on one side, and the maximum takeoff gross weight. The estimation developed by Boeing is formulated around the wing tips of the Boeing 777. The final weight penalty is calculated by finding the ratio of the result of the equation mentioned earlier to the 777's result from the same equation. This ratio is multiplied by 3 klb (the weight of the mechanism on the 777) to calculate the weight.

8.5.3 Fuel Weight Analysis

The ultimate fuel weight and volume must at minimum be dependent on the missions which will be required by the aircraft. As discussed in previous sections, the aircraft must have the capability to complete three different types of missions, wherein the distance and payload required vary between them. The addition of fuel, as well as the mission payload, has great implications on the final gross takeoff weight for each mission profile. A breakdown of the takeoff weights for each mission is given in Figure 53. The weight is broken down between operating empty weight, payload, reserve fuel, and mission fuel. The weight of the reserve fuel is calculated from the takeoff gross weight; it is taken to be 8% of the maximum takeoff gross weight, which gives a value of 88,000 lbs for our aircraft. This gives a comprehensive overview of the range of loadings to which the aircraft will be subjected in its lifespan.

Weights Breakdown per Mission
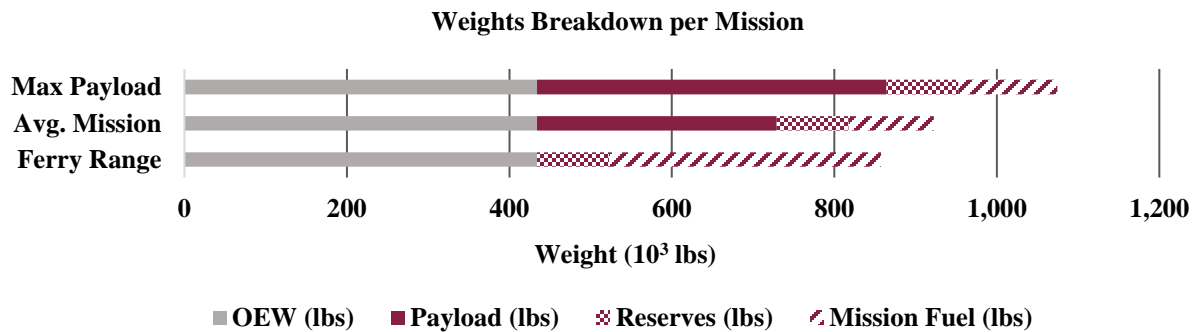
Figure 53. Gross takeoff weight breakdown for each of three required missions

8.5.4 Determination of Center of Gravity

This section details the process by which the longitudinal center of gravity is located. In a previous section, the determination of the aircraft's empty weight components was discussed. The values found through those methods are utilized here, in tandem with the longitudinal locations dictated by the configuration of the PW-24 Harpy. The method of determination was drawn from the last section of Chapter 20 in Nicolai [11]. Nicolai prescribed a method wherein the weight of each component is multiplied by its distance behind the nose. All moments are then summed, and that total is divided by the sum of all component weights. The resulting value is accepted to be the longitudinal center of gravity.

This determination is most easily done in a MATLAB script. The implementation in a computational script allowed for changes to be easily made or considered when design iterations required the updating of the center of gravity location. The behind-the-nose locations of critical components were made variable through the addition of a differential *d*. This made it possible to quickly assess the implications of lengthening the fuselage, which has a major effect on the locations of the lifting surfaces and the landing gear. Initially, the length of the fuselage was 262 feet. However, this created conflict between the requirements of the stability and subsystems teams. A compromise needed to be found which avoided tail-striking on takeoff and kept the static margin of the aircraft within a reasonable range. This issue arose when the travel of the center of gravity at the maximum payload configuration was considered.

A study was conducted which compared moving the wings and landing gear back 0, 5, and 10 feet. The team also considered moving the wing back a further distance than the landing gear and vice versa. Through the use of simple loops, the base determination method described above was implemented with the variability method previously discussed. Through this study, the fuselage was lengthened by approximately 10 feet. The final behind-the-nose locations of the major components are given in Table 27.

Table 27. Major components' weights and longitudinal locations

Component	Weight (lbs)	Distance Behind the Nose (ft)
Wing	253,000	126
Horizontal Tail	9570	254
Vertical Tail	1720	254
Fuselage	60,800	136
Landing Gear – Nose	5530	32
Landing Gear – Main	17,800	122
Engines	57,200	104
Cockpit	306	18
Crew Bunks	55	48
Lavatories	508	83
Wing folding mechanism	2,700	134

9. Subsystems

9.1 Electrical Systems

The PW-24 Harpy relies on a powerful electrical system to operate due to its bleed-less design. The power requirements for flight are shown in Table 28:

Table 28. Subsystem Power Requirements

Subsystem	Power Requirement (kW)
De-icing	186
Pressurization	1,250
Hydrostatic Actuators	1,120
Folding Wingtip	224
Avionics	~2
Total	2,780

To meet the aircraft's total power requirements, two Trent 1000 J-2 turbofan variable frequency engine generators per engine are combined with dual Auxiliary Power Units (APUs), their respective batteries, and another main battery. Combined, these units generate 2.9MW of power which is distributed from four buses. These buses consist of the 235VAC primary power, 270VDC for electrically driven pump motors, and 115VAC and 28VDC for smaller avionics systems, lighting, and galley power [38]. Remote power distribution units located throughout the aircraft as indicated in Figure 54 manage the flow of electrical power from the main power to the various subsystems and allow for remote monitoring of independent system status through integration with the onboard avionics systems. The power generated at any given time is larger than the needed power to compensate for growth in power consumption. When ground power is available, the engines are started by an external ground unit; while when this option is not available, the APU batteries are used to start the main engines. The electric motor pumps operating at 270VDC provide power for the actuators and motors of the following systems:

- Flight Controls: The electronic motor pumps provide the necessary hydraulic power to actuate the elevator, aileron, and rudder surfaces.

- Landing Gear: Both the Main Landing Gear's (MLG) and Nose Landing Gear's (NLG) actuation and control is electrically powered, along with the electronic braking system.

- De-Icing: de-icing is handled through an integrated heating mat in the spars of the wings and leading edge of the tail. This system provides cyclic heating as necessary to prevent formation of ice on control surfaces. [39]
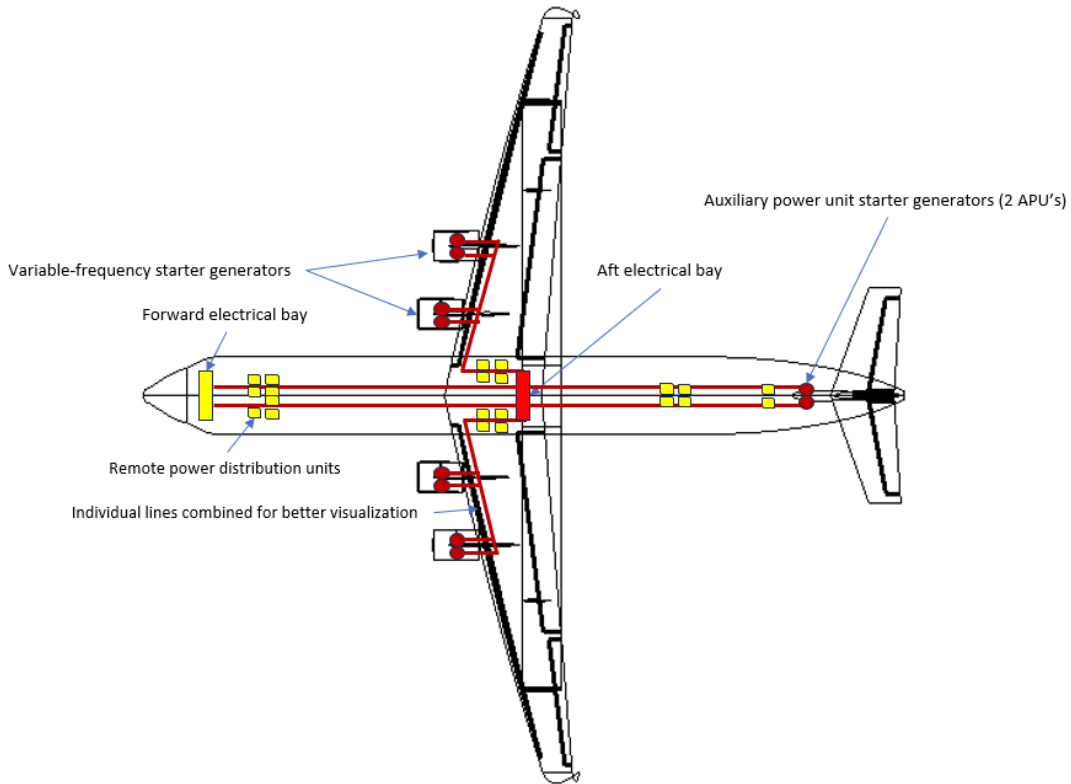
Figure 54. Electrical Systems Schematic

9.2 Hydraulic Systems

Unlike conventional aircraft, the PW-24 Harpy will utilize a highly distributed hydraulic system to actuate the primary flight controls, landing gear retraction and extension, and the cargo gates. Most conventional aircraft rely on bleed air to drive hydraulic pumps which pressurize the hydraulic fluid throughout the aircraft [40]. The Harpy, on the other hand, incorporates a more-electric design which eliminates the need for bleed air. Instead of a central hydraulic system, the PW-24 Harpy will use a network of electrohydrostatic actuators (EHA) to actuate the fast-moving primary flight controls and electromechanical actuators (EMA) to control slower moving secondary controls (landing gear, flaps/slats, cargo gates, etc.). The actuators selected for the Harpy are the Type V CEHA. They were chosen for their quick actuation speed and control authority which well suits the Harpy's needs [41].

One of the primary advantages of using a more electric system is the weight savings as a result of removing the traditional hydraulic system. Following the parametric equations presented in [11], the traditional hydraulic system weight was estimated to be 9,600-lbs. The more electric hydraulic system, shown in Figure 55 below, has a total weight of approximately 8,400-lbs [41]. This results in significant weight savings from eliminating the hydraulic system. Another advantage of the more electric system is that it reduces the amount of maintenance required. In the event of component failure, the broken system can be quickly replaced independently. This is particularly important if repairs are required in areas of limited resources.

Lastly, the Harpy will use electromechanical actuators to open and close the main cargo gates. Once again, this reduces the total weight of the hydraulic system since this design removes the need for heavy hydraulic lines, fluid, and actuators.
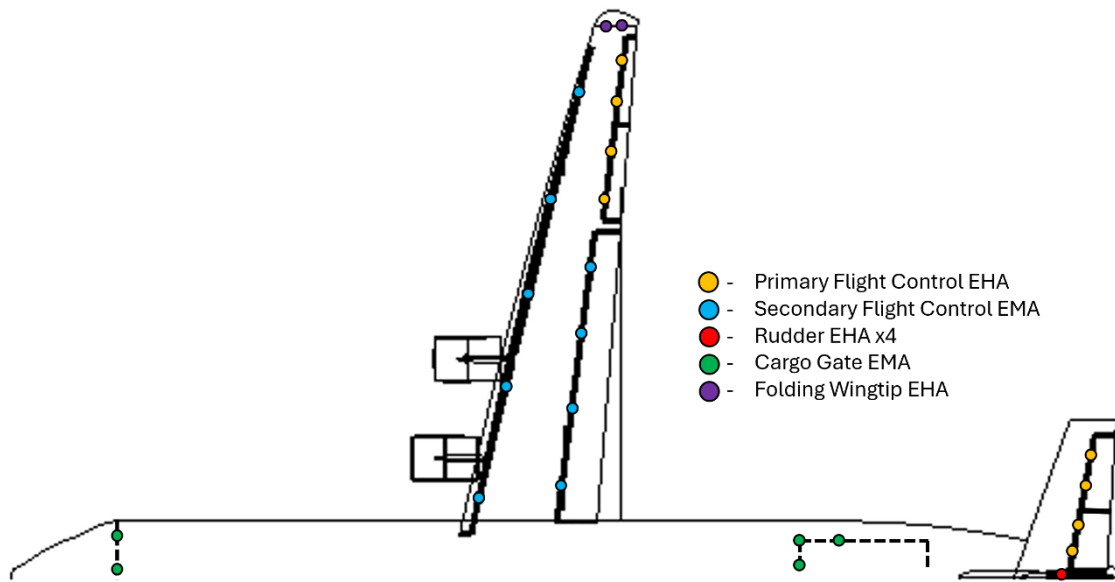
Figure 55. PW-24 Harpy's Distributed More Electric Hydraulic System Schematic

9.3 Fuel Systems

The PW-24 Harpy's fuel system is designed with maintainability and redundancy in mind. The required 280,000lbs of fuel is stored in four integral wing tanks, two in each wing. Owing to Jet-A-1's tendency for its density to fluctuate with temperature (6.89lb/gal; 0°F and 6.57lb/gal; 100°F) the fuel tanks were sized using the lowest density, i.e. the condition that requires the most volume [40].

Due to the anhedral angle of the Harpy's wings, the outboard side of the fuel tank will accumulate more fuel than the inboard tanks resulting in a weight shift further out towards the wing tips. The dual tank design will allow for fuel to be preferentially consumed from the outboard tanks in as to limit the amount of weight being transferred towards the wing tips. Moreover, the fuel pickups and pumps will be located along the bottom of the fuel tanks and at the outboard edge to ensure the pumps are continuously fed with fuel.

Figure 56 below shows the PW-24 Harpy's fuel tank and transfer systems. It is important to note that the Harpy contains an extra fuel line extending towards the nose of the aircraft which is used for aerial refueling. This line can feed both port and starboard fuel tanks via automatic or pilot-controlled fuel transfer valves.
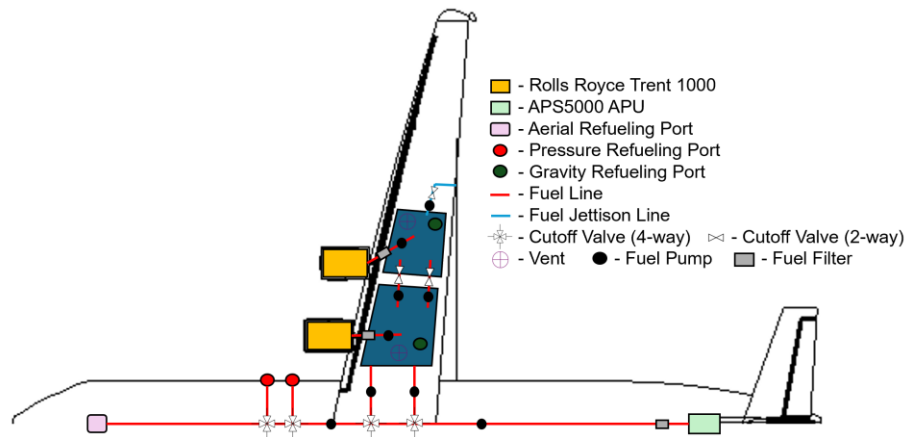
Figure 56. The PW-24s Fuel System Schematic

The fuel transfer valves can be controlled automatically using inputs from both the Trent 1000's FADEC computer and the Harpy's FMS computers to ensure efficient fuel transfer and flow to the four engines. The pilots have a manual revision of this system in the cockpit in case of a system failure. An active monitoring system, like the Collins Aerospace "Kidde Dual Spectrum," will watch for any potential fires and deploy necessary extinguishers to put out any potential fires [41].

Ground refueling is facilitated via four pressure points located on the forward section of the landing gear pod. This system, like the C-5 Galaxy's, allows for a shorter refueling time than a single pressure point design [11]. Also, the refueling points are located near the bottom of the Harpy's fuselage to reduce the amount of ground personnel and equipment needed as opposed to a wing-mounted refueling point. The four pressure points serve to expedite the refueling process and it is possible to refuel the Harpy using only one pressure

point if the airport's infrastructure is limited. Lastly, there will be four over-wing gravity refueling points to serve as a backup to the pressure points.

9.4 Landing Gear

The PW-24 Harpy's landing gear is designed to support takeoff weights in excess of 1 million pounds and for safe landings at vertical speeds up to 15ft/s. The Harpy's main landing gear has four bogies each containing six tires (total of 24 tires) and the nose gear contains six tires. This allows for a distributed load which reduces the size and pressure of the tires and limits the Harpy's impact on softer airfield surfaces. Using the FAA's COMFAA 3.0 software, the Harpy's aircraft classification number (ACN) was calculated to be 40.5 for flexible runways with a B subgrade (CBR 10).

Additionally, the landing gear is located following the method outlined in [24, 11]. The main landing gear is placed such that the tip-back angle is approximately greater than the angle of attack when the aircraft generates 90% of C_{Lmax} [11]. The combined nose gear and main landing gear placement results in 9.5% of the Harpy's weight to be carried by the nose gear. This is desirable as it provides enough force for the Harpy to have adequate turning authority. Lastly, the Harpy's tires are chosen using the parametric equations presented in [24], the calculated maximum loads, and Goodyear Tire's product catalogue [42]. Table 29 and Figure 57 below outline the key design metrics and layout/location of the Harpy's landing gear.

Table 29. PW-24 Harpy Landing Gear Design Parameters

Design Aspect	Value
M.L.G Wheel Loading	40,700-lbs
M.L.G Tire Size and Pressure	49x17-in, 195-psi
N.L.G Wheel Loading	27,200-lbs
N.L.G Tire Size and Pressure	49x17-in, 195-psi
Oleo Strut Diameter	7-in
Oleo Strut Travel	17-in
Tip-Back Angle	9.5°
Overturn Angle	59.7°
Vertical CG Angle	18.7°
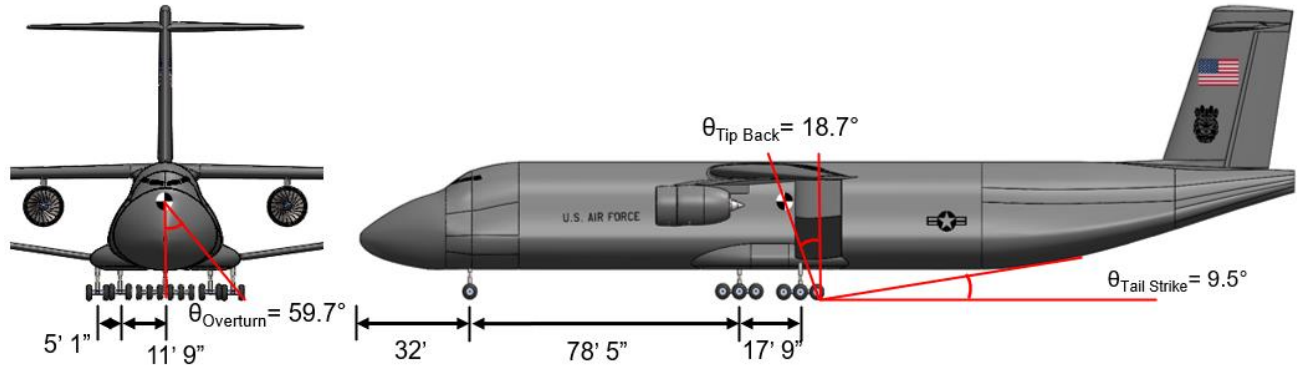
Figure 57. The PW-24 Harpy's 30-Tire Landing Gear Design

Lastly, a kneeling system is installed in the Harpy's landing gear to lower the cargo floor during loading and unloading. This system, inspired by the C-5 Galaxy, partially retracts the nose landing gear until the fuselage rests approximately 18 inches from the ground. The main landing gear will also recede slightly into the fuselage to maintain a flat cargo floor. This reduces the necessary total length of the front cargo ramp from 66 ft to 42 ft while maintaining the same down angle of 12°.

9.5 Cargo Handling and Interior Layout

To accommodate the three load conditions of the main cargo bay of forty-eight 463L pallets, or three M1A2 Abrams Main Battle Tanks (MBT), or 330 passengers, three main cargo bay configurations are used. Cargo loading and egress is available through a forward and aft loading ramp. This ramp allows for drive-on drive-off capabilities for vehicle cargo. The ramp can be angled down or locked horizontally to the ground for ease of pallet loading through forklifts. The cargo ramp itself will be 42' in length, with a down angle of 12 degrees and a ramp toe angle of 16 degrees. Two paratrooper doors are featured in the main cargo bay behind the wings on either side of the aircraft.

- MBT configuration: Twenty-seven individual tie-down rings per tank rated at 25,000lbs are located in accordance with the following diagram to allow for proper securement of the three vehicles. These tie-down rings are permanently attached to the floor of the cargo bay and lay flat when not in use to avoid damage to equipment [43]. MB-2 chain gear of forty-two individual chains rated at 25,000lbs are stored in the aircraft's cargo bay to secure the tanks to the appropriate tie-down rings [44]. As per the Air Force's Transportability Guidance on the MBT four persons can prepare, load, and tie down the vehicle in 45 minutes, while it can be unrestrained and unloaded in fifteen [45].

71
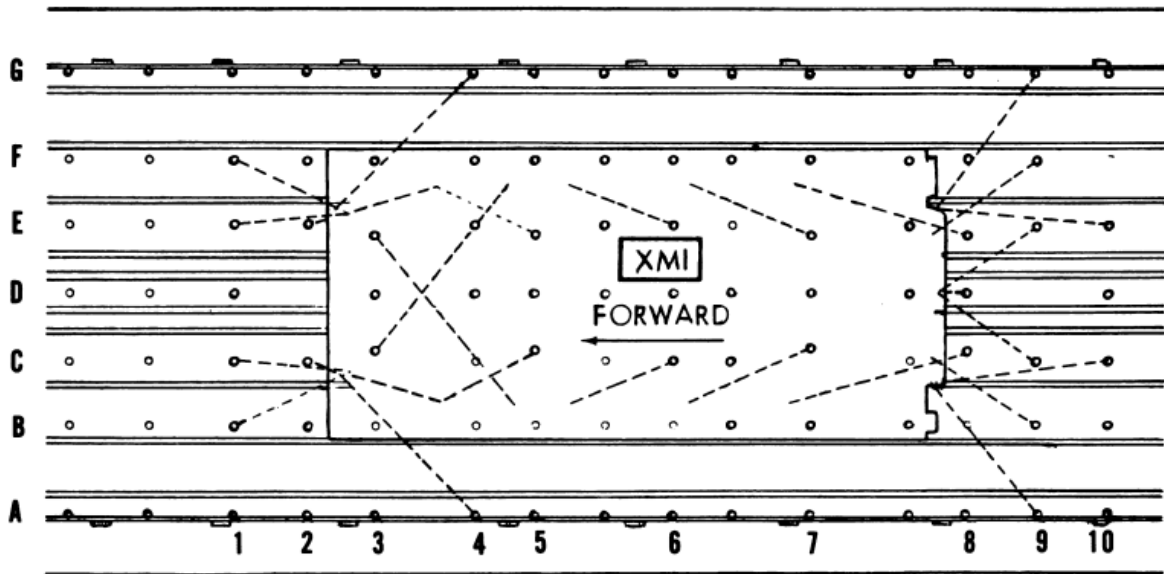
ALL CARGO TIEDOWN FITTING - RATING 25,000 LB EACH.

Figure 58. Cargo Fastening Locations

- Pallet configuration: Removable gravity roller conveyors will be installed when palletized cargo is needed [46]. These conveyors are tailored to the 463L pallet system, rated for a maximum weight of 10,000lbs, and include a locking mechanism which secures the individual pallets in place during normal operations. When loaded, the pallets will be arranged into 3 rows of 16, for a total payload of 48 pallets. Provisions for a single top net and two side nets per pallet will be integrated into the cargo bay for loose stacked pallets, along with nylon tie down straps rated at 5,000lbs [47, 48]. In accordance with U.S. Transportation Command [48], pallets are to be spaced 2 inches apart and 14 inches from each wall to allow for the loadmasters and crew to move about the cargo bay.

- Passenger configuration: The passenger configuration relies on a palletized seating system which uses seats mounted to standard 463L pallets to meet the 330-passenger requirement in the main cargo bay. Each passenger pallet includes fifteen seats, requiring a total of twenty-two pallets. These pallets will use the same roller conveyor locking system as the pallet configuration for securement during normal operations. The spacing of the passenger pallets will be the same as that of the cargo pallets.

To accommodate 100 more troops, the second floor has a passenger bay directly behind the cockpit, shown in Figures 59 and 60. For crew and passenger comfort, a galley, bathroom, and crew quarters are included on

72

the second floor directly behind the passenger bay. The crew quarters include sleeping quarters for the four-person relief crew relief crew. The second floor also has a partitioned section in the rear of the aircraft's fuselage for storage of environmental controls including pressurization equipment and air conditioning, along with a section to house the dual APS5000 APU system. A forward avionics bay is located under the main cargo bay's forward section.
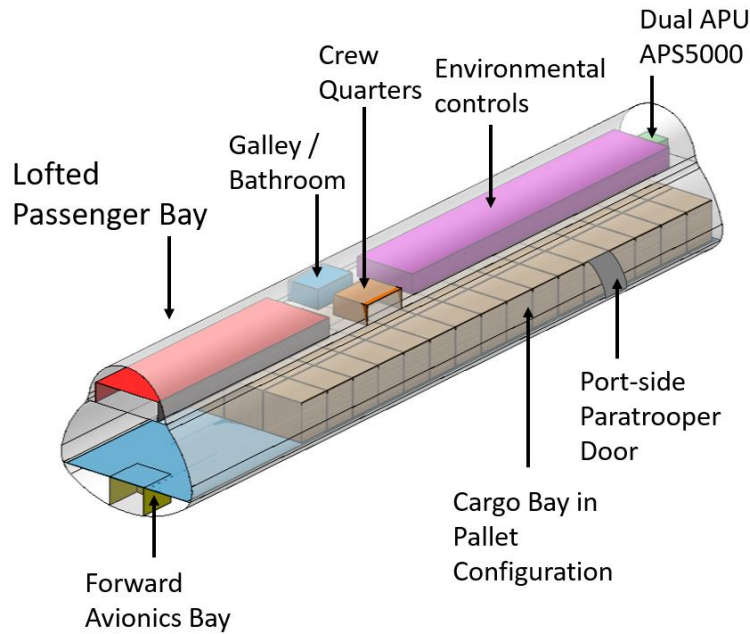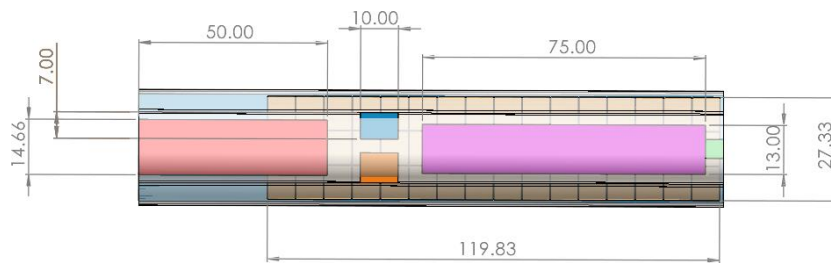

Figure 59. Internal fuselage layout

Figure 60. Internal fuselage dimensions

9.6 Cockpit Layout

The cockpit of the PW-24 Harpy is designed with the goal of minimizing the need of pilot training when switching over from the C-5 Galaxy platform. With this in mind, both the flight displays and general layout of the cockpit, shown in Figure 61, are similar to those of the C-5.

- The pilot and copilot each have two VDT-1209 Video Display Terminals, capable of each functioning as both a primary flight display (PFD) and navigation display (ND). [49]

- The engine indicating and crew alerting system panel (EICAS) is located between the pilot and copilot's VDT's. This system allows for real-time monitoring of various subsystems including the engines, flight controls, hydraulics, electrical, and environmental systems. Monitoring of the Trent 1000's Full Authority Digital Engine Control (FADEC) is made available through this system's Engine Monitoring Unit (EMU). [50]

- The Electronic Flight Instrument Panel (EFIS) is also available for both pilot and copilot, providing additional displays for fuel quantity, system status, weather radar, and traffic information.

- An Environmental Control System (ECS) is overhead between the pilot and copilot. This panel provides control and real-time tracking of the environmental systems including temperature control within the cabin, pressurization, ventilation, and humidity controls.

- BAE LiteWave Heads-Up Displays (HUD) are provided for both pilot and copilot; and are responsible for displaying critical flight information within the pilot's line of sight. This system provides a 70% reduction in size and weight compared to conventional HUDs, and features an "Eye Motion Box", allowing for increased head movement by pilot. This system was selected to reduce the workload of the flight crew. [51]

- An Electronic Flight Book (EFB) is included for both the pilot and copilot, serving as a tablet-based replacement for paper-based flight manuals. The EFB provides tools for flight planning, checklists, and documentation relevant to the platform.

- Two Control Display Units (CDU) are centrally located in the cockpit to allow for interface with the aircrafts Flight Management System (FMS). This interface allows entry of flight plans as optimized by performance, weather, and fuel efficiency.

- Communications equipment consists of several systems in accordance with the RFP. These include very-high frequency/ultra-high frequency VHF/UHF radio transceivers [52], satellite communications (SATCOM), and Identification Friend of Foe (IFF).

- Controls corresponding to flight surfaces are arranged the same as the C-5 platform with rudder, pedals, sidestick controller, trim, and throttles to facilitate the ease in adoption of the platform.
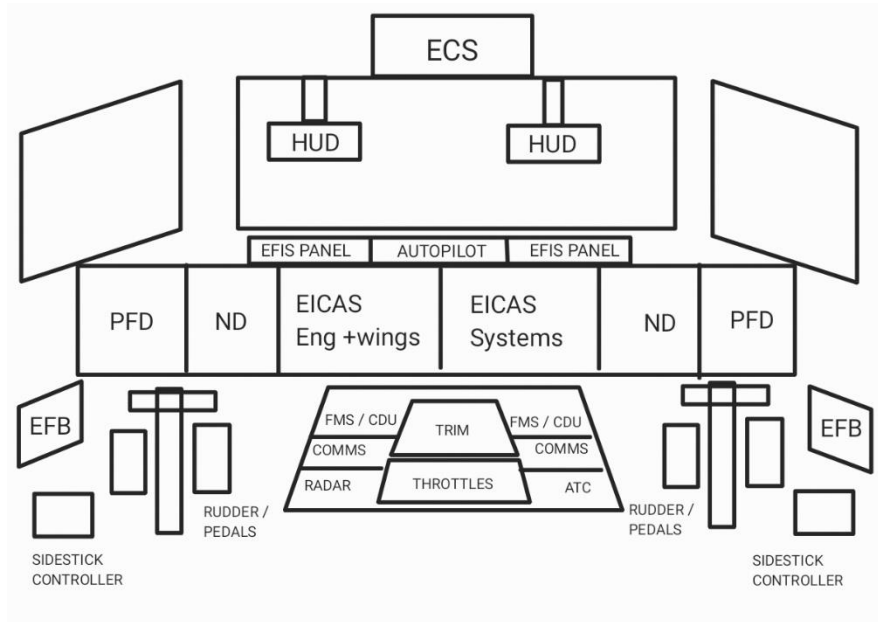
Figure 61. Cockpit Avionics Layout Diagram

9.7 Avionics and Data Communication

The PW-24 Harpy's avionic suite is based off commercial the shelf systems (COTs). This helps to alleviate some of the upfront procurement costs associated with the design and manufacture of the aircraft. It also ensures that the Harpy will receive state-of-the-art equipment while reducing project timeline risk caused by delays in product development. All avionics equipment used are considered Line Replaceable Units (LRUs) and easy access to this equipment will be provided through a compartment under the forward-most location of the fuselage.

The equipment selected to be used in the Harpy is shown in Table 30 below. This table outlines the type of equipment, the model/manufacturer, and the quantity included for redundancy.

Table 30. PW-24 Harpy Avionics Equipment List

Avionic System Type	Avionic System	Manufacturer/Model	Quantity
Communication	VHF/UHF/SATCOM Radio	**Collins Aerospace:** ARC-210 RT-2036 (C)	3
Communication	ATC Mode S/IFF	**Collins Aerospace:** APX-119	2
Communication	SATCOM Antenna	**Collins Aerospace:** HGA-2100B	3
Communication	TACAN/DME	**L3 Harris:** TRC2634	2
Electronic Countermeasures	Radar Warning Receiver (RWR)	**BAE Systems:** AN/ALR-56M	2
Electronic Countermeasures	Large Aircraft Infared Countermeasures LAIRCM	**Northrop Grumman:** MWS/GLTA	2
Navigation	Terrain Following Radar	**Collins Aerospace:** TERPROM	2
Navigation	GPS	**Rockwell Collins:** GPS-400S	3
Navigation	INS	**Safran:** Sigma 95N	3
Flight Displays	Video Display Terminal (VDT)	**Intellisense Systems:** VDT-1209	6

The PW-24 Harpy uses a MIL-STD-1553B military data bus with a federated digital architecture. This bus is a bi-directional, centralized control, linear topology, command/response bus. Traffic throughout the bus is managed by a centralized bus controller (BC). Networks within the aircrafts avionics systems are implemented for dual redundancy.

9.8 Life Support Systems

9.8.1 Zero-Zero Crew Escape

The PW-24 Harpy does not incorporate a zero-zero crew escape system. These systems are extremely complex and require extensive maintenance efforts to ensure their safety and reliability. The Air Force's B-52 and B-1 utilize crew escape systems like what would have been found in the Harpy, but they require 3+ weeks of maintenance every 4-5 years [53]. This maintenance program requires highly skilled technicians, people who may not be readily accessible if a failure occurred in an austere environment. Additionally, these aircraft typically fly into more contested airspace where the likelihood of encountering hostile threats is far greater. The PW-24 Harpy, on the other hand, is a strategic airlifter that tends to avoid hostile airspaces (a job more

suited for a tactical airlifter like the USAF's C-130). This means that the Harpy is much less likely to encounter enemy threats which would necessitate the implementation of a complex and costly crew escape system.

9.8.2 Pressurization and Environmental Control System

A traditionally designed aircraft would rely on bleed air tapped from the engine's compressor section to provide compressed air to pressurize the fuselage. The PW-24 Harpy's more electric design removes the bleed air and pneumatic system in favor of electrically powered subsystems. The Harpy's design includes five electric environmental control system (ECS) packs. These packs require a significant amount of power to operate and are one of the primary drivers in electrical system sizing. The number of packs was obtained by extrapolating the fuselage volume and quantity of packs in the Boeing 787 (two ECS packs) to the PW-24 Harpy. It was found that the Harpy's pressurized volume is roughly 2.5x the size of the 787 resulting in a system designed with five ECS packs. Also, the power consumption was extrapolated in the same manner resulting in a total power draw of approximately 1.25MW (787's power consumption is 500kW per [40]). This value is further supported by extrapolating the data presented in Figure 2 of [54]. The data is presented in terms of power consumption per passenger, a metric that is not applicable to the Harpy, but it was assumed that one passenger was equal to $10ft^3$. This, once again, yielded an approximate total power consumption of 1.25MW.

9.8.3 Anti-Icing

The PW-24 Harpy boasts a wingspan 70' greater than that of the C-5 platform, requiring a powerful and efficient de-icing system to maintain the effectiveness of its flight surfaces. To meet this requirement, the Harpy integrates a heater mat that runs the full length of the wings' slats, as well as the leading edge of the tail. These heater mats are a cured composite constructed of carbon and glass fiber, along with a spray-on metal. [39] The power requirements for this system were calculated based on a formula defining power usage of the cyclic heating system on a Boeing 787. [55] The total power draw of the system is calculated to be 186kW at a 5% cyclic heating cycle.

9.8.4 Emergency/Backup Systems

Since the PW-24 Harpy is highly dependent upon its electrical system, a loss of electrical power is a significant risk that requires mitigation. To minimize the impact of an electrical failure, the Harpy will employ

three ram air turbines (RATs) to power critical systems. The batteries are each capable of supplying 2,000 Watt-hours of power which can be used for environmental control, flight control actuation, and for critical avionics/radios [56]. Likewise, the RATs will be able to supply ~70kW of power (based on A380 system) indefinitely for the same purposes [40].

10. Program Management

10.1 Production Cases

The team at Prestige Worldwide conducted a cost analysis on the production runs prescribed by the RFP. These include 90 units, 180 units, and 270 units production runs. The nominal target production run for the PW-24 Harpy is a production of 180 units, 20 of which will be produced with the goal of selling to United States' Military Allies and commercial cargo transport companies.

10.2 Flyaway Cost Analysis

The research, development, tooling, and engineering costs of the PW-24 Harpy was found using the tried-and-true DAPCA IV model. DAPCA IV is the Development and Procurement Costs of Aircraft model created by the RAND corporation [57]. This model computes the total flyaway cost using the overall cost of engineering, tooling, quality control, manufacturing, and propulsion systems. This is done by finding the going rate for each of these processes in 1989 US Dollars. These are then multiplied by the man-hours required for each process to find the total cost for each portion of the flyaway cost.

DAPCA IV is a powerful tool for early-project aircraft cost analysis, but its inputs must be procured from other sources. The equations used to calculate the hours and hourly rates are found in Nicolai Chapter 24 [11], which deals in life cycle cost estimation. Chapter 24.2 of the textbook covers the calculation of required hours and hourly rates for cost components from airframe engineering to manufacturing. These are used as inputs for the DAPCA IV model. In addition, the inflation factor is incorporated to make the final cost values relevant to the strength of 2024 US Dollars as well as a material adjustment factor for any materials other than aluminum. The inflation factor is acquired from the US Bureau of Labor Statistics [58]. A breakdown of the inputs for the DAPCA IV model can be found in Table 31.

Table 31. Inputs for DAPCA IV Cost Model

Input Parameter	Value
Aircraft Type	'cargo'
Engineering Rate	155.824
Tooling Rate	169.192
Manufacturing Rate	135.584
Inflation Factor	2.83
Material Adjustment Factor	1.0 (Aluminum)

The per-unit flyaway cost falls considerably as the number of aircraft produced is lowered. This is in part due to the nature of manufacturing processes becoming more efficient as the learning factor increases. That is to say, as the employees manufacturing the aircraft spend more time on the assembly line, they become faster with their individual time. In turn, this lowers the wages paid to build a single aircraft and thus the effective price of the aircraft. The impact of each parameter in cost computation is shown in Figure 62. A large part of this price decrease, however, is the percentage of fixed pricing that must be covered by each aircraft that is sold. At a production run at 90 units, the price of engineering, tooling, and testing must be covered and exceeded by just those 90 sales. Therefore, it follows that when the cost is spread among three times as many units, the price of the aircraft can be much lower and still turn a profit.
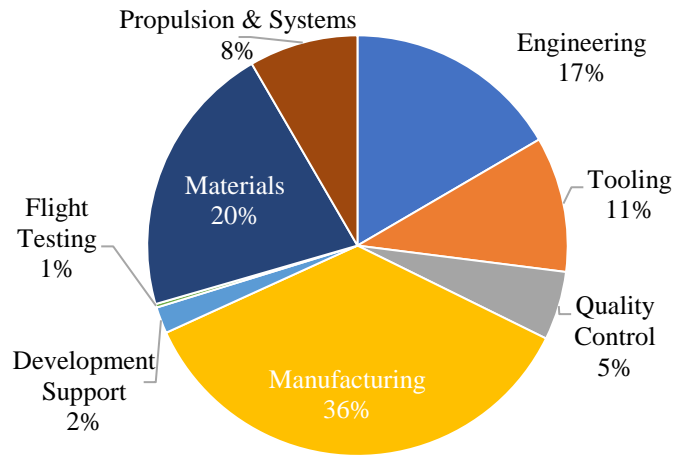

Figure 62. Flyaway cost breakdown

The unit cost for the three production runs required by the RFP, as mentioned above, are shown in Table 32. The calculations for these runs consider an aircraft production number of 90, 180, or 270 + 5 test aircraft. The unit cost for each case is given as a combination of the cost of engineering, manufacturing, and

testing spread across the number of units. A 10% profit is then added onto the unit cost to create a unit price. These are also displayed in Table 32. It is worth noting that we propose a 40% cost share with the DoD as the Harpy will be used for defense purposes.

Table 32. Unit cost and price for each production run

Number of Aircraft	Unit Cost	Unit Price
90	$532,000,000	$585,000,000
180	$383,000,000	$421,000,000
270	$322,000,000	$354,000,000

10.3 Operations Cost

The cost of operations was developed using the methods listed in Raymer, chapter 18.5 [24] and readily available information from the internet. Operations are broken down into three major categories: fuel, salaries, and maintenance, which are explained in further detail below. For this section's purpose, a production run of 180 aircraft was used with an estimated 1200 flight hours per year per aircraft. A service life of 40,000 hours was used as designated by the RFP, giving each aircraft a service life of just over 33 years.

Fuel costs were found by calculating the gallons of fuel burned per year from the flight hours per year and average fuel burned per flight hour. This was then multiplied by the national average jet fuel cost (August 2nd, 2024) of $6.03 per gallon [59].

Crew salaries made up the majority of the operating costs for the Harpy. Each aircraft requires a crew of two pilots and two loadmasters, with provisions for a relief crew of the same size. Salaries for these crew members was determined by examining the pay rates for military pilots and the pay rates for loadmasters. Due to the wide range of pay rates of service members based on their pay grade and years of experience, the average crew salary was estimated to be $80,000 per year. This was multiplied by the crew ratio, which is 1.5 for military transport aircraft flying at 1200 flight hours per year, the number of aircraft in service, and the number of crew members per aircraft.

The total time spent on maintenance was found using the Harpy's MMH/FH value and the average flight hours per year. This was multiplied by the manufacturing wrap-rate to find the maintenance labor cost

per year. For military aircraft, the maintenance material cost is roughly equal to the maintenance labor cost, which gives the total maintenance cost per aircraft. The total operations cost breakdown is shown in Table 33.

Table 33. Operations cost for each aircraft per year

Category	Cost
Fuel	$38,000,000
Crew Salaries	$86,400,000
Maintenance	$5,180,000
Total	$130,000,000
Total per Flight Hour	$108,000

10.4 Marketing Plan

Per the RFP, 20 units of the 180-unit production run are to be sold to United States military allies and commercial cargo transport entities. Therefore, a marketing plane must be created which aims to market the PW-24 Harpy to these potential customers. The marketing strategy emphasizes creating public excitement and intrigue around the PW-24 Harpy.

10.4.1 Website Development

The first step in marketing Prestige Worldwide and the PW-24 Harpy is to develop and launch and company website. The overarching goal of this website is to introduce customers and the public to Prestige Worldwide and its aircraft. The website will feature sections about getting to know the company and its mission, high-level specifications of the aircraft, and location and dates of demonstrations and air shows in which our aircraft can be seen. This means that potential customers can quickly learn about our company and aircraft in one place. This website will draw digital foot traffic to our product. Having a single location in which company updates and news can be spread helps to strengthen the Prestige Worldwide brand [60]. This in turn gives our product more legitimacy within the market, improving the chances of selection of our aircraft. An online presence also generates more "random" traffic to our product, as we are able to appear in any search related to heavy lift mobility platforms or similar inquiries.

10.4.2 Social Media Campaign

In addition to the online presence created by a company website, a social media marketing campaign will be conducted to further flood Internet spaces with the PW-24 Harpy. The purpose of the website is to

provide a professional and succinct location to learn about the aircraft. The social media campaign will strive to create excitement and more general interest in the plane and its abilities. Featuring video clips of the airplane in action, behind the scenes of the aircraft in production, and meet the team content, the marketing campaign will take a more "fun" approach to the selling of large cargo transport aircraft. On our various social media platforms, we will be able to communicate with the public in real time about updates to demonstration dates and exciting news about the development of our company [61]. General interest will bring our product to the top of the list of candidates that our potential customers will consider. Another benefit the social media presence is that it allows for another way to draw traffic towards our website, which will give the most complete view of our product.

10.4.3 Air Demonstrations

The best way to show off a new aircraft is to demonstrate its capabilities in flight. There are air shows and flight demonstrations across the country and world. We have developed the largest production line aircraft to grace the skies, and seeing this large an air vehicle cruising at transonic speeds will inspire awe in all those able to see it in person and on social media. This will further the excitement around the aircraft and increase the likelihood of purchase by potential customers.

10.5 Risk

In conjunction with the selection of the Heavy Lift Aircraft (HLA) baseline design, a project risk assessment was conducted to identify potential challenges. The assessment includes an analysis of project risks (shown in Table 34), with each risk undergoing a dual assessment, considering both impact and probability. A numerical value for impact and probability ranging from zero to one is assigned to every identified risk. To determine the overall risk, both values for each risk are multiplied. The results are shown in Figure 63. To strengthen the project against potential risks, we developed strategic mitigation strategies (Table 34) in response to each identified risk. This risk analysis serves as a fundamental element in ensuring the resilience and success of the HLA development project.

Table 34. Risk Analysis Stating Risk Factors and Their Mitigation Strategy

| Risk Factor	Mitigation Strategy
Cost Risk due to inflation	Contingency Cost Allowance
Production takes longer due to lack of facilities and understaffing	Develop a comprehensive project tracking program to maintain schedule
Legal risk of failing to get certified	Precise planning and control of policies
Cost Share Failure	---
Customer decision changes	Initial Contracts and Agreements
Competition from peer aircraft	Make optimal design decisions
Schedule and Management deficiencies (e.g. Task dependencies don't work out & increasing complexity and interfaces add unplanned time)	Maintain close ties to every department - keep everyone in the loop throughout the project.
New technologies and designs are found to be technically infeasible	Assign sufficient time for quality assessment during prototype stage
Production supply shortage	Qualify multiple suppliers at prototyping stage
Discrepancies between test results and flight/ground tests	Realistic testing
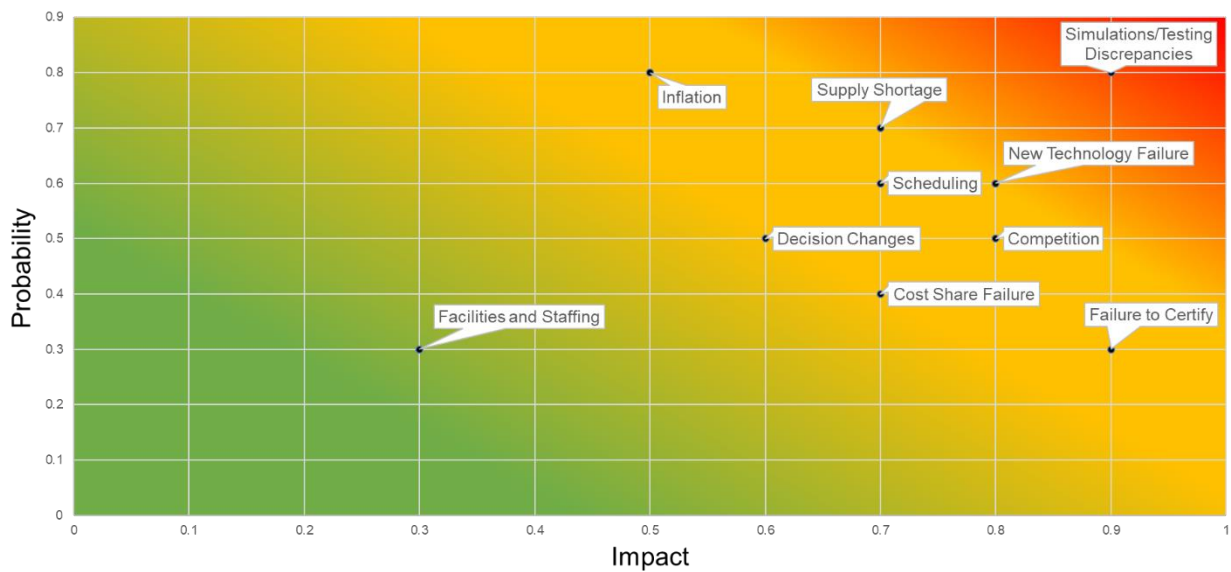
Figure 63. Project Risk Analysis Diagram Stating Impact and Probability

10.6 Gantt Chart
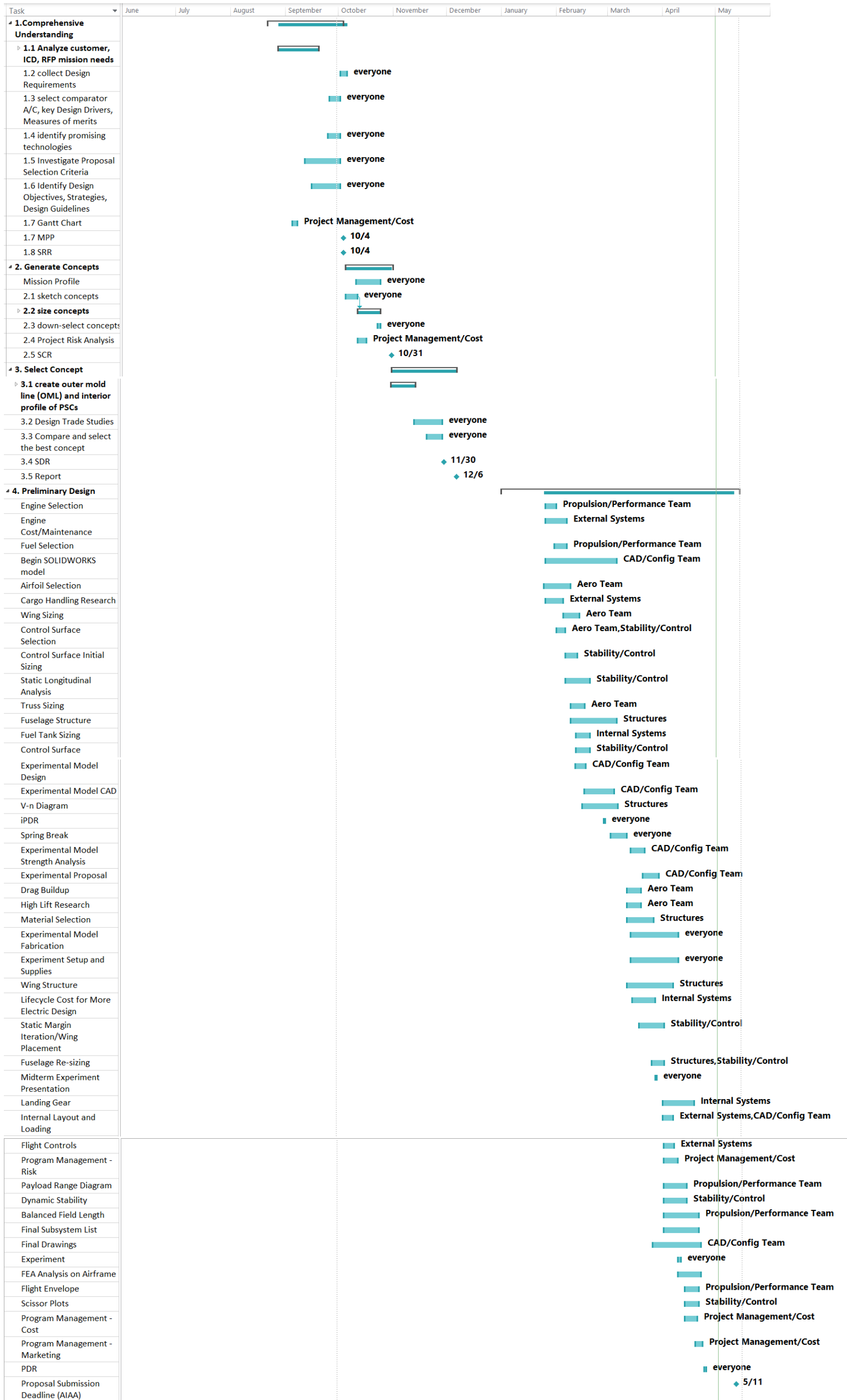
11. Conclusion

In the 2030s and 2040s, the US Air Force will need a new heavy-lift strategic transport aircraft to replace their ageing strategic air mobility platforms. In response to the AIAA's RFP, Prestige Worldwide has designed an innovative heavy lift mobility platform, the PW-24 Harpy, to bridge the Air Force's looming capability gap. Our aircraft utilizes emerging technologies to transport heavier loads further than any existing platform. The Harpy takes advantage of a truss braced wing design to decrease the aircraft's total drag and increase the wing's aspect ratio and overall efficiency. The Harpy maintains its versatility by employing folding wingtips, allowing for operation out of smaller airfields without compromising on the performance benefits of a larger span wing. The more electric subsystem architecture, made possible because of the bleedless air engine system, further increases the fuel efficiency of the Harpy. The PW-Harpy stands out against its competitors and is the clear choice for the USAF's strategic transportation needs and as the next generation of heavy lift aircraft.

References

[1] "Code of Federal Regulations: Title 14 - Part 25 - Airworthiness standards: Transport category airplanes" *National Archives,* 04 Dec. 2014.
https://www.ecfr.gov/current/title-14/part-25

[2] "MIL-A-8861B, MILITARY SPECIFICATION: AIRPLANE STRENGTH AND RIGIDITY FLIGHT LOADS (7 FEB 1986)," *Every Spec,* published online. http://everyspec.com/MIL-SPECS/MIL-SPECS-MIL-A/MIL-A-8861B_6743/.

[3] "MIL-HDBK-516, DEPARTMENT OF DEFENSE HANDBOOK: AIRWORTHINESS CERTIFICATION CRITERIA (01 OCT 2002)", *Every Spec,* published online.

[4] "Lockheed C-5 Galaxy Heavy Transport" *Aerospace Web,* published online 15 Apr. 2011.
https://aerospaceweb.org/~aerospa1/aircraft/transport-m/c5/

[5] "C-17 Globemaster III", *United States Air Force*, published online.
https://www.af.mil/About-Us/Fact-Sheets/Display/Article/1529726/c-17-globemaster-iii/

[6] "Antonov An-225 Mriya (Cossack)", *Military Factory,* published online 15 Apr. 2022.
https://www.militaryfactory.com/aircraft/detail.php?aircraft_id=58

[7] Buckley, J., "AN-225: Plans to rebuild world's largest plane confirmed," *CNN* published online 10 Nov. 2022.
https://www.cnn.com/travel/article/antonov-an225-mriya-rebuild-2022/index.html#:~:text=Originally%2C%20Ukrainian%20state%20defense%20company,to%20rebuild%2C%20said%20the%20company.

[8] Mitchell, B. "Air Force selects AI-enabled predictive maintenance program as system of record," *Defense Scoop,* published online 10 May 2023.
https://defensescoop.com/2023/05/10/air-force-selects-ai-enabled-predictive-maintenance-program-as-system-of-record/

[9] Hill, E., "Higher performance head-up", *Aerospace Manufacturing*, published online 25 Jun. 2022.

[10] Ting, E., et al. "Aerodynamic Analysis of the Truss-Braced Wing Aircraft Using Vortex-Lattice Superposition Approach", *NASA,* Atlanta, Georgia, 16 Jun. 2014.

[11] Nicolai, L. M., Carichner, G., and Nicolai, L. M., "Fundamentals of aircraft and Airship Design," *Aircraft Design,* Vol. 1, Reston, Virginia, 2010. American Institute of Aeronautics and Astronautics.

[12] "ILFC selects Rolls-Royce Trent 1000 for 40 Boeing 787s," *Rolls Royce,* published online 06 Jul. 2006.
https://www.rolls-royce.com/media/press-releases-archive/yr-2007/ilfc-selects-rr.aspx

[13] "Record Year For The World's Largest, Most Powerful Jet Engine" *GE Aerospace,* Evandale, Ohio, published online 19 Jan. 2012.
https://www.geaerospace.com/press-release/ge90-engine-family/record-year-worlds-largest-most-powerful-jet-engine

[14] Harris, C. D., *NASA supercritical airfoils* Available:
https://ntrs.nasa.gov/api/citations/19900007394/downloads/19900007394.pdf.

[15] "WHITCOMB INTEGRAL SUPERCRITICAL AIRFOIL (whitcomb-il)," *Whitcomb integral supercritical airfoil (Whitcomb-IL)* Available: http://airfoiltools.com/airfoil/details?airfoil=whitcomb-il.

[16] Roman, D., "3. Drag: An Introduction," Jan. 1997.

[17] "Induced drag coefficient," *NASA* Available:
https://www.grc.nasa.gov/www/k-12/VirtualAero/BottleRocket/airplane/induced.html.

[18] Ivaldi, D., *Aerodynamic shape optimization of a truss ... - deep blue* Available:
https://deepblue.lib.umich.edu/bitstream/handle/2027.42/140535/6.2015-3436.pdf?sequence.

[19] European Union Aviation Safety Agency. "EASA Publications." Accessed May 1, 2024.
https://www.easa.europa.eu/en/downloads/7733/en

[20] Trent Data - Aircraft Commerce. "RR Trent Engine Guide." Aircraft Commerce, Issue 83. Accessed May 1,
2024. https://www.aircraft-commerce.com/wp-content/uploads/aircraft-commerce-
docs/Aircraft%20guides/RR%20TRENT/ISSUE83_TRENT_GUIDE.pdf

[21] EASA Datasheet - GE: General Electric Company. "Type Certificate Data Sheet for [GEnx Series Engines]."
EASA, No. IM.102, 22 November 2022

[22] RR Press Release - Rolls-Royce. "ILFC selects Rolls-Royce Trent 1000 engines for Boeing 787 Dreamliner
fleet." Press Release, Year 2007. Accessed May 1, 2024. https://www.rolls-royce.com/media/press-releases-
archive/yr-2007/ilfc-selects-rr.aspx

[23] GE Press Release - GE Aviation. "Best-Selling GEnx Engine Enters New Era." Press Release. Accessed May 1,
2024.
https://www.geaerospace.com/press-release/genx-engine-family/best-selling-genx-engine-enters-new-era

[24] Raymer, D. "Aircraft Design: A Conceptual Approach", Aerospace Research Central, 6th ed. 30 Sep.
2018. https://doi.org/10.2514/4.104909

[25] Delta TechOps. "Trent 1000 Engine Maintenance Services." Accessed May 1, 2024.
https://deltatechops.com/services/engine-maintenance/trent-1000-engine/

[26] CO2 List. "Carbon Dioxide Emissions by Source." Accessed May 1, 2024.
http://www.co2list.org/files/carbon.htm#RANGE!A83

[27] Federal Aviation Administration. "FAA Docket No. FR-ADFRAWD-2023-25521." Accessed May 1, 2024.
https://drs.faa.gov/browse/excelExternalWindow/FR-ADFRAWD-2023-25521-
0000000000.0001%3FmodalOpened%3Dtrue?modalOpened=true

[28] Filippone, A., Flight performance of fixed and rotary wing aircraft, Reston, VA: American Institute of Aeronautics
and Astronautics, 2006.

[29] "Stability and Control Complete Vehicle Pitch Stability and Control",
https://archive.aoe.vt.edu/lutze/AOE3134/Vehicleproperties.pdf

[30] "Determining the Horizontal Tail Optimum Dimension of Civil Transport Class Aircraft Based on the Previous
Model for Upgrading the Passengers Number", N Aditya and W Nirbito, IOP Conf. Series: Materials Science
Engineering 449, 2018. https://iopscience.iop.org/article/10.1088/1757-899X/449/1/012012/pdf

[31] "Aircraft Design: A Systems Engineering Approach" , John Wiley & Sons, Inc., 2013.
https://onlinelibrary-wiley-com.ezproxy.lib.vt.edu/doi/book/10.1002/9781118352700

[32] "MILITARY SPECIFICATION FLYING QUALITIES OF PILOTED AIRPLANE", NOV 5 1980,
MIL-F-8785C.pdf

[33] Aerospace Metals. "Contact Aerospace Metals." Accessed May 1, 2024.

https://aerospacemetals.com/contact-aerospace-metals/

[34] "Pros and cons of composite materials: Pacific Aerospace Corp," Pacifc Aerospace Corp (PAC) Available:
https://www.pacificaerospacecorp.com/what-are-the-pros-and-cons-of-composite-materials/.

[35] Niu, M. C., Airframe structural design, Hong Kong: Conmilit Pr, 1990.

[36] Roskam, J., Airplane Design, Lawrence, Kan: DARcorporation, 2018.

[37] Gur, Ohad & Bhatia, Manav & Schetz, Joseph & Mason, William & Kapania, Rakesh & Mavris, Dimitri. (2010). Design Optimization of a Truss-Braced-Wing Transonic Transport Aircraft. Journal of Aircraft. 47. 1907-1917. 10.2514/1.47546.

[38] Ray, J., "System design: Fixing the 787's batteries," Avionics International Available:
https://www.aviationtoday.com/2013/06/01/system-design-fixing-the-787s-batteries/.

[39] Sloan, J., "787 integrates new composite wing deicing system," CompositesWorld Available:
https://www.compositesworld.com/articles/787-integrates-new-composite-wing-deicing-system.

[40] Moir, I., and Seabridge, A., Aircraft Systems Mechanical, electrical, and avionics subsystems integration, West Sussex, England: John Wiley & Sons Ltd, 2008.

[41] Crone, C., "COMMON ELECTRO-HYRDOSTATIC ACTUATORS (CEHA)", Actuation, 2018. Available:
https://www.moog.com/content/dam/moog/literature/sdg/space/actuationmechanisms/moog-common-electro-hydrostatic-actuators-datasheet.pdf

[42] "Aircraft Tire Data Book," The Goodyear Tire & Rubber Co., Akron, OH, Oct. 2002.
https://www.aps-aviation.com/wp-content/uploads/goodyear-aircarft-tire-data.pdf

[43] "Tie down rings," Davis Aircraft Company Available: https://davisaircraft.com/products/tie-down-rings/.

[44] "Chain Gear," Davis Aircraft Company Available: https://davisaircraft.com/products/chain-gear/.

[45] Department of the Navy, "Military-references," Technical Manual Available:
https://www.military-references.com/wp-content/uploads/books/tanks/usa/m1_abrams/M1_Abrams_Turret_Organizational_Troubleshhoting_Vol_II_Part_1_TM_9-2350-255-20-2-2-1_1984.pdf.

[46] "Gravity Roller Conveyor," International Automated Systems Available:
https://www.iasmn.com/wp/air-cargo/gravity-roller-conveyors/.

[47] "463l nets," 463L Nets Available: https://www.463lnets.com/.

[48] "463L tensioners, 463L chains and 463L tie downs," 463L Tie Downs, 463L Chains, 463L Tensioners Available:
https://www.463lpallet.com/463ltiedowns463ltensioners463lchains.htm.

[49] "VDT-1209 Datasheet download," Intellisense Systems, Inc. Available:
https://www.intellisenseinc.com/thank-you/vdt-1209-datasheet-download.

[50] "TYPE-CERTIFICATE DATA SHEET," Apr. 2024.

[51] "LiteWave® head-up display (HUD)," BAE Systems | International Available:
https://www.baesystems.com/en/product/litewave-head-up-display.

[52] "ARC-210 RT-2036 (C) networked communications airborne radio," CA Available:

https://www.collinsaerospace.com/what-we-do/industries/military-and-defense/communications/airborne-communications/vhf-uhf-l-band/arc-210-rt-2036-c.

[53] Armstrong, B. J., "No margin for error at Tinker bomber egress shop," *72nd Air Base Wing Public Affairs*, published online 12 Mar. 2009.
https://www.af.mil/News/Article-Display/Article/120938/no-margin-for-error-at-tinker-bomber-egress-shop/

[54] Herxog, J., "Electrification of the Environmental Control System" *25th International Congress of the Aeronautical Sciences*, Liebherr Aerospace Lindenberg GmbH, 2006.
https://www.icas.org/ICAS_ARCHIVE/ICAS2006/PAPERS/344.PDF

[55] Meier, O., and Scholz, D., "A Handbook Method for the Estimation of Power Requirements for Electrical De-Icing Systems,"
https://www.fzt.haw-hamburg.de/pers/Scholz/MOZART/MOZART_PUB_DLRK_10-08-31.pdf

[56] Boeing. "787 Batteries Backgrounder." Accessed May 1, 2024.
http://787updates.newairplane.com/Boeing787Updates/media/Boeing787Updates/Aviation%20Experts/787-BATTERIES-BACKGROUNDER.pdf

[57] Boren, H. E., "DAPCA: A computer program for Determining Aircraft Development and production costs | Rand," *DAPCA A Computer Program for Determining Aircraft Development and Production Costs* Available: https://www.rand.org/pubs/research_memoranda/RM5221.html.

[58] "CPI Home," *U.S. Bureau of Labor Statistics* Available: https://www.bls.gov/cpi/.

[59] "100ll & jet fuel prices at U.S. Airports & Fbos by region," *Globalair.com* Available: https://www.globalair.com/airport/region.aspx#:~:text=Latest%20Jet%20Fuel%20%26%20100LL%20Aircraft%20Fuel%20Prices&text=The%20national%20average%20price%20for%20jet%20fuel%20is%20%246.48%20per%20gallon.

[60] Kaplan, K., "Council post: Why every business needs a website," *Forbes* Available: https://www.forbes.com/sites/theyec/2020/02/03/why-every-business-needs-a-website/?sh=ae516b16e75c.

[61] Adobe Communications Team, "15 benefits of social media marketing | adobe," Business Adobe Available: https://business.adobe.com/blog/basics/smm-benefits.